UNIVERSITÀ DEGLI STUDI
DI GENOVA

PhD PROGRAM IN BIOTECHNOLOGY IN TRASLATIONAL MEDICINE
Curriculum: Translational Medicine
XXX CYCLE
Department of Experimental Medicine, Università & Ospedale Policlinico San Martino

PLATELET DERIVATIVES: FROM BENCH TO BEDSIDE. MOLECULAR CHARACTERIZATION OF THE EFFECT OF PLATELET DERIVATIVES ON CELLS AND THEIR USE FOR SKIN CHRONIC ULCER TREATMENT

Candidate
Marta Nardini

Supervisor
Prof. Ranieri Cancedda

Co-Supervisor
Dott.ssa Maddalena Mastrogiacomo

TABLE OF CONTENTS

PREFACE

Our interest in skin regeneration arises from the evidence that chronic ulcers, and especially those in diabetic patients, are difficult to cure and are widespread in all countries. The incidence of this disease is particularly high in our region (Liguria, Italy), affecting mainly elderly population that need of home care for the treatment of chronic ulcers.

Skin ulcers are sore localized on the skin or on a mucous membrane, accompanied by the disintegration of tissue that occurs predominantly in bedridden patients. The ulcers are due to a re-epithelization process not physiologic determined by several factors during the regeneration of the skin. One of the pathologies that can lead to the development of skin ulcers is diabetes, which incidence in recent years, has strongly increased. One of most important problems related to the diabetic skin ulcers is the chronicity of the lesion that leads to a constant and prolonged demand for care by the patient, becoming a big social issue.

To date, the "conventional" treatment for the healing of crucial ulcers is the *debridement*, that results in the reduction of the infection at the site. This approach induces a stimulation of the reepithelization process, that in most cases is intercepted by the presence of necrotic tissue. Subsequently, the wound bed is threated with different techniques such as physical stimulation (hyperbaric oxygen therapy, negative pressure therapy, and ultrasound treatment) [1,2] and advanced methods including growth factor therapy. The average duration of an ulcer is approximately 26 weeks, with a range that vary from 4 weeks to 30 years in the worst cases. However, in 46% of patients the clinical course exceeds 26 weeks and in 15% of patients is over two years.

The care of these critical lesions represents one of the main aim of the regenerative medicine.

In this regard, recently, it has been introduced the treatment of the skin ulcers with Platelet Rich Plasma (PRP) gel. The PRP gel is a matrix consisting mainly of platelets, that are activated by thrombin to release growth factors important in the starting and sustaining of the process of tissue regeneration.

In this field I carried out my PhD course project in Regenerative Medicine with Curriculum Translational Medicine during which I studied the role of growth factors derived from the platelets in term of their effect on the cell proliferation and their use in the treatment and care of skins ulcers.

The Thesis, here presented, is organized in three chapters:

1) Platelet derivatives effect on the proliferative stage of mesenchymal stem cells and cell lines, and MYC pathway activation;

2) Electrospun silk fibroin fibers for storage and controlled release of human platelet lysate;

3) Sericin, alginate and platelet lysate combined in a biomembrane for the treatment of skin ulcers.

In support of the original design of the thesis project, there were publications that our team had previously published on the role of PRP as a potential substitute of the fetal calf serum in cell cultures and as its potential use for tissue regeneration.

Zaky et al. and Muraglia et al. [3,4] have described in different papers a platelet derivative able to stimulate cell proliferation, allowing cells to maintain their phenotypical characteristics and differentiation capacity. In 2016 were published the first results regarding the efficiency of a PRP bioactive membrane fabricated according to the standard protocols used in the Blood Transfusion Centre. The novelty of this membrane respect to others is the standardization of growth factors content based indirectly on the number of platelets/microliter associated to the membrane. This allowed the generation of different typologies of membranes adaptable to different applications in relation to the severity of the lesions.

Based on this background, the aim of the Thesis was the study of the effects of platelet growth factors on the cells to understand the molecular activated mechanisms responsible for the increased proliferation. In parallel with the aim to identify a cutaneous patch based on PRP, we studied a new membrane based on the combination of platelet derivatives and silk proteins that are considered good scaffolds in the tissue regeneration. Here either fibroin or sericin were used in combination with platelet derivatives to generate a membrane able to release, in a controlled fashion, platelet growth factors to simulate the microenvironment for the repair of the skin wound. To achieve this goal, we established collaborations with two different research groups.

OUTLINE

To date, the major part of culture medium supplements is based on animal sera. The use cell culture is increasing, and innovative supplements to expand cells are constantly developed.

As it is well known, there are several problems related to the use of animal sera. These problems are not only scientific, ethical and technical, dealing with the conservation, starvation and lot to lot variation [5–7], but also regarding the limited use of the Fetal Calf Serum (FCS) for the expansion of cells intended for clinical applications [4]. In June 2011, the European Commission released guidelines to minimize the risk of transmitting animal spongiform encephalopathy agents via human and veterinary medicinal products (EMA/410/01 Revision 3). These guidelines suggested the preferential use of supplements of non-animal origin for the cultivation of cell cultures [4]. For this reasons, the human derivatives, in particular the platelets derivatives, have earned a huge success based on the presence of a mix of growth factors that promote cell proliferation and differentiation, one of most important step in the regenerative process.

In literature there are several publications related to the use of platelet derivatives as supplement for culture medium: however, these publications, report controversial results. This can be explained by the different procedures that are applied for the supplement preparation resulting in different contents of platelets and growth factors released [8].

In 2015, the research group in which I worked during the PhD training, published an article that showed for the first time a dual component based on platelet and plasma derivatives to be used in replacing FCS in cell culture system. The main characteristics of this platelet derivative were the derivation from discarded pool of human healthy donor blood donations, and the standardization in term of their content of growth factors to reduce the variability in the different preparations [4].

Starting from these observations, I designed the first part of my PhD program to understand the effect of platelet derivatives on cell proliferation, investigating its efficiency respect to FCS, the standard used supplement, and the activated molecular pathways at the base of its proliferation stimulation efficiency.

Traditional treatments of degenerative pathologies include, physical stimulation (hyperbaric oxygen therapy, negative pressure therapy, and ultrasound treatment) [1,2] and advanced methods such as growth factor therapy [2,9]. Furthermore, these treatments are, in most cases, merely palliative. The well-known capability of platelet derivatives in promoting cell proliferation, suggested their use in the clinical practice, in most cases in the form of autologous Platelet Rich Plasma (PRP) [9-12].

In orthopaedic, PRP has been used for the treatment of bone, tendon and ligament disorders, while in the dentistry it has been employed to promote tissue growth and to speed up the healing process.

Recently, many experimental attempts to favour faster healing of the wound, have been done with a tissue engineering approach in order to develop medical bioactive devices (patches, membranes etc.) [14].

At the beginning of my PhD, I participated in a work which had the objective to characterize a biomembrane based on allogenic PRP with a standardized platelet concentration for the treatment of

skin chronic ulcers. This work yielded a manuscript entitled Platelet Rich Plasma-based Bioactive Membrane as a New Advanced Wound Care Tool [15], where two different bioactive membranes (BAM) based on a different platelet concentration [2.0E6 (Low-BAM) and 10E6 (High-BAM) platelets/mL] were compared and characterized for their ability to release growth factors and their regenerative potential in an animal model. The BAM were prepared by a standardized method, starting from human derived components, to ensure the biocompatibility and a complete biodegradation and resorption [16]. The growth factors release and the speed of biodegradation of the BAM were controlled by varying the platelet concentration inside the PRP, in the presence of cryoprecipitate. The control of the gel biodegradability and of the growth factor release is very important issues. BAM maintain a wet environment in the wound area that is favourable for the best tissue regeneration [17]. This feature, in combination with the strong pro-inflammatory induction determined by the platelet release, should restore the correct micro-environment in the wounded area, thus enhancing wound healing and closure [18]. In the skin chronic wound animal mouse model, the L-BAM performed better than H-BAM. However, it remains to be investigated if, unlike in the mouse model, in the human chronic wounds, where the skin layers are thicker than in rodents, both BAM could be of benefit in enhancing wound closure. In particular, H-BAM could be used for the treatment of deeper skin lesions, where it is necessary a stronger tissue granulation formation, while the L-BAM could be used for the treatment of more superficial skin lesions.
The conclusions lead to consider the PRP-BAM a new powerful tool for the treatment of chronic and difficult to heal skin ulcers.
The skin lesions, in particular the ulcers, represent especially for a diabetic patient, one of most common cause of, infections, ischemia and lower limb amputations in the United States and Europe. Despite the introduction of endovascular revascularization techniques, wound therapeutics, and advances in the medical management of diabetes, the number of patients that need limb amputation have not decrease in the last years.

The physiologic wound healing process consists of four phases that overlap at some points and are summarized in Figure 1:
• Coagulation and haemostasis,
• Inflammation,
• New tissue formation,
• Remodelling.

The first wound healing phase occurs immediately after tissue damage with the coagulation and haemostatic process [19,20]. This mechanism starts to prevent exsanguination. This first phase occurs to provide a matrix for invading cells that are needed in the late phase [21]. The amount of fibrin deposit at the wound site is represented by a changing balance between different types of cells and process [22]. Simultaneously with haemostatic events begin the coagulation cascade that starts with the release of factors that activate the extrinsic and intrinsic pathway: platelets that occur firstly during this phase are recruited at the site of the wound where release growth factors

necessary for the recruitment of the cells of the immune system. At the same time platelet factors and thrombin co-ordinate the formation of a gel, the basis of the clot, mainly consisting of fibrin which will form the "scaffold" for cellular infiltration of the next stage.

The second stage turns up within 24-72 hours. This phase is divided in two parts, an early inflammatory phase and a late inflammatory phase [23]. In the early inflammation neutrophils invade the wound site in order to remove the bacteria or other molecules present in the site [23]. Neutrophils in this phase become sticky and begin to adhere to the endothelial cells in the post-capillary venules surrounding the wound [22-24]. Then, the neutrophils, move along the endothelium surface and begin to be pushed forward by the blood flow [25]. To complete the phase, the neutrophils must be eliminated from the wound, so the redundant cells are eliminated by extrusion or apoptosis, without creating damage to the wound or potentiating the inflammatory response [23,26]. The debris that remain in the wound site are later phagocytized from the macrophages. This part of the wound healing process represents the late inflammatory phase, while continuing the phagocytosis mechanism. The macrophages that participate in this phase are important cells that act as key regulatory cells providing abundant growth factors, that activate other cells like keratinocytes, fibroblasts and endothelial cells that are important for the starting of new vessels formation [26]. At the end of this phase also intervene the lymphocytes recalled by interleukin-1 (IL-1) playing and important role in the collagen remodelling, that is crucial for the following phase [25].

The third stage of the process takes place within 3-10 days from the injury and continues with the migration of different tissue-specific cell to the wound site. This phase is characterized by the migration of fibroblasts, new vessels formation (angiogenesis) and the synthesis of new extracellular matrix, that replace the deposit of fibrin and fibronectin leading to the formation of granulation tissue [25].

The fourth stage begins 2-3 weeks after lesion, when most of the endothelial cells, macrophages and myofibroblasts that have participated in the previous phases, undergo apoptosis, promoting the formation of a mass, composed mainly of collagen and proteins of the extracellular matrix [27] that will be remodelled in the next phase. This phase may last up to one year or two years, or sometimes even much longer periods [28,29].

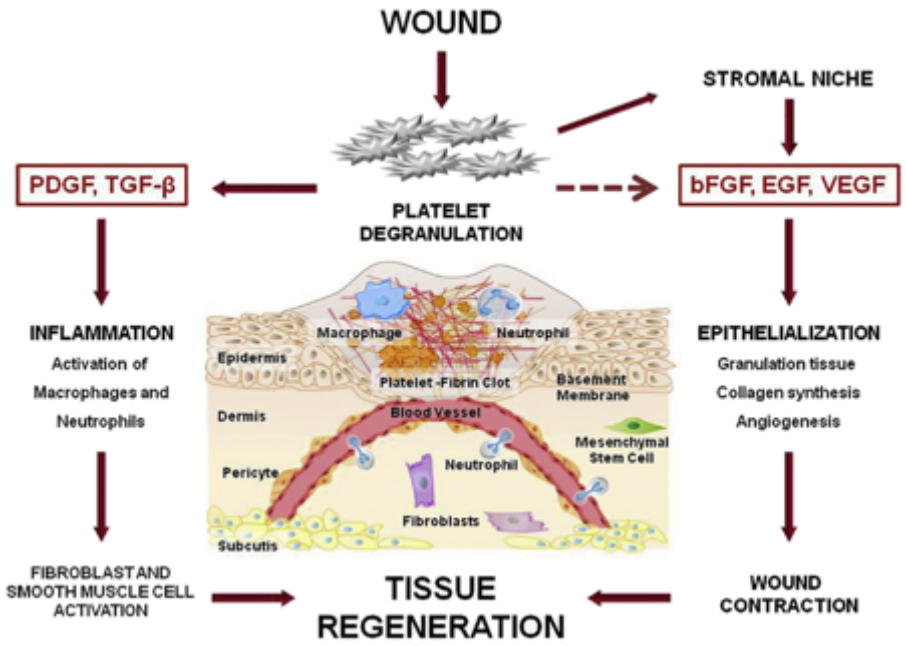

Figure 1: Phases of wound healing progress and the principal factors involved in the process.

The estimated costs for wound dressing in the next 5 years will grow by 4-7% a year [30], leading to an increasing interest in the development of new matrix or scaffold to regenerate the cutaneous tissue.

Recently, many experimental attempts have been done in the field of tissue engineering in order to develop medical devices (patches, membranes, etc.) to favour faster healing of the wound [14].

The ideal wound dressing should have different properties according to the wound requirements.

These wound dressing are divided into two main groups: the traditional one that played no active role during wound healing process and the nanotechnology-based wound dressing, that acts as a substrate to load different typologies of biological materials such as antibacterial, anti-inflammatory and drug/growth factor [31]. Recently wound dressing containing biological compounds like cells or growth factors have been developed as helpful new tool for skin regeneration.

For every thousand inhabitants there were 12 hospital admissions diagnosed with diabetes, of which 2 admissions had diabetes as the leading cause of hospitalization. Up to 25% of diabetic patients suffer from a foot ulcer during their lives, being the ulceration the major cause of infection and amputation. Approximately 50% of diabetic foot ulcers become infected, and 20% of these require amputation. In more than 85% of amputations of the lower limbs, the ulcer is a critical aspect of the disease in diabetic patients. The incidence of diabetes-related amputation is more than two times higher in men than in women, while it is similar among racial and ethnic groups. Approximately 50% of amputations involves the foot, while 50% are below or above the knee. In particular, in Italy, amputations among diabetic patients account for about 60% of all admissions for non-traumatic amputations (ISTAT data).

Although the conventional treatment of ulcer in diabetic patient, including the revascularization of the limb, leads to ulcer healing in 70% of the patients, within the first year after the surgery the 30% of them still need to undergo amputation (ISTAT data).

Diabetes is a serious burden on economic budgets of national health systems. The total estimated cost of diagnosed diabetes in 2010 has been 11.6 % of total expenditure worldwide, 10% in the European Countries and 9% in Italy.

In Europe it is estimated that approximately 1-3% of the population will suffer from chronic ulcers during their lifetime, and this percentage will increase as a result of the gradual elongation of life expectancy. The prevalence of skin ulcers in European hospitals range from 5% to 28% of patients admitted. Ulcers, in particular those related to the lower limbs, represent a very important clinical problem especially for diabetic patients. Approximately 50% of foot ulcers undergo recurrent infections that, in 20% of patients lead to amputation of the limb (ISTAT data).

Chronic injuries not only have a significant impact on public health, but also represent a large component of medical expenditures. In Italy, the cost of treating chronic lesions (decubitus wounds, diabetic ulcers and surgical injuries) reaches 1 billion euros per year, representing an important burden for the health system.

For these reasons, all health systems, both public and private, pay particular attention to new therapeutic strategies for the management of skin ulcers in order to improve patients' quality of life and reducing the costs of therapeutic treatments. However, clinical treatment of chronic ulcers remains a problem, especially in terms of complete wound healing process [14].

AIMS OF PhD

Based on our previous manuscripts [15,32], our long-term goal is the development of a new therapeutic approach to regenerate the cutaneous tissue by the use of platelet derivatives.
The Thesis is divided in three different chapters:

1. Platelet derivative effect on the proliferative stage of mesenchymal stem cells and cell lines, and MYC pathway activation;
2. Electrospun silk fibroin fibers for storage and controlled release of human platelet lysate. In collaboration with Dr. Atanassiou's group of Smart Materials, Nanophysics, IIT of Genoa;
3. Sericin, alginate and platelet lysate combined in a biomembrane for the treatment of skin ulcers. In collaboration with Dr. Torre's group of University of Pavia from the department of Drug Science.

1. PLATELET DERIVATIVES EFFECT ON THE PROLIFERATIVE STAGE OF MESENCHYMAL STEM CELLS AND CELL LINES AND MYC PATHWAY ACTIVATION.

ABSTRACT

The present paper is related to the field of cell culture medium supplements. In particular, it refers to (i) an heparin-free human Platelet Lysate devoid of serum or plasma components (v-PL) and (ii) an heparin-free human serum devoid of platelet lysate components (Pl-s), and to their use as single components or in combination in primary or cell line cultures.

Human Mesenchymal Stem Cells (MSC) primary cultures were obtained from adipose, bone-marrow and umbilical cord. The cumulative cell doubling number in the presence of the different culture medium supplements was determined at different culture times. In general, MSC expanded in the presence of Pl-s alone showed a low or no proliferation in comparison to cells grown with the combination of Pl-s and v-PL. Confluent, growth arrested cells, either human MSC or human articular chondrocytes, treated with v-PL resumed proliferation, whereas control cultures, not supplemented with v-PL, remained quiescent and did not proliferate. Interestingly, signal transduction pathways distinctive of proliferation were activated also in cells treated with v-PL in the absence of serum, when cell proliferation did not occur, indicating that v-PL could induce the cell re-entry in the cell cycle (cell commitment), but the presence of serum proteins was an indispensable requirement for cell proliferation to happen. Indeed, Pl-s alone supported cell growth in constitutively activated cell lines (U-937, HeLa, HaCaT, V-79) regardless the co-presence of v-PL. Plasma and plasma-derived serum were equally able to sustain cell proliferation although, for cells cultured in adhesion, the Pl-s was more efficient than the plasma from which it was derived. Moreover, cell expanded in the presence of the new additives maintained their differentiation potential and did not show alterations in their karyotype.

In a different work we showed how Platelet Lysate (PL) derived from Platelet Rich Plasma (PRP) was capable to support growth and isolation of MSC (Mesenchymal Stromal Cell). However, the molecular mechanisms involved in these processes were still unknown. We focused our attention on a family of highly conserved proteins involved in different cellular mechanisms such as cell growth, proliferation and apoptosis, MYC's family. In particular, MYC is a transcription factor that activates or inhibits the transcription of several genes by interacting with other proteins.

The three proteins of *C-MYC* gene have the same c-terminal part, differing in the N-terminal region due to an alternative translation at the start site. The three forms are C-MYC1, C-MYC2 and C-MYCS, differently expressed during cell growth.

INTRODUCTION

Platelet growth factors can support cell proliferation and differentiation and human platelet derivatives were proposed as tissue culture supplements alternative to Fetal Calf or Fetal Bovine Serum (FCS or FBS). The adoption of an animal–free culture medium is particularly relevant in establishing culture conditions for isolation and expansion of cells intended for clinical applications. Platelet derivatives used as cell culture medium supplements, are commonly provided in the form of platelet-lysate (PL) within a small amount of plasma.

Plasma is the physiological fluid of blood, while serum is the fluid remaining from plasma after fibrinogen, prothrombin, and other clotting factors have been removed. *In vivo*, cells are normally exposed to plasma and come in contact with serum only at the time of clot formation following an injury. Though, the use of plasma in cell culture presents some problems. Citrate, a calcium chelator, is the standard plasma anticoagulant used in the process of blood and plasma collection, but, fibrin clots may still form when plasma is added to culture media, which contain calcium [33]. This is often prevented by adding heparin to the platelet lysate [34]. However, heparins are active factors that bind growth factors and may interfere with cell growth [35–38]. Heparin negatively affected proliferation and motility of vascular smooth muscle cells [39,40] and inhibited growth of osteoblasts and Mesenchymal Stem Cells (MSC) under conventional culture conditions [41–43]. It was also shown that a relatively high concentration of heparin in culture media supplemented with human platelet lysate (PL) impaired adipogenic and osteogenic differentiation of MSC [44]. Others reports showed that heparin interfered with the functional capacity for migration and homing of bone marrow (BM)-derived mononuclear cells used in cardiovascular repair [45]. Moreover, commercially available heparin is manufactured primarily from porcine sources and, being of animal origin, it represents a limit in the development of a totally xeno-free medium. Although porcine heparin is approved for human use, there are examples of hypersensitivity to the molecule [46,47].

To overcome the need of heparin to prevent clotting after PL addition to the culture medium, different options, including the use of serum, were proposed. In principle a human serum could be obtained by letting fresh whole blood, collected without any anticoagulant, to clot several hours before high-speed centrifugation. Being deprived of coagulation factors, this serum, containing also platelet factors, can be added to the cell culture medium without that fibrin clots may form. However, this method yields only small aliquots of PL, suitable mainly for research use. In fact, this type of strategy does not allow the preparation of large batches of standardized, quality controlled PL starting from outdated blood donations. Indeed, an adopted approach is the production of a serum-converted PL from pooled Platelet Rich Plasma (PRP) derived from buffy coats, i.e. fractions of blood which are by-products of plasma preparations routinely performed in the Blood Banks. The plasma-coagulation step is performedd by the addition of calcium chloride and/or thrombin (in most cases of animal origin). However, by this procedure the relative concentration of factors before and after coagulation can vary. When the concentration levels of 100 soluble factors were measured in plasma and serum using a multiplexed ELISA assay, a comparison revealed that

concentrations of 2 factors were higher in plasma, whereas the concentrations of 18 factors, including 11 chemokines, were higher in serum [33]. Conflicting results exist in the literature with regard to the comparison of the biological activities of plasma and its derived serum. Mojica-Henshaw et al reported that PL-serum was less efficient than the sister counterpart PL-plasma in supporting MSC proliferation although both lysates supported the cell tri-lineage differentiation potential [48]. A beneficial effect of the fibrinogen depleted lysate was instead observed with regard to the immunosuppressive properties of MSC [49].

An additional possibility to avoid the use of heparin, is the production of a PL devoid of plasma through repeated cycles of platelet washing with a saline solution prior their rupture and release of bioactive factors. This PL sustained cell proliferation, comparable to FBS, in short term (1-7 days) cultures of renal epithelial cells, of either animal or human origin, in adhesion as well as of human lymphoblastoid cells in suspension [50]. The mitogenic effect induced by the PL addition was confirmed also by the activation of the ERK1/2 factors. However, the sustainability of long term cell expansion in the presence of PL obtained from washed platelets was not investigated and no experimental evidence was given in the published reports of a long term cell culture in the continuous presence of a plasma-free or serum-free PL as the only medium supplement.

As mentioned above, serum is usually obtained by allowing a whole blood specimen to clot prior to centrifugation. The first studies, using human serum obtained by conventional blood coagulation as cell culture supplement, showed the efficient isolation and expansion of bone marrow MSC that maintained their osteo-adipogenic differentiation potential (osteogenic differentiation was higher in autologous serum rather than in FBS) [51]. Furthermore, bone marrow derived MSC expanded in the presence of autologous human serum from whole blood presented a higher cell motility compared to the ones expanded in the presence of FCS [52]. Autologous serum was shown to be a suitable supplement also for the *in vitro* expansion of dental pulp stem cells without altering their multi-lineage differentiation ability [53]. In some cases, serum was also successfully derived by the clotting of umbilical cord whole blood. Human MSC from bone-marrow and umbilical cord, isolated and expanded in allogenic cord blood serum (CBS) displayed higher self-renewal and a delayed senescence compared to cells cultured in fetal bovine serum, [54]. Moreover MSC cultured in the presence of CBS showed an enhanced and accelerated osteogenic differentiation and a repressed adipogenic differentiation [55]. Off the clot AB serum is commercially available and was successfully used for isolation and expansion of cells, such as bone-marrow MSC and hematopoietic stem cells [56,57]. Human AB-serum was successfully used also for adipose MSC long-term culture [34]. Contradictory results however have been reported on the use of allogeneic human serum [58–61].

Alternatively, serum can be derived from blood plasma that has been treated with anticoagulants and from which blood cells, including red blood cells, white blood cells and platelets, were removed by centrifugation (Platelet Poor Plasma; PPP) or by plasma directly collected by apheresis. Also in this case, coagulation is obtained by addition of calcium cations and/or thrombin treatment. However, depending on the protocols to obtain the PPP, preparations may contain residual platelets.

These residual platelets are activated during the centrifugation steps and the coagulation process and undergo a degranulation of the alpha granules, resulting in the release of their growth factor content. Therefore, the level of platelet growth factors in the final serum may change depending on the presence of platelets in the source material and this may significantly change the biological effect of serum when used as supplement in a cell culture medium. Tanaka et al. described a more pronounced stimulation of proliferation of human articular chondrocytes when a serum derived from plasma including platelets was compared to a serum derived from a plasma depleted of platelets although no significant differences were observed on the cartilage matrix deposition by chondrocytes cultured under the different serum conditions [62]. Recently, a comparison was performed between two different plasma sources to obtain human serum, plasma removed from blood after 24 h from collection and plasma devoided of cryoprecipitate. Serum was obtained after coagulation in the presence of calcium ions. Both forms of plasma-derived serum were effective in sustaining fetal umbilical cord matrix derived MSC proliferation as the standard supplement bovine serum [63].

The different abilities of plasma and serum to modulate cell growth were already investigated already in the '70s. Initial studies indicated that cells did not proliferate in plasma containing medium, but they proliferated actively when they were exposed to serum [64]. However the initial comparison was made between platelet-free plasma and serum containing platelet mitogens. Indeed, the addition of platelets and calcium to platelet-free plasma increased the activity of the obtained plasma serum to the same level achieved with blood serum [65]. Also the tridimensional environment to which cells are exposed to is crucial in modulating cell behavior. Gospodarorowicz and Ill reported that bovine vascular smooth muscle cells in Petri dishes exposed to plasma proliferated poorly compared to when exposed to serum from whole blood, but, when the same cells were seeded on extracellular matrix (ECM) coated dishes, they proliferated equally well in the presence of either plasma or serum [66]. Since this pioneering work, taking advantage of different cell types, different substrates and different culture conditions, other authors have investigated the abilities of plasma and serum to promote cell growth [51,59,67]. Although published results are sometimes contradictory, some general conclusions can be made out of these publications: (i) platelet depleted plasma or serum derived from this plasma are poor cell growth inducers in cultures of primary cells [65,68,69]; (ii) serum allows a better adhesion of the cells to the substrate than plasma, unless a coating of the culture dishes by serum or extracellular matrix proteins is adopted.

Several years ago, Rutherford et al. reported that exposure of quiescent cells to whole blood serum or platelet-free plasma serum plus crude platelet factors preparations stimulated cell proliferation [70]. However, no accurate investigations were ever done to distinguish between the role played by factors and molecules released by platelets and the serum components. We report that, although factors and molecules released by platelets (PL in saline solution) were capable of activating the cell proliferation machinery (ERK and AKT phosphorylation, Cyclin D1 induction, etc.) and of recruiting quiescent, and even differentiated or senescent cells back in the cell cycle, the PL itself was unable to support cell proliferation unless the plasma or serum components were also present in the culture medium. Interesting, in cells that were constitutively stimulated, such as different cell

lines of human or animal origin, or in some cultures of cells derived from fetal tissues, the addition of PL to the culture medium was not an absolute requirement and cell proliferation could be obtained by the simple addition of PL-free serum.

To fill this gap, we studied the molecular mechanisms underlying the effects of PL on proliferation of the primary cell culture and cell lines we focused the study on molecular mechanisms that are at the base of this result. From previous works we know that stimulation with PL activated the phosphorylation of some genes involved in cells proliferation [71,72] like ERK, AKT and Cyclin D1. Given the critical role of *MYC* gene family in the cell proliferation, we evaluated the expression of *C-MYC* gene, in cell primary cultures derived from adult and fetal tissues and cell line. [73].

The human *C-MYC* is translated into three different isoforms that give rise to three corresponding protein products: C-MYC1, C-MYC2 and C-MYCS. The C-MYC protein plays a critical role in cellular proliferation, cell size, differentiation, stem cell self-renewal and apoptosis [74]. This gene encodes preferentially for the two major nuclear proteins that are found in the species ranging from *Xenopus* to human [75]. The most abundant protein is represented by C-MYC2, that initiates his translation in exon 2 from the first AUG codon, whereas C-MYC1, starts upstream in exon 1 at a non-AUG site. These two proteins were identified in 1984 [76], using antiserum prepared against a synthetic peptide corresponding to the C-terminus of human *C-MYC* sequence. They identified two protein of 64 and 67 kD as the major products of *C-MYC* gene. Hann et al. in 1988 [75] demonstrated that this two proteins are derived from alternative translational initiations in the same reading frame in exon 1 and 2.

In 1997 Spotts at al. [77] reported that human, murine, and avian cells express smaller C-MYC proteins in addition to the full-length C-MYC1 and 2 protein. These proteins, called C-MYCS, similarly to full-length protein appeared to be localized in the nucleus. The synthesis of these proteins, in contrast with C-MYC1 and 2, is transient during growth [77].

The three proteins have the same C-terminal part, differing in the N-terminal region [78] due to an alternative translation at the start site. These three forms are differently expressed during cell growth: the C-MYC2 protein, preferably expressed in proliferating cells [75]; the C-MYC1 form, which prevails in cells that break the growth due to the high density or lack of methionine [79,80]; the C-MYCS form, present in vertebrate cells, is transiently present [77] and less abundant.

In PL culture condition the C-MYC1 isoform appeared to be modulated respect to the standard, showing an increment, contrary to what is shown in the literature, in which C-MYC1 is expressed only under conditions of cellular stress. In this regard we evaluated the activation of this isoform in critical culture condition in presence and absence of PL. Cells stimulated with PL showed expression of C-MYC1 in a proliferative step also when they were cultured at low confluence and at high methionine concentration in the medium, condition in which C-MYC1 should not be activated.

MATERIALS AND METHODS

Production of virgin-Platelet Lysate (v-PL) and Plasma-serum (Pl-s)

An outline of the manufacturing process is reported in Figure 1. All separation steps were performed within a sterile closed system. The high-speed centrifugation of a whole blood unit separates different phases: the plasma at the top, the buffy coat (BC) layer (enriched in platelets and leukocytes) at the interface and the red blood cells fraction at the bottom. For the preparation of the virgin-Platelet Lysate (v-PL), pools of BC units (not usable for transfusion purposes; up to 300 total units) were centrifuged at low speed. The Platelet Rich Plasma (PRP) was recovered from the upper part of the blood bag and high-speed centrifuged to separate an upper phase, the Platelet Poor Plasma (PPP) and a lower phase, the platelet concentrate. Recovered platelets were subjected to three washes in sterile saline solution. After the third wash, the platelet concentrate was suspended in saline solution and the platelet concentration adjusted to 10 $x10^6$ plt/μL. The platelet concentrate underwent three freeze-thaw cycles. A high-speed centrifugation was then performed to sediment platelet membranes and debris. The different obtained supernatants, the plasma-free Platelet Lysates (v-PL) were combined in a single pool before being divided into aliquots and lyophilized.

The Plasma-serum (Pl-s) was obtained from several frozen plasma units. Each plasma unit was slowly thawed at 4°C to separate the cryoprecipitate and the cryo-poor plasma (CPP). The CPP was added of calcium chloride (2 mg/ml) and then subjected to a coagulation step at 37°C up to 6 hours. After the coagulation step, the blood bag was high-speed centrifuged to separate the coagulum. The liquid phase, the Plasma-serum (Pl-s), was recovered, and the pool of several units was divided into aliquots and lyophilized.

Cell culture

Adult mesenchymal stem cells

Human bone marrow stromal cells (BMSC or BM-MSC) were obtained from discarded adult femoral heads of patients undergoing orthopaedic surgery for hip prosthesis, with the approval of the Institutional Ethic Commitee of San Martino Hospital (Genoa, Italy). The bone marrow was washed 5 times with PBS 1X. The obtained liquid was centrifuged at 1500 rpm for 10 minutes at room temperature (RT). The supernatant was discarded while the pellet was recovered and re-suspended in a quantity of α-MEM (Lonza, Belgium) so that it had an adequate cell count (50-100 nucleated cells per square in Burker's chamber). Counting was carried out using a nuclear dye (0.1% methyl violet in 0.1M citric acid). After counting, the cells were plated at a consonant density. The only cells that will be able to adhere to the plate will be those of our interest (BMSC). The cells were cultivated in α-MEM.

Human adipose tissue cells (ADAS or AD-MSC) were obtained by treating lipoaspirate samples derived from discarded liposuction performed in adult patients with the approval of the Institutional Ethic Commitee of San Martino Hospital (Genoa, Italy). The sample was washed 4-5 times with

PBS 1X and subsequently digested with an enzymatic solution (type I collagenase 0.1% in PBS 1X) at 37 °C for 1 hour vigorously agitating every 15 minutes to facilitate digestion.
The sample was then centrifuged twice at 1200 rpm for 5 min at RT, re-suspending the pellet between both centrifugations. After centrifugation, three different phases were obtained: the supper and the intermediate, containing fat cells and the enzymatic aquous solution, respectively, were discarded. The stromal vascular fraction (SVF) containing mesenchymal stromal cells was re-suspended in 5 mL of α-MEM supplemented with 10% FBS in order to inhibit the activity of any remaining enzyme activity. The resulting solution was again centrifuged under the same conditions and the new pellet formed was re-suspended in in basic medium to remove the remaining traces of FBS. After a subsequent centrifuge under the same conditions as described above, the pellet obtained was re-suspended in a volume of medium corresponding to the initial volume of lipoaspirate. The sample was cultivated into flasks in α-MEM.

Fetal stem cells

Human amniotic fluids stem cells (AFS) were obtained from discarded samples of amniocentesis performed at the Cytogenetic Laboratory of Galliera Hospital (Genoa, Italy) for fetal karyotyping, between 15 and 17 weeks of gestation with the approval of Ethical Commitee of Galliera Hospital (in collaboration with Dr. C. Gentili). Primary cells were isolated from amniotic fluid by centrifugation and suspended in Chang Medium. After 5-6 days, non-adherent cells and debris were discarded and adherent cells were c-Kit selected by magnetic cell sorting on a Mini-MACS apparatus. AFSC were then expanded in α-MEM.

Umbilical Cord derived MSC (UC-MSC) were kindly provided by Dr. M. Introna (AO Papa Giovanni XXIII USS Center of Cell Therapy 'G. Lanzani' USC Hematology, Bergamo, Italy). Cells were isolated from cord blood tissue collected from pregnant women after either normal vaginal delivery or cesarean sections. The UC processing was performed in accordance with the protocol for the isolation and expansion of UC-MSC as previously described [81]. The cells were cultivated in α-MEM.

Other cell types

Human bone samples (hOB) were obtained from discarded trabecular bone of adult patients undergoing orthopaedic surgery with the approval of Ethical Committee of San Martino Hospital (Genoa, Italy). The bone sample was cleaned of adherent soft tissue and cut into small pieces, washed in Ringer solution and digested at 37 °C by consecutive treatment with 1 mg/mL trypsin for 10 min; 2 mg/mL dispase for 20 min; 3 mg/mL collagenase type II, for 30 min repeated twice. The products derived from the first two digestions were discarded, whereas cells released by the collagenase digestions were collected by centrifugation, washed, plated and cultured with Iscove.

Human articular cartilage (hAC) was obtained from discarded biopsies from adult patients undergoing orthopaedic surgery withg to the approval of Ethical Committee of San Martino Hospital (Genoa, Italy). The cartilage sample was cut into small fragments, washed several times with PBS and centrifuged at 1500 rpm for 10 min at RT. The supernatant was discarded and replaced with an enzymatic solution made of 0.25% trypsin, 400 U/mL collagenase type I, 1000 U/mL collagenase type II and 1 mg/mL hyaluronidase at 37 °C for 1 h. The supernatant derived from the first enzymatic digestion was discarded and the enzymatic digestion steps were repeated until the all biopsy material was digested. For each cycle of digestion after the first one, the supernatant was collected and the enzymatic activity blocked with Coon's modified Ham's F-12 medium containing 10% FBS. Isolated chondrocytes were then washed with basal medium to remove any residual of FBS and then cultured in Coon's modified Ham's F-12 medium. In some experiments, dedifferentiated chondrocytes were transferred to suspension culture in the presence of ascorbic acid to allow the formation of a cartilage-like tissue [82].

Cell lines

HeLa cells (human cervical adenocarcinoma) were purchased from Interlab Cell Line Collection of the Biological Bank and Cell Factory of the Ospedale Policlinico San Martino (Genoa, Italy). They were thawed and plated in Petri plates. Cells were expanded in D-MEM High Glucose (Euroclone, Italy).

U-937 cell line (human histiocytic lymphoma) was purchased from the Interlab Cell Line Collection of the Biological Bank and Cell Factory of the Ospedale Policlinico San Martino (Genoa, Italy). They were thawed and plated in Petri plates. Cells were expanded in RPMI (Euroclone, Italy).

HaCaT cell line (human immortalized keratinocytes) was kindly provided by Dr. G. Pellegrini (Centro di Medicina Rigenerativa "Stefano Ferrari" Modena, Italy). They were thawed and plated in Petri plates. Cells were expanded in DMEM (Euroclone, Italy).

V-79 cells (lung of Chinese hamster) were purchased from the Interlab Cell Line Collection of the Biological Bank and Cell Factory of the Ospedale Policlinico San Martino (Genoa, Italy). They were thawed and plated in Petri plates. Cells were expanded in MEM (EBSS).

In all culture conditions, the basal medium was supplemented with 100 IU/mL penicillin and 100 μg/ml streptomycin, 2 mM L-glutamine and, when indicated, with Pl-s and v-PL used alone or in different combinations or with 5% PL (indicated as PL). In some control experiments, medium was supplemented with 10% Fetal Calf Serum (FCS, Invitrogen, USA) as control of standard culture condition of mesenchymal stem cells, with, in some cases, the addition of FGF-2 growth factor. Cells were detached from the culture dish with 0.05% trypsin and 0.01% EDTA (Euroclone, Italy).

Trypsin activity was neutralized with a trypsin soybean inhibitor solution (0.5 mg/ml in PBS; GIBCO, USA).

BMSC, ADAS, AFS, hOB, hAC and HeLa cells were used also for MYC pathway analyses, after reaching confluence, were detached, counted and plated at a density of 70000 cells for a 60 mm Ø Petri dishes, while HeLa cells were seeded at a density of 30000 cells per 60 mm Ø Petri dishes.

Cell proliferation assays

Long-term cell proliferation assay – Cumulative doubling number calculation

For determining the number of doublings of BM-MSC, AD-MSC and UC-MSC in a long term culture, after the initial selection of the cells (passage 0) in FCS supplemented medium, cells at 70-80% confluence were detached with trypsin/EDTA solution and replated at the density of 7 x 10^4 cells for UC-MSC and 1 x 10^5 cells for all the other cell types, in 60 mm Ø Petri dishes, in duplicate with medium supplemented with 10% Pl-s or 10% Pl-s + 5% v-PL or 10% Pl-s + 1% v-PL. Number of doublings were calculated by counting the number of cells at each passage until the end of the culture.

The human cell lines U-937 (pro-monocytic cells growing in suspension), HeLa (epithelial cells with adhesion growth), HaCaT (keratinocytes with adhesion growth) and the animal cell line V79 (hamster lung fibroblasts, also growing as adherent cells) were cultured with the same supplements used for the primary cell cultures. To monitor cell proliferation, the cumulative number of doublings performed at different culture times was determined. At each passage, cells were plated at the following densities: U-937, 2 x 10^5 cells/mL in T25 flask; HeLa, 2,5 x 10^5 cells/60 mm Ø plate; HaCaT, 2,5 x 10 cells/plate 60 mm Ø; V79, 4 x 10cells/ 60 mm Ø plate.

Unless differently stated, results were expressed as the average of at least three independent experiments.

Short-term cell proliferation assay

For determining cell proliferation rate during a short time period, BM-MSC, HeLa and U-937 chosen as representative of primary cell cultures and cell lines growing in adhesion and in suspension respectively were plated for BM-MSC at 5 x 10^4 cells in 6 multi-well plates and for Hela, at 1 x 10^5 cells/60 mm Ø plate. U-937 were seeded at 1 x 10^5 cells/ml in T25 flask. The number of cells was determined at different time intervals during a week. Results were expressed as the average of at least two independent experiments.

Cell proliferation assay for articular chondrocytes - Crystal violet staining

Cells were seeded in 96 multi-well plates and cultured in the presence of different medium supplements as indicated. At different times of the culture, after extensive washing with PBS, cells were stained with 50 µl staining solution [0.75% (g/ml) crystal violet (Sigma-Aldrich, USA), 0.35% (g/ml) NaCl, 32.3% (v/v) absolute ethanol and 8.64% (v/v) formaldehyde 37%] for 20 minutes at

RT. Cells were then washed 5 times with water and dried by exposing the plate to air under a chemical hood. To each well 100 µL eluent solution [50% (v/v) absolute ethanol and 1% (v/v) acetic acid] were added and the absorbance at 595 nm measured within 10-30 minutes with a spectrophotometer AD 200 (Beckman Coulter, USA). For each experimental condition quintuplicate assays were performed. Results were expressed as the average of at least three independent experiments.

Cell differentiation assays

Osteogenic differentiation

Confluent BM-MSC and AD-MSC were cultured in osteogenic differentiation medium containing 10% Pl-s, 50 µg/ml ascorbic acid, 10 mM ß-glycerophosphate and 10−7 M dexamethasone (all from Sigma Aldrich). Negative control cultures were maintained in medium containing 10% Pl-s. The medium was changed three times weekly and osteogenic stimulation took place for 3 weeks. Alizarin red S staining was performed at the end of the induction period.

Chondrogenic differentiation

Dedifferentiated chondrocytes were transferred in suspension culture in 15 ml Falcon tubes to prevent cell attachment, but still ensuring cell-cell interactions, and in the presence of 100 µg/ml ascorbic acid (Sigma Aldrich, USA) to allow the organization of a cartilage matrix and the formation of a cartilage-like tissue. Cell aggregates were washed 3 times with PBS, fixed with 3.7% paraformaldehyde (PFA) for 20 minutes at 40 °C and embedded in paraffin. Paraffin embedded samples were sectioned in slices of 5-6 µm thickness. Slices were adhered on Superfrost Ultra Plus Slides (Thermo Scientific, Germany) coated with poly-L-lysine (Sigma Aldrich, USA), dewaxed to remove paraffin and processed for immunohistochemistry.

Sections were permeabilized with 0.2% Triton in PBS for 10 minutes, treated with 4% H_2O_2 for 30 minutes at room temperature (RT) to inhibit endogenous peroxidase activity, rinsed with PBS 3 times x 5 minutes, incubated with hyaluronidase type II (Sigma Aldrich, USA) at concentration of 1 mg/ml in PBS (pH 6) for 30 minutes at 37 °C and washed with PBS. After incubation with 10% normal goat serum in PBS for 1 hour at RT to inhibit nonspecific binding, the sections were incubated at 40 C for 16 hours with primary antibodies against α-collagen type II (1:100; CIIC1-Developmental Studies Hybridoma Bank, University of Iowa), washed 3 times with PBS and incubated for 1 hour at RT with Labeled polymer HRP anti-mouse (Dako, Denmark). Sections were stained with *3,3'-Diaminobenzidine* (DAB, Enzo Life Sciences, USA) for 3-5 minutes, counter-stained with Mayer's hematoxylin for 2 seconds, submersed in 0,1% $NaHCO_3$ for 1 minute, and finally mounted with Eukitt (O. Kindler GmbH, Germany). Images were acquired by a microscope Axiovert 200M (Carl Zeiss, Germany).

Molecular analysis

Protein extraction

For western blot (WB) analysis, the cells used for the C-MYC analysis were exposed to cell lysis that was performed on cells that have reached 80% of their confluence, to avoid detachment during collection process.

The plates were placed on ice during the whole process. The medium was removed from the cells and then they were washed with cold PBS 1X. A lysis buffer (500 µL per 60 mm Ø plate) was added to each plate. Concurrently to the lysis buffer, phosphatases and proteases inhibitors (PhoStop and Complites) were added to avoid the protein degradation.

The lysis buffer was allowed to act for 5 minutes, always keeping the plate on ice. Then, the cells were dislodged from the bottom of the plate and collected all within a 1.5 mL eppendorf. The eppendorf was placed on ice for 40 minutes and was vortexed every 10 minutes. At the end of the incubation the samples were centrifuged at 4 °C for 20 minutes at 13000 rpm. The resulting cell pellet was discarded while the supernatant containing the proteins was aliquoted for protein analysis by WB.

Cells, whose lysates were subjected to WB, were treated in several ways. Some cells were directly isolated in presence of platelet derivatives used at the appropriate percentage depending on cell type. Other cells were plated in the 10% FBS condition. Some of the plates in the 10% FBS condition, after reaching 60% confluence, were switched to platelet derivatives at the appropriate percentage, collected at 5 minutes, 30 minutes, 1 hour and 24 hours, and processed as described above.

Methionine stimulation

HeLa cells were, for preliminary experiments, stimulated with lower doses of methionine (30,60, or 90 mg/L) and for subsequent experiments with a solution of methionine 5-10 mM. Cells were plated in 60 Ø mm Petri dishes (two plates for each condition). Methionine was added at several concentrations to the supplemented base medium (10% FBS or 5% platelet derivatives). All conditions were monitored during proliferation by microscopic acquisition. When sub-confluence was reached, the cells were collected and lysed as described above.

Western blot analysis

Confluent dedifferentiated chondrocytes were supplemented with 5% v-PL either in presence or absence of bovine serum. At different times after the addition of the supplement, cells were washed with phosphate buffered saline (PBS) and collected for western blot analysis.

The protein content of cell lysate, was determined by Bradford assay and after quantification WB analyses were performed.

Electrophoresis was performed in reducing conditions using 20-70 µg of protein loaded on a 4-12% NuPAGE Bis-Tris gel (Invitrogen, USA) and proteins were transferred to a AmershamTM ProtranTM 0.45 µm NC nitrocellulose blotting membrane. The blot was saturated with 5%

skimmed cow milk in TTBS (20 mM Tris HCl pH 7.5, 500 mM NaCl, 0.1% Tween 20) for 2h at RT and washed several times with TTBS and and then incubated in a cold room overnight with antibodies specific for pERK (1:1000, Cell Signaling), ERK (1:1000, Cell Signaling) pAKT (1:500, Cell Signaling), AKT (1:1000, Cell Signaling), Cyclin D1 (1:250, Santa-Cruz Biotechnology) and Actin (1:500, Santa-Cruz Biotechnology). For C-MYC analyses membranes was also incubated with specific antibody against C-MYC (1:1000, DSHB). After incubation, with the primary antibody, the membrane was washed with TTBS at RT for 1h and incubated with 1:5000 Mouse/Rabbit specific HRP-conjugated secondary antibody. The bands of WB were detected with enhanced chemiluminescent (ECL) and exposed to an X-ray film (GE Healthcare).
Images were scanned using the Epson perfection 1260 scanner (Epson, Italy) and band densities were quantified using the ImageJ software (NIH, USA, http://rsbweb.nih.gov/ij/download.html). Western blots were performed on three different independent primary cultures.

Karyotype analysis

Forty thousand BM-MSC expanded in medium containing 10% Pl-s + 1% v-PL were plated in slide flasks (Thermo Fisher Scientific, Denmark) and cultured at 37°C in 5% CO2 atmosphere. After 1-2 days the medium was replaced with 2,5 mL of fresh medium containing Colcemid solution (6μg/mL; Sigma Aldrich, USA) and incubation continued. After 2 hours of incubation, the medium was removed and replaced with 5 mL of hypotonic solution [tri-Sodium citrate dehydrate 17 mM/potassium chloride 75 mM (1:1) solution] followed by an incubation of 10 minutes. Then, that 0,5 mL of fixative ethanol/acetic acid (3:1) solution were added to the flask for 10 minutes at RT. The solution was then removed and replaced by 2,5 mL of fresh fixative followed by an incubation of 15 min (repeated three times).
Chromosome staining was performed by Q-banding technique (Quinacrine stain, DBA Italia, Italy). Each slide was examined and photographed under a fluorescence microscope (Olympus) using software MACTYPE 5.4.1 (Apple). A minimum of 10 metaphases for each sample were captured and analysed.

Growth factors quantification

The platelet growth factors were quantified by an ELISA assay on Pl-s and v-PL. The adopted kits were from RayBiotech (USA) for PDGF-BB and from Invitrogen (USA) for VEGF respectively. The assays were performed according to the manufacturer directives.

Immunofluorescence analysis

Cells were grown on 1 cm Ø sterile slides placed on the bottom of a 24-well plate. The cells were fixed with paraformaldehyde (PFA) 3.7% at RT for 10 minutes. All subsequent steps were carried out on ice as well as all the solutions and reagents used. Once the cells were fixed, they were washed with PBS and treated with a permeabilizing solution (HEPES 20 mM, NaCl 50 mM, Triton x-100 0.5%, $MgCl_2$ 3 mM and saccarose 300 mM) for 5 minutes. Then the slides were washed with

PBS for 5 minutes and treated with 20% normal goat serum in PBS 1X for at least 30 minutes. After blocking, cells were incubated with primary antibody against Ki67 (1:4000, Oncogene) for 2 hours at 4 °C. Subsequently, hybridization was performed with specific fluorescent secondary antibody (mouse 1:800). Prior to final assembly, the slides were incubated with HOECHST (1:5000), a fluorescent blue dye used to mark the DNA and then highlighting the nuclei of cells. Slides were mounted on object-mounted slides with an aqueous mounting and subsequently analyzed at different magnifications, using a fluorescence microscope.

Apoptosis assay

The apoptosis assay was performed using Vybrant® Apoptosis Assay Kit (Molecular Probes) with sligh modification. We induced apoptosis in control cells, putting them at 96 °C for 10 minutes. All the cells (control and other cells), were centrifuged, and the supernatant was discarded, and each pellet was re-suspended in 1X annexin-binding buffer (provided by the kit) at a concentration of $1*10^6$ cells/mL. We added 5 μL of Annexin-APC (BD), 1 μL of the 50 uM C_{12}-resazurin working solution and 1 μL of 1 mM Sytox Blue stain working solution to each 100 μL of cell suspension. We incubated the cells at 37 °C in an atmosphere of 5% CO_2 for 15 minutes. After the incubation period, we added 400 μL of 1X annexin-binding buffer, and we kept them on ice.

We analysed the stained cells by flow cytometry, measuring the fluorescence emission at 530 nm, 575 nm and 660 nm.

Statistical analysis

All the experiments, when it was possible, were conducted in triplicate on different primary cell cultures. Statistical analyses were performed using Student's *t*-test to compare two groups or two-way ANOVA to assess statistical differences among several groups, provided by the Graphpad Software (www.graphpad.com).

RESULTS

CELL PROLIFERATION

Growth factors quantification in the v-PL and the Pl-s

v-PL and Pl-s were produced according to the protocol described in Materials and Methods and outlined in Figure 1. An ELISA assay was performed for the quantification in the two culture medium supplements of PDGF-BB and VEGF as representative indicators of platelet factors present in a relatively high and relatively low concentration respectively (Table I).

Stimulation of cell proliferation by v-PL: primary cell cultures vs cell lines

Primary cultures of cells derived from adult tissues, AD-MSC (from adipose) and BM-MSC (from bone-marrow) or from a fetal tissue, UC-MSC (from umbilical cord) were initially isolated and expanded in 10% FCS (passage 0). At the time of the first passage the culture medium was replaced with medium supplemented with Pl-s and v-PL in different relative ratios (10% Pl-s or 10% Pl-s + 1% v-Pl or 10% Pl-s + 5% v-PL) and the cultures continued by passaging the cells before they reached confluency for about 30 days. By the evaluation of the cumulative number of population doublings performed in the different culture conditions, the following conclusions were inferred: (i) In general, cells cultured with Pl-s alone showed a low or no proliferation rate in comparison to cells grown with the combination of Pl-s and v-PL; (ii) In particular, BM-MSC essentially did not proliferate in the presence of Pl-s alone (about 2 cell doublings in 30 days) whereas underwent 10.5 and 17 cell doublings in 10% Pl-s + 1% v-PL and 10% Pl-s + 5% v-PL culture medium respectively; (iii) whereas AD-MSC and UC-MSC performed about 10 doublings in 10% Pl-s and about 25 and 20 doublings in the presence of Pl-s and v-PL respectively; (iv) For both AD-MSC and UC-MSC no major differences were observed between the condition 10% Pl-s + 1% v-PL and 10% Pl-s + 5% v-PL (Figure 2).

The same culture medium supplements, used in the same combinations as for the primary cell cultures, were tested with human, U937, HeLa, HaCaT and animal V-79 cell lines. Also in this case the cell proliferation was monitored by determining the number of cell doublings at different culture times. v-PL was not required to support cell proliferation. Indeed, Pl-s alone was able to support human cell growth in a manner comparable to the different combinations of Pl-s and v-PL both for suspension (U-937) and adhesion (HeLa and HaCaT) cultures. Moreover, the human additives sustained survival and proliferation of animal derived cells (V-79, growing in adhesion) comparably to human cells (Figure 3).

v-PL promotes re-entry in the cell cycle of confluent resting cells

Confluent growth-arrested dedifferentiated human articular chondrocytes were maintained in the original culture medium supplemented with 10% FCS or additionally supplemented with 5% v-PL. A crystal violet proliferation assay was performed in parallel on both cultures (Figure 4 upper

panel). Confluent cells treated with v-PL resumed proliferation, whereas the control culture maintained in FCS only remained quiescent and did not proliferate.
A western blot analysis of proteins extracted from control cells and cells treated with 5% v-PL for different times (1, 4, and 8 hours) was performed using α- cyclin D1, α- phospho Akt, α- phospho Erk1/2 antibodies. Actin was blotted as an internal control. After 1 hour from the v-PL treatment, we observed an increase in the amount of phospho Akt and phospho Erk1/2 (Extracellular signal-regulated protein kinases 1 and 2). After 8 hours the activation of these proteins was almost completely over. Instead at the same time an expression of the Cyclin D1 protein reached its maximum. Interestingly, the western blot analysis also showed that these proliferation pathways were activated by PL not only in cells resuming proliferation, but also in cells treated with v-PL in the absence of serum (Figure 4 bottom panel).
This confirmed and expanded our previous observation that confluent quiescent osteoblasts [72] that did not proliferate when maintained in serum, once exposed to the PL mitogenic stimulus were able to activate signal transduction pathways that promoted cell growth in response to the extracellular signals.

v-PL can rejuvenate a culture of senescent MSC

The positive effect of v-PL on resting cells was confirmed on a primary culture of BM-MSC (Figure 5). Cells, isolated and expanded in 10% FCS for about 10 population doublings, were split and transferred to different culture conditions: (i) 1% v-PL; (ii) 10% Pl-s; (iii) 10% Pl-s + 1% v-PL. Both the 1% v-PL only and the 10% Pl-s only culture conditions were not permissive for the cell growth and did not support cell proliferation. However, the combination of the two supplements allowed a good proliferation rate. After about 7 doublings, to half of the growing cells the v-PL was removed, leaving the cells in 10% Pl-s only. The cells maintained in 10% Pl-s + 1% v-PL remained fully viable and continued to grow up to about 25 duplications. On the contrary, in the half culture where the mitogenic stimulus of v-PL was removed, the cells, after a period of adaptation to the new condition, stopped growing and entered a senescent status. At this point, half of this culture was maintained in 10% Pl-s only, whereas the other half was transferred again to 10% Pl-s + 1% v-PL (restoring in this way the mitogenic stimulus of the v-PL). When v-PL was provided, senescent MSC resumed proliferation (Figure 5).

Pl-s versus plasma

A comparison of the efficacy of Pl-s and plasma in sustaining cell proliferation was performed taking advantage of primary cultures of BM-MSC and different cell lines growing either in adhesion (HeLa) or in suspension (U-937) (Figure 6). Plasma and plasma-derived serum were equally able to sustain cell proliferation. However, especially for BM-MSC and HeLa, both cell types growing in adhesion, the Pl-s was slightly more efficient than the plasma from which it was derived.

Population doublings of cells cultured with the new supplements versus FCS

AD-MSC were initially isolated and expanded in a medium containing either the standard animal-based 10% FCS or 10% Pl-s + 1% v-PL (Figure 7). Cultures were monitored for about 30 days and the population doublings were calculated. Cells grown with 10% FCS performed a significant lower number of doublings in comparison to the parallel culture maintained in 10% Pl-s + 1%v-PL (6 vs 22 doublings respectively).

Differentiation potential of cells cultured with the new supplements

Maintenance of the differentiation potential by the cells expanded in the presence of the new medium supplements was confirmed. Specific *in vitro* assays routinely performed in the lab were adopted. In particular, osteogenic differentiation was tested for BM-MSC and AD-MSC and chondrogenic differentiation for dedifferentiated articular chondrocytes. Representative images of the Alizarin Red S staining of MSC and of the type II collagen immunolocalization in the chondrocyte culture are presented in Figure 8. In the stimulated culture condition, it is clearly evident a calcium enriched matrix and a type II collagen positivity for the MSC and the chondrocytes respectively.

Karyotype stability of cells cultured with the new supplements

Cytogenetic analysis was performed on passage 2 of 3 cultures of BM-MSC in 10% Pl-s + 1% v-PL, in order to obtain information on the genetic stability of the cells grown in this condition. One of the cultures was also analyzed after a more extensive expansion in the presence of the new supplement (passage 7). The genetic stability was confirmed in all cultures (Figure 9 and Table II).

MYC MOLECULAR ANALYSIS

Evaluation of protein pathway involved in cell cycle

The cell systems on which this project is intended to work are all the primary cell cultures derived from discarded adult or fetal tissues, according to the guide lines of the Ethical Commitee of San Martino Hospital: BMSC or BM-MSC (Bone Marrow Stromal Cell), AD-MSC or ADAS (Adipose Derived Mesenchymal Stromal Cells), hOB (human Osteo Blast) hAC (human Articular Chondrocyte) hAFS (human Amniotic Fluid Stem cells). Regarding the cell line, we have tested the effect of PL on several cell types and obtained reproducible results among all of them, therefore, for the next experiments we decided to work only on HeLa cells (human cervical cancer cells). In these experiments all cells were treated with 10% FBS and 5% PL from isolation FBS as control condition or expanded in FBS and subsequently treated at different times with PL.

We investigated the different gene expression on MSCs undergoing the two treatments (control/stimulated). In agreement with one of our previous our manuscripts [72], we showed that phosphorylation of ERK and AKT protein was influenced by PL stimulation. The ERK protein in its phosphorylated form, is involved in various processes such as cell adhesion, mitosis, meiosis and

post-mitotic functions. AKT protein is also involved in various processes such as glucose metabolism, apoptosis, cell proliferation, transcription, and cell migration. (Figure 10)

At the same time, we evaluated the protein produced by the *C-MYC* gene encoding for a transcription factor also involved in different cellular processes such as growth, differentiation and apoptosis [49-52].We focused on this gene because preliminary analysis by western-blot on BMSC and AD-MSC cells showed the presence of a double band in PL treated samples at both short and prolonged time of treatments (Figure 11) when blots were incubated with an antibody against C-MYC protein. As suggested by the available literature, these two bands do not correspond to an unspecific recognition by antibody used, but reflect the existence of two isoforms of the same protein.

The lower band, equally present in all samples, represents the most well-studied C-MYC2 protein, while the upper band, which is only apparent in samples treated with PL, even for very short times, corresponds to the protein (which differs from only 3 kD) C-MYC1 [75]. This result was evident also in all other primary cell types analysed as showed in Figure 12.
In hOB cell culture we analysed the expression of C-MYC1 in low and high cell confluence to evaluate the C-MYC modulation as reported in literature [79]. As reported in figure 12c three different culture conditions (isolated in FBS or PL; isolated in FBS and stimulated with PL for 30 minute), at low (20%) and high (90%) confluences were tested. The data showed that only cells isolated or stimulated with PL expressed the C-MYC1 protein independently from the confluence reached.

It has been shown that C-MYC1 protein is expressed not only in cells that stop growth due to the contact inhibition arising from confluence, but also in cells subjected to lack of the essential amino acid methionine [79]. Our proliferation experiments showed that all primary cultures treated with PL are able to proliferate even for prolonged periods, without stopping their growth [4], as showed. by immunofluorescence for Ki67, a proliferation marker. Stimulation with PL for 24 hours showed expression of Ki67 (red spots in nuclei) as reported in Figure 13. This protein is a nuclear protein present in cells that are in interphase, but absent in the G0 phase of the cell cycle, which suggest that cells treated with PL are proliferating cells. So, cells expressing the C-MYC1 isoform, and therefore considered quiescent cells, were activated by PL treatment.

Again to understand the role of C-MYC1 in the proliferation under PL conditions, by Vybrant® Apoptosis Assay Kit we evaluated if our cells, when treated with platelet derivatives, were apoptotic cells. We applied this analysis on BMSC and ADAS cells, in the same condition described above.
With this analysis we find that our cells, when treated with platelet derivatives, did not show an apoptotic profile, respect to the cells isolated in platelet derivatives and treated for 24 hours with FBS that are alive but show a low percentage of cells that are late apoptotic cells. For all the

treatment the cells appeared alive at the flow cytometry analysis showing a statistical difference from the death cells (Figure 14).
Verified that PL treated cells, expressing the C-MYC1 isoform, did not show a proliferation stoppage due to reach of confluence, we went to search in literature what other causes were associated with the expression of the C-MYC1 isoform.

C-MYC1 expression and the possible lack of methionine

In literature was reported that this protein isoform is expressed from cells cultured in medium deprived of the essential amino acid methionine [79], a typical condition found in high confluence status. To understand the effect of PL in this condition, we evaluated the C-MYC1 expression in presence and absence of PL. The results reported in Figure 15, showed that the HeLa cells have also an increase in the C-MYC1 isoform after stimulation with PL, although apparently less marked than in primary cell cultures. We attribute these results to the weaker response of the cell lines to the treatment with PL respect to primary cell cultures [4]. Given the greater availability of HeLa cells, we used this cell line to test if the lack of methionine in culture medium could be responsible for the expression of the C-MYC1 isoform. This was evaluated in presence and absence of PL in an increasing gradual concentration of methionine in the medium (30-120 mg/L). As shown in Figure 16a, the different concentrations of methionine, in the medium, did not lead to a change in the expression of protein isoforms compared to PL alone in the medium (30 mg/L). Increasing methionine concentration up to 5mM and 10mM, the limit of tolerance by the cells, any effect was evident (Figure 16b).

DISCUSSION

Most of the studies done so far with *in vitro*–expanded human MSC for therapeutic purposes used, as the main cell culture medium supplement was the fetal bovine serum (FBS or FCS). However, in this case, the use of FBS or FCS as medium supplements is undesirable because of the risk of transmitting animal viruses, prion diseases, including the bovine spongiform encephalopathy (BSE) in cows, and proteins that may trigger a xenogeneic immune response. The use of a human autologous serum avoids the zoonotic infection risk, but generation of autologous serum has significant limitations from a manufacturing, regulatory, and quality assurance perspective. Indeed, the large variability observed with sera from different patients deters their use for expansion of cells intended for therapy. Moreover, it is expected that the supply of bovine serum will be highly diminished in the near future years and that research and cell factory labs will be forced to modify their cell culture protocols and to adopt substitutes of FBS. For these reasons, human blood platelet lysate supplements are gaining an increasing interest as bovine serum substitutes, especially when cells that eventually will be implanted in a patient are cultured.

Different procedures and protocols have been adopted for the preparation of these platelet lysate supplements [87] reviewed in [8,88]. In essentially all published protocols, including the recently published one of ours for the production of a two component supplement [4], the final human platelet derived additive included, in addition to growth factors and active molecules present within platelets, also a significant amount of proteins and other molecules component of plasma. To avoid coagulation of the plasma fibrinogen upon addition of the supplement to the culture medium, heparin is normally added as an anticoagulant agent. However, as already mentioned in the introduction, it has been reported by several authors that heparin is capable of interfering with the activity of several growth factors. Hemeda et al. have described that higher heparin concentrations impaired cellular proliferation in a dose-dependent manner [44]. At high heparin concentrations colony-forming unit frequency and the in vitro differentiation toward adipogenic and osteogenic lineages of human BM-MSC were also reduced. Moreover, being of animal origin, the addition of heparin should be discouraged whatever possible, especially when the culture medium is adopted for the expansion of cells intended for cell therapy.

Compared to plasma, proteins and factors involved in the coagulation process are missing in the serum. Conflicting results have been reported on the use of allogenic serum, obtained by conventional blood coagulation or by coagulation of plasma, as culture medium supplement. Initial studies performed more than 10 years ago with human serum, revealed the possibility of efficiently isolate and expand human BM-MSC that maintained their differentiation potential [51]. Shetty et al. observed an increase of cell proliferation when human BM-MSC cultures were performed in the presence of human serum from whole blood compared to FCS [54]. In the presence of human serum. an enhancement in the adipogenic differentiation of the same cells was observed by Oreffo

et al. [89]. Enhancement of MSC differentiation induced by allogenic human serum or autologous plasma was observed also by other authors [56,57]. However, Shahdadfar reported an increased proliferation of human BM-MSC induced by autologous serum compared to FCS, but not by allogenic serum [59]. An increase in the proliferation, but a less effective differentiation of human pre-adipocytes was observed by Koellensperger et al [90]. Simões et al. observed an increase in the cell yield when MSC of different origins were cultured with human serum compared to FCS as medium supplement throughout passage 3 to passage 7 [91]. Recently a comparable UC-MSC proliferation was shown in cultures with human serum from two different plasma sources as medium supplement, plasma removed from blood after 24 h from collection and plasma devoid of cryoprecipitate [63]. However, in most, if not all, of the above cited papers and similar ones in the literature, a careful determination of the platelet factor concentration in the serum was not done and the adopted protocols not always guaranty the absence of platelets or platelet content as serum contaminants.

Here we reported the development of two standardized lyophilized cell culture medium supplements: a completely plasma-free platelet lysate (v-PL) obtained from extensively washed platelets and a platelet lysate-free serum (Pl-s) obtained by a plasma cryo-precipitation, to remove the bulk of the fibrinogen molecules, followed by a calcium-mediated coagulation, to remove the residual fibrinogen. Characterization of these two products and investigation on their biological activity when used as cell culture supplements lead us to conclude that v-PL recruited quiescent, and even differentiated or senescent cells back to the cell cycle by activating the cell proliferation machinery (ERK and AKT phosphorylation, Cycline D1 induction, etc.). Instead, v-PL was unable to support cell proliferation unless the plasma or serum components were also present. These observations are in agreement with the interesting results obtained with primary cultures of monkey arterial smooth muscle cells [65] and Swiss mouse 3T3 cells, embryo derived cells with a high degree of sensitivity to contact inhibition of growth [92,93], both types of cells requiring platelet derived growth factors in association to plasma components to sustain the cell growth, where platelet factors alone did not promote proliferation. Indeed, despite the fact that platelet derived mitogens were crucial to promote the reentry in the cell cycle (commitment) of confluent cells of early passages and even senescent cells of late passages of primary cultures, v-PL used as single component did not sustain viability and proliferation of either cell lines or primary cell cultures. On the contrary Pl-s was ineffective in quiescent resting cells, but supported proliferation of the same cells after v-PL treatment and of cells constitutively stimulated as in the case of established cell lines. In agreement with these findings, the combination of the two components was highly effective in supporting proliferation of primary cell cultures at a higher level than FBS in control cultures, whereas, the Pl-s added to the medium as a single component sustained the growth of several human cell lines in adhesion or in suspension at a growth rate comparable to the one of FBS control cultures. These results are in line with previous studies, dated back to almost forty years, where virally transformed cells grew well in plasma derived serum without the need of exogenous

platelet extract whereas malignant cells of mesodermal origin directly derived from tumors showed a range of dependence on platelet derived factors [94].

When we determined the efficiency of Pl-s and the plasma from which it was derived with regard to the ability to sustain cell proliferation in cultures of both primary cells and cell lines, we observed a comparable activity in the two medium supplements. However, a slight proliferation advantage was observed in cultures supplemented with the Pl-s. This was especially true for cells growing adherent to the Petri dish compared to cells growing in suspension. This finding suggests that, during the coagulation process, an activation of proteins and factors favoring adherence of proliferating cells is occurring, possibly through enzymatic proteolysis.

The use of the two combined products allowed to establish cell cultures from tissue biopsies or aspirates in complete absence of animal components and to *in vitro* expand different types of cells, intended for cell therapy in humans, maintaining their differentiation potential and without introducing karyotype alterations. These cells include, but are not limited, to MSC derived from bone marrow, adipose or cord blood and articular chondrocytes. To note is that this, not only could consent to perform cell therapies with cells expanded in a safer condition (absence of animal components in the medium), but, in some cases, could allow to isolate and expand transplantable cells otherwise not achievable with conventional culture medium supplements. This is particularly relevant in case of elderly patients from which conventional culture medium supplements often do not permit to obtain an adequate number of cells.

The C-MYC protein is involved in different cellular roles like cellular proliferation, cell size, differentiation, stem cell self-renewal and apoptosis [74]. In the last 30 years many investigations were made about this protein. C-MYC is implicated in different and critical biological roles at molecular level but its total implications are not clearly identified [85]. In particular, the protein is involved in several cellular pathways, interacting with different cofactors, and regulating the expression of different genes. In 1984 Hann S.R et al. [76], identified two protein of 64 and 67 kD as the major products of the *C-MYC* oncogene. These two different proteins have different exons where they initiate. C-MYC2 initiates from the first AUG site codon in *C-MYC* exon2, whereas C-MYC1 initiates from a non-canonical site, indeed it starts from a CUG codon located near the 3' end of exon 1 and differ from C-MYC2 by 14 or 15 N-terminal amino acids [75]. In 1992 it was demonstrated how C-MYC 1 appears to be specific for growth inhibition mediated by methionine deprivation, as a consequence of a physiological stress, because the deprivation of other amino acids did not cause its expression. Indeed, C-MYC2 is expressed during the cell cycle when the cells do not show any sufferings. In our work a strong activation of the C-MYC1 isoform is showed in primary cells culture under the stimulation or the isolation of the cells in PL (Platelet Lysate) but not when the cells are expanded in the control condition (10% FBS), whereas the cell line have a different behaviour, showing a lower constitutional expression of C-MYC1 isoform that is modulated under the stimulation or expansion with PL but without statistical differences respect to

the control condition. Considering the data of the literature [4,72], PL have different effect on the proliferation of cell line respect to primary cells cultures and activates some genes involved in cells proliferation like ERK, AKT and Cyclin D1 in osteoblast primary cells culture. In fact, the PL addition to cell line cultures allows to maintain growth rate standards similar to the control condition, instead for primary cell culture, the effect of PL is statistical better than the FBS expansion.

Primary cells cultures stimulated with PL showed a double band in correspondence of C-MYC protein after 5 minutes, instead this double band was absent in cells that were in the standard condition.

The second band had was nearly the first one, because the C-MYC1 protein differ from the second isoform (C-MYC2) only for few basis, indeed the two protein have a molecular weight of 64 and 67 kD respectively. The presence of C-MYC1 band was also observed in other primary cells cultures like AFS (Amniotic Fluid Stem cells), hAC (human Articular Chondrocyte) and hOB (human OsteoBlast).

As demonstrated from Hann S.R et al. [79] the expression of C-MYC1 protein was associated to high confluence reached by cells that lead to a deficiency of methionine in the medium.

Our results performed in osteoblast at different confluence (high with 90% of confluence and low with 20% of confluence) showed how in presence of PL the C-MYC1 isoform was expressed independently from the confluence reached by the cells. This experiments showed that the confluence of the cells was not the cause of C-MYC1 expression, because the expression of this isoform was present also in cells that were in contact with PL even just for 30' independently from the confluence reached.

For the cell line, the result showed a scene slightly different because for this type of cells we obtained a modest expression of this isoform also in the standard condition (FBS).

Some experiments were performed to show that the cells that express the C-MYC1 isoform are not growth arrested cells. Indeed, from previous observations [4], we know that cells grown in PL are proliferating cells. In this work the data demonstrate that the expression of C-MYC1 isoform was not associated with cells cycle arrest, on the contrary they resulted positive for Ki67 staining. Ki67 is a typical nuclear marker associated with cellular proliferation. Experiments with Vybrant® Apoptosis Assay Kit revealed that these cells were not apoptotic.

Experiments were carried out to show that the presence of PL in the medium was not responsible for the "sequestration" of the methionine in the medium. With these analyses the expression of the C-MYC1 isoform was observed also when the methionine concentration in the medium was at the higher level tolerable by cells leading to the result that the expression of that particular isoform was not due to the lack of methionine in the medium.

All these experiments showed that PL was responsible for the induction or increasing of C-MYC1 isoform in primary cells culture and much more slightly in the cell line. Surely this not sufficient to explain all the molecular mechanism that are at the base of the different response of the two types of cells to PL stimulation, but it paves the way to a deeper molecular study in order to understand peculiar differences of PL stimulation on various types of cells.

This work is presented in the publications:

Culture Medium Supplements Derived from Human Platelet and Plasma: Cell Commitment and Proliferation Support.

*Muraglia A, Nguyen VT, **Nardini M**, Mogni M, Coviello D, Dozin B, Strada P, Baldelli I, Formica M, Cancedda R, Mastrogiacomo M.*

Front Bioeng Biotechnol. 2017 Nov 20;5:66. doi: 10.3389/fbioe.2017.00066. eCollection 2017.

In preparation

Role of C-MYC in the proliferation stage of mesenchymal stem cells cultured and selected by platelet derivatives

***Nardini M.**, Gentili C., Cancedda R., Castagnola P.,Mastrogiacomo M.*

TABLES

Table I). Concentrations of PDGF-BB and VEGF in the culture medium supplements

Sample	**PDGF-BB ng/ml °** *(mean ± st dev)*	**VEGF ng/ml *** *(mean ± st dev)*
Plasma-Serum (Pl-s)	0.11 ± 0.06	0.02 ± 0.01
virgin-Platelet Lysate (v-PL)	64.58 ± 9.10	4.35 ± 1.23

° Average of 4 different preparations; * Average of 2 different preparations

Table II). Karyotype stability in cells expanded in the presence of the new culture medium supplements

donor	**age (years)**	**passage**	**doublings**	**karyotype**
#1	73	2	10	46, XY
#1	73	7	15	46, XY
#2	94	2	11	46, XX
#3	51	2	14	46, XX

FIGURES

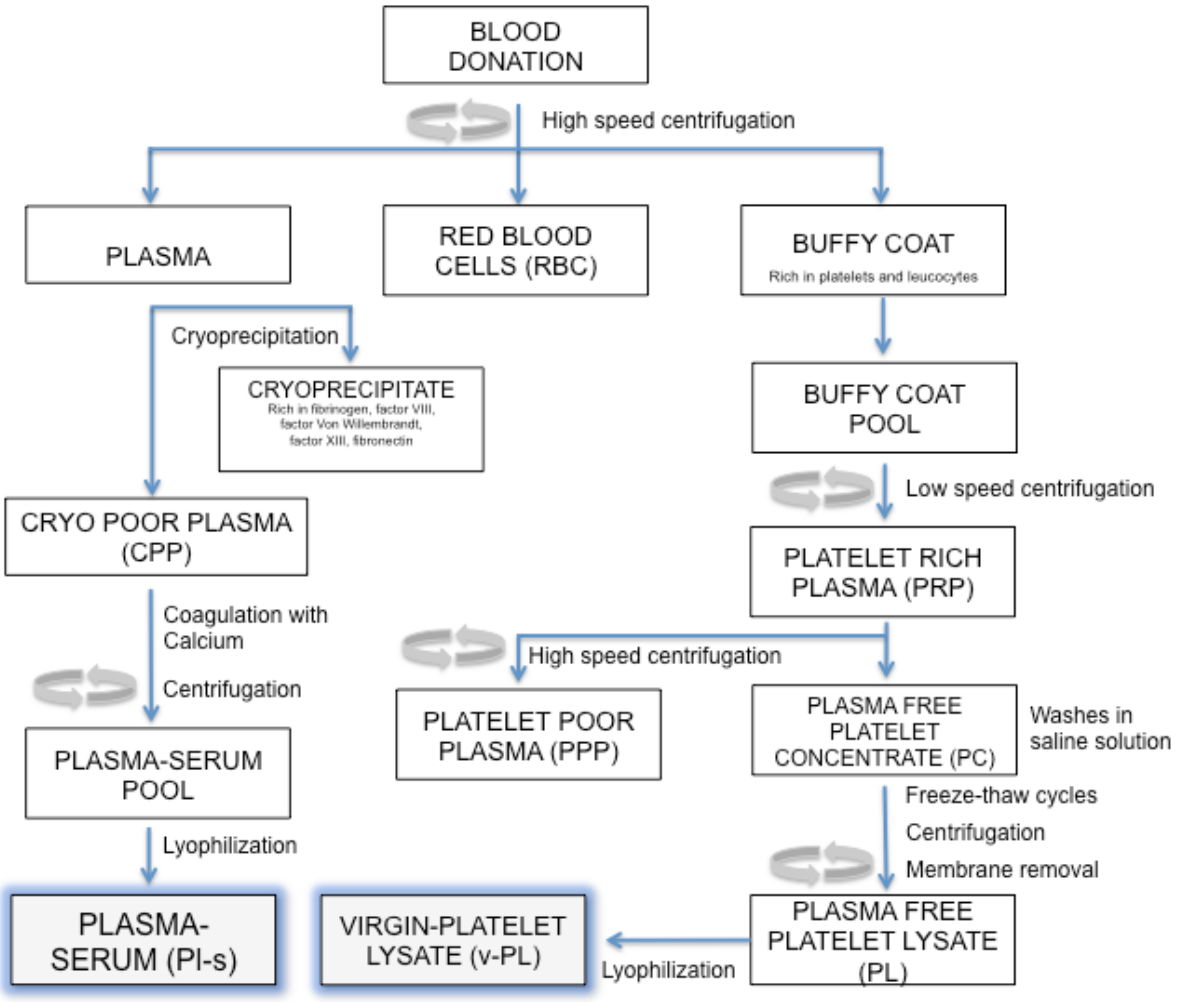

Figure 1: Manufacturing process outline: Steps in this procedure occur within a sterile closed system thanks to the possibility of performing sterile connections between blood bags.

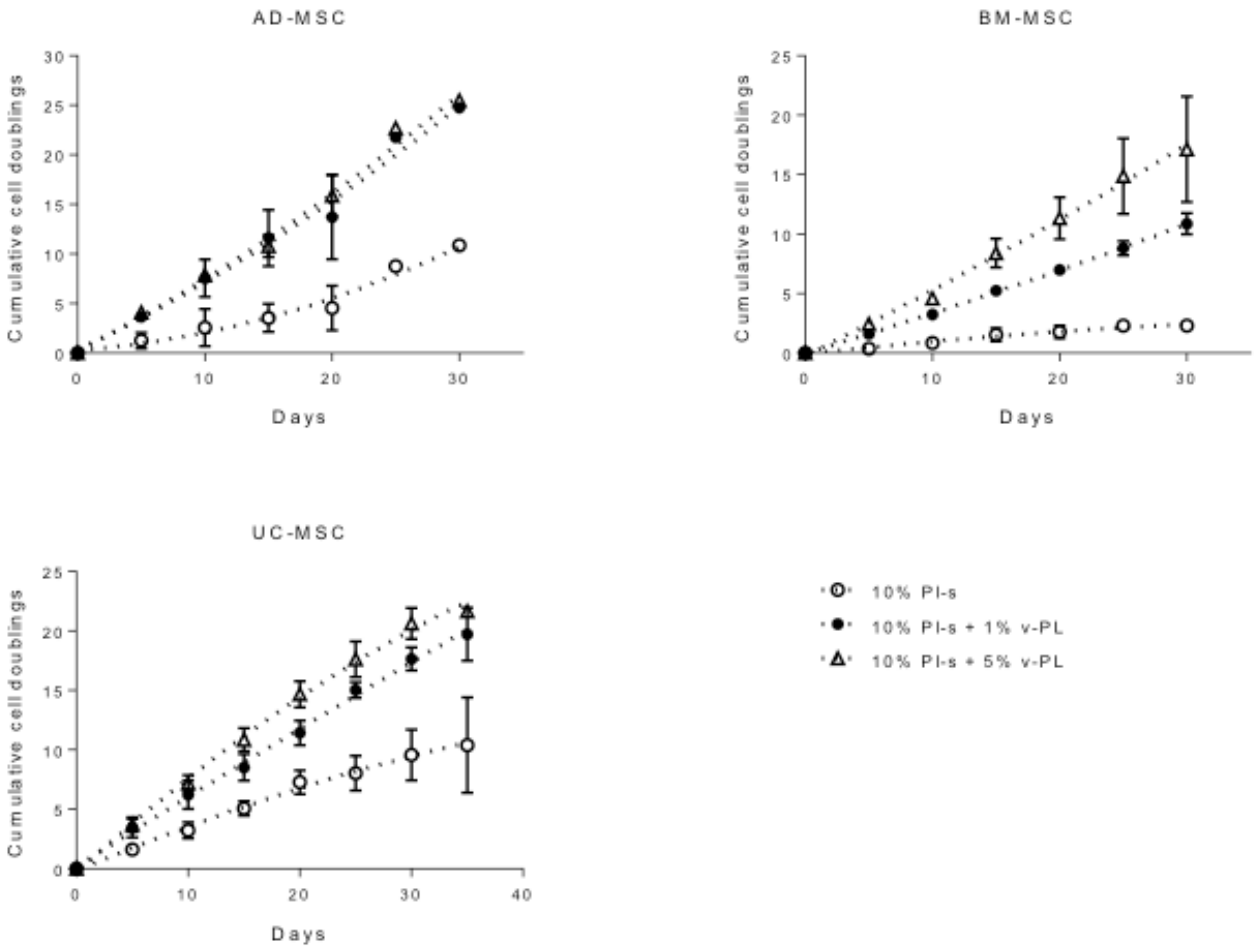

Figure 2: v-PL effect on cell proliferation – primary cultures: Adult tissue derived primary cells, AD-MSC and BM-MSC or fetal tissue derived cells, UC-MSC initially selected and expanded in medium supplemented with 10% FCS were transferred to media with different platelet and plasma derived supplements. Their proliferation rate was monitored by calculating the number of doublings performed during the time in culture.

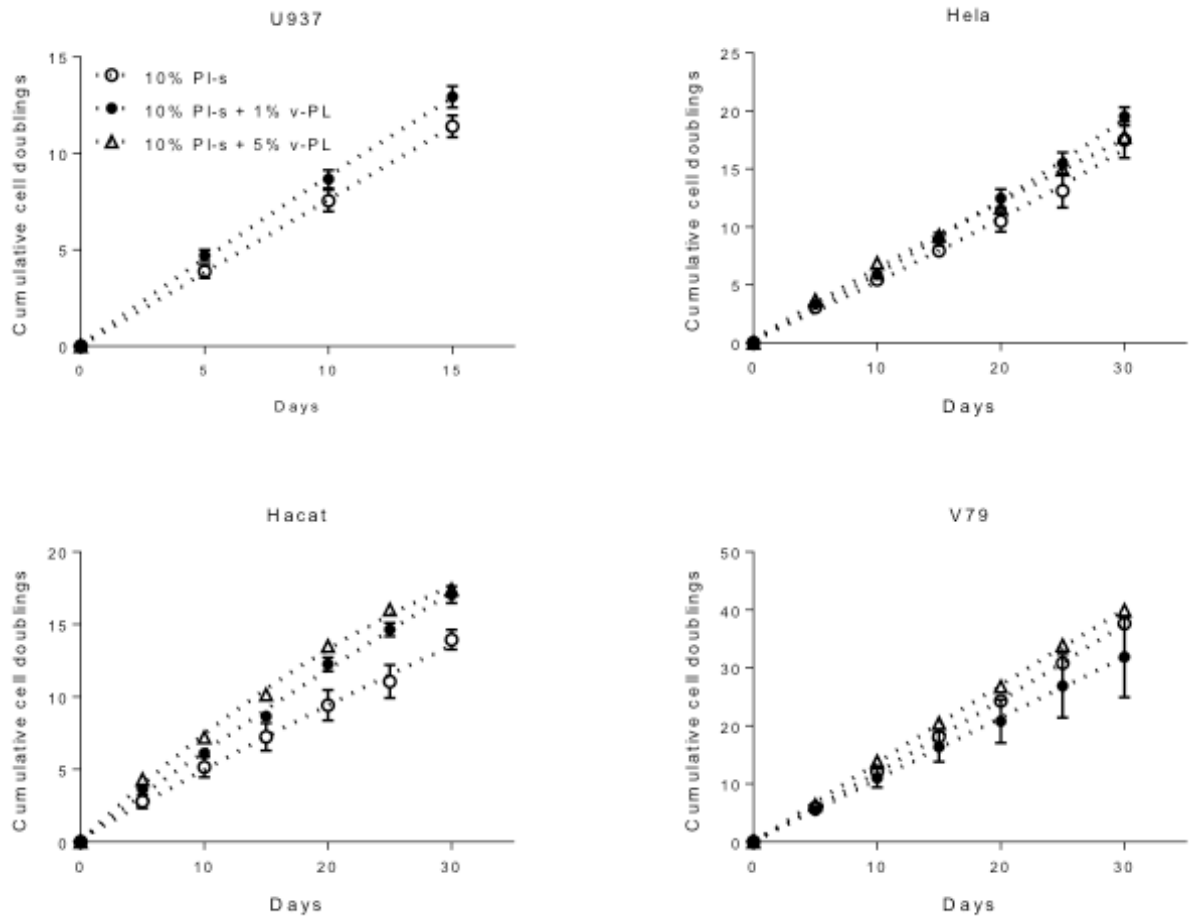

Figure 3: v-PL effect on cell proliferation – cell lines: The human cell lines U937, HeLa, HaCaT and the hamster V79 cell line were cultured in the presence of different platelet and plasma derived supplements and their proliferation rate was monitored by calculating the number of doublings performed at different culture times. On the contrary to the behaviour of the primary cell cultures, cell lines are less responsive to the v-PL mitogenic stimulus and the culture condition in the presence of only serum, is permissive to the proliferation of the cells both in adhesion or in suspension.

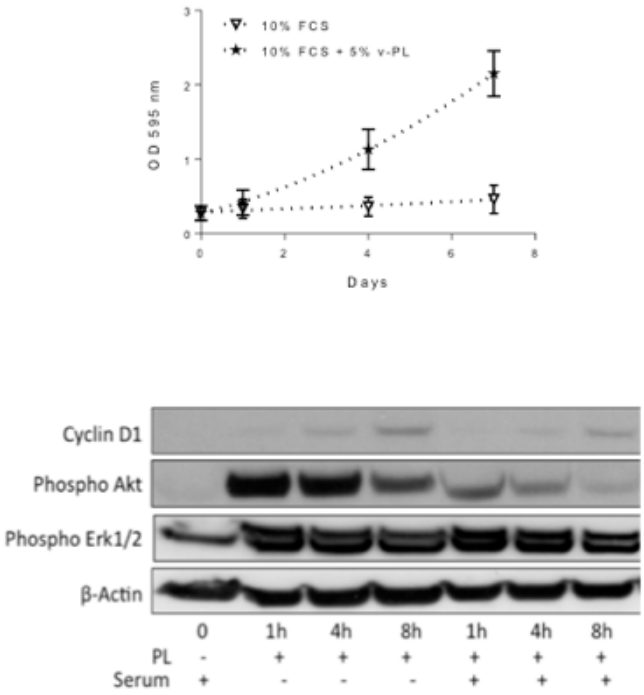

Figure 4: v-PL promotes re-entry in the cell cycle of confluent resting cells: Upper panel: Confluent growth-arrested chondrocytes, obtained from cartilage biopsies and expanded in vitro in the presence of 10% FCS, were maintained in 10% serum or additionally supplemented with 5% v-PL. A crystal violet proliferation assay was performed in parallel on both cultures. Confluent cells treated with v-PL resumed proliferation whereas the parallel control culture did not. Lower panel: Western blot analysis of proteins extracted from the cells treated with 5% PL probed with Cyclin D1, phospho Akt, phospho Erk1/2 and Actin antibodies shows that proliferation pathways were activated by v-PL also in the absence of serum.

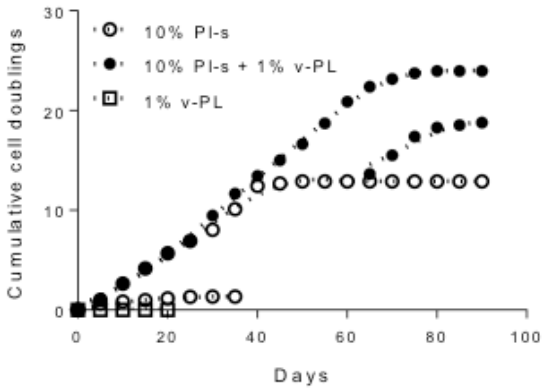

Figure 5: v-PL can rejuvenate a culture of senescent MSC: A culture of BM-MSC previously expanded in the presence of 10% FCS for about 10 population doublings was split in the different culture conditions. After 3 weeks, one part of the cells of the culture in 10% Pl-s + 1% v-PL was transferred in medium supplemented with Pl-s without v-PL. After additional passages, at a time that proliferation was arrested (senescent cells), part of the Pl-s culture was transferred again in medium supplemented with 10% Pl-s + 1% v-PL (restoring in this way the v-PL mitogenic stimulus). As shown by the graph, 1% v-PL cannot support cell proliferation, but the addition of v-PL to senescent cells, maintained in the presence of Pl-s as the only supplement, rejuvenate the cells that resume proliferation.

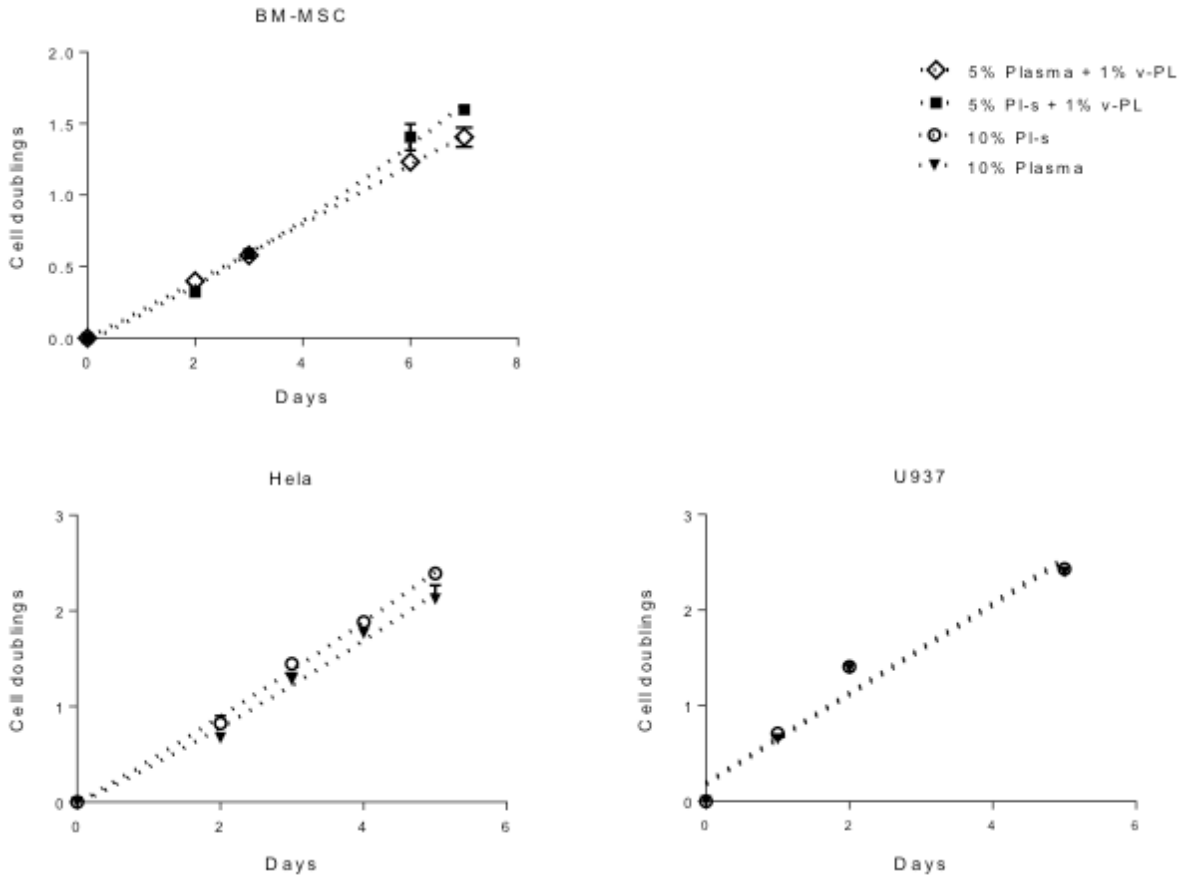

Figure 6: Comparison of Pl-s and plasma as medium supplements Human primary cells (BM-MSC) and human cell lines growing either in adhesion (HeLa) or in suspension (U-937) were cultured either with Pl-s or plasma as medium supplements. Cell proliferation was determined by direct cell counting.

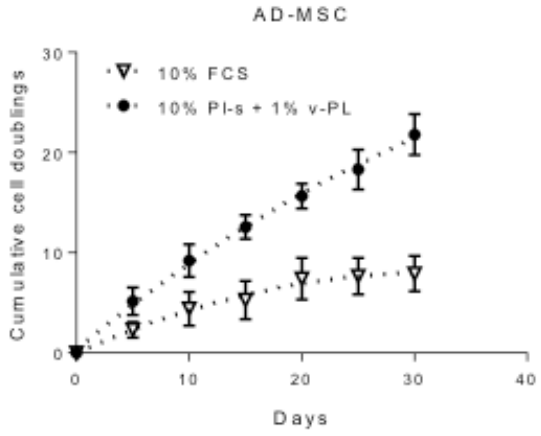

Figure 7: Growth rate of cells cultured with the new supplements: The combined effect of Pl-s and v-PL on cell growth was tested on primary cultures of AD-MSC and compared to the control condition where cells were grown with the standard supplement FCS. The proliferation rate was monitored through the evaluation of the cumulative population doublings performed by the parallel cultures.

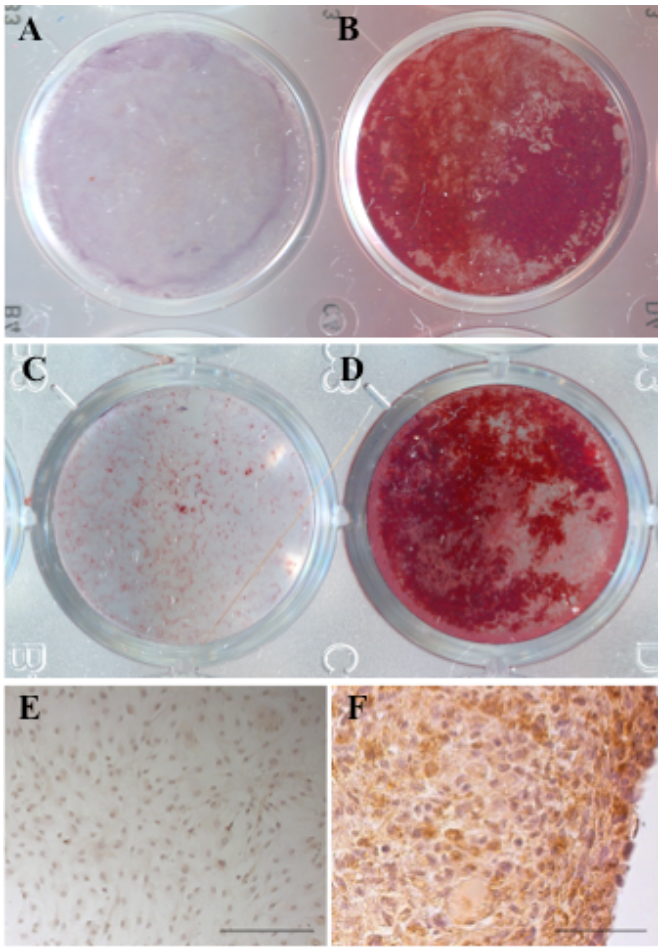

Figure 8: Maintenance of the differentiation potential by cells cultured in the presence of v-PL and Pl-s: Panel A-B) Primary cultures of BM-MSC (passage 2); Panel C-D) Primary cultures of AD-MSC (passage 2); Panel B,D) Cells osteogenically induced for 3 weeks; Panels A, C) Not osteogenically induced control cells; Panel E-F) Human articular chondrocytes cultured as adherent dedifferentiated cells (Panel E) and transferred to suspension cultures (panel F) stained with antibodies against αII collagen.

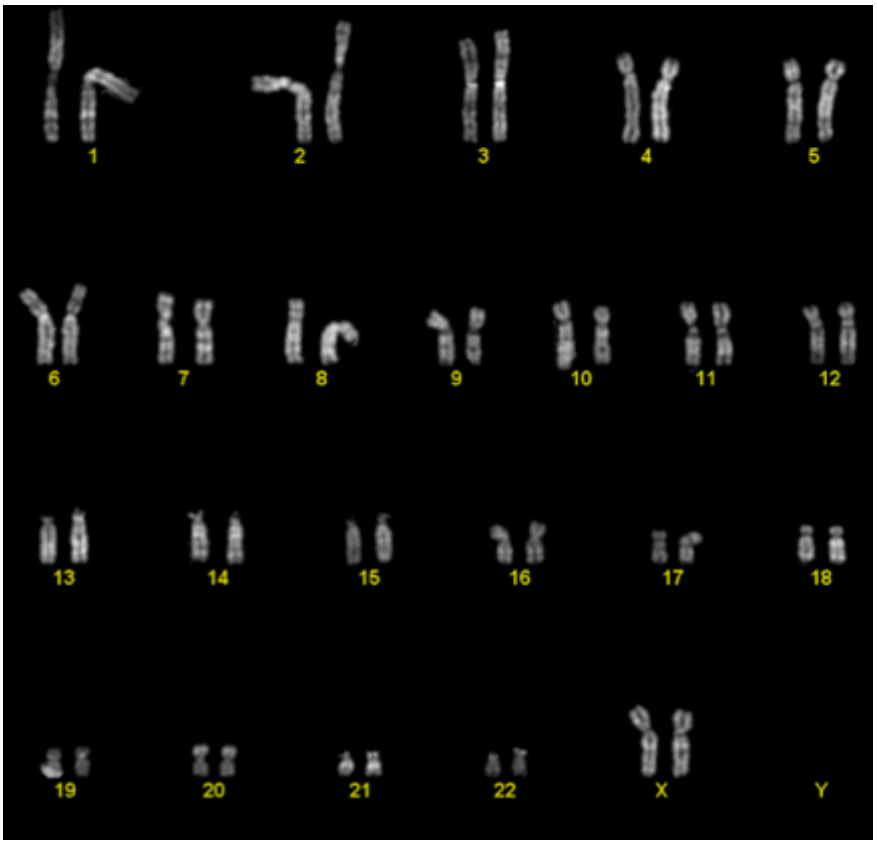

Figure 9: Representative Karyotype of a passage 2 BM-MSC culture: Analyses of more than 10 metaphases revealed a normal 46 XX karyotype.

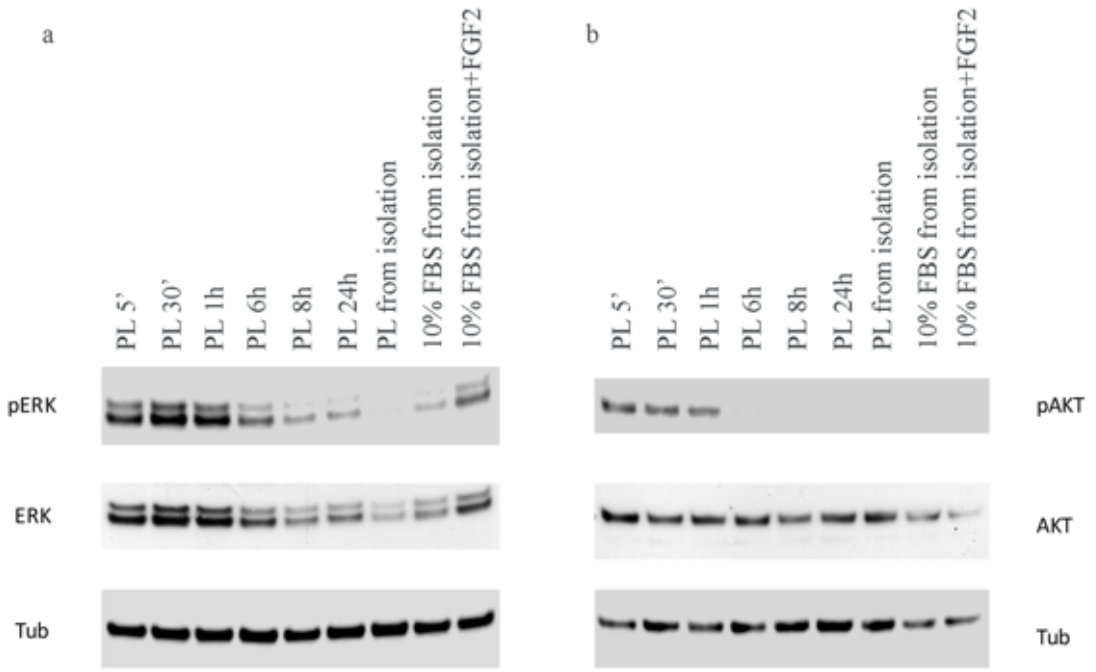

Figure 10: PL activates AKT and ERKs pathways. Sub-confluent cells were treated with PL and collected at different times starting at 5 min. Western blot analysis of cell lysates probed for ERKs (a) and AKT (b) and their phosphorylated forms. Tubulin was blotted as an loading control.

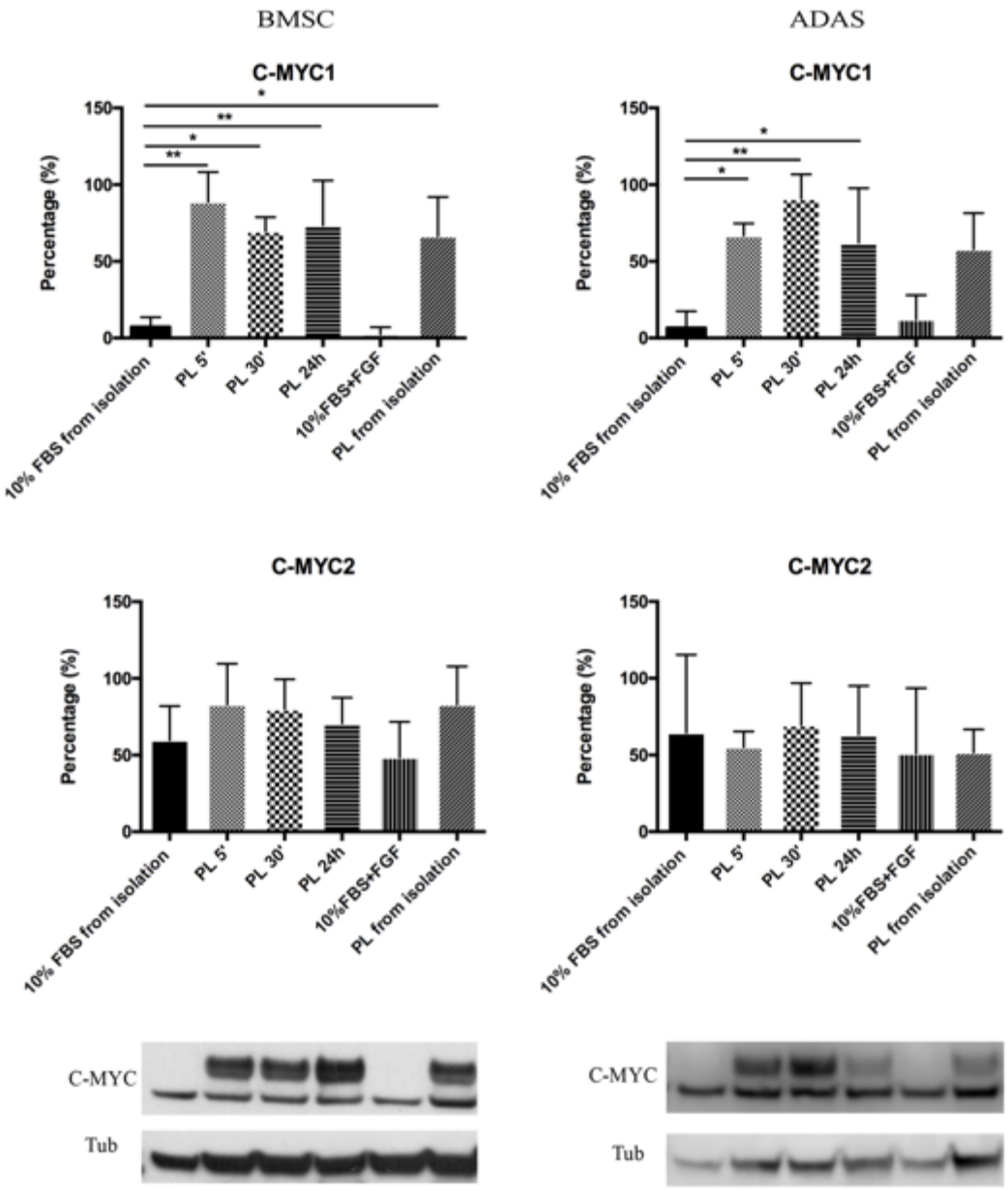

Figure 11: PL activates c-Myc1 isoform. Sub-confluent cells were subjected to different treatments and collected at different times starting at 5 min. Western blot analysis of cell lysates BMSC (a) and ADAS (b). Tubulin was blotted as an internal control.

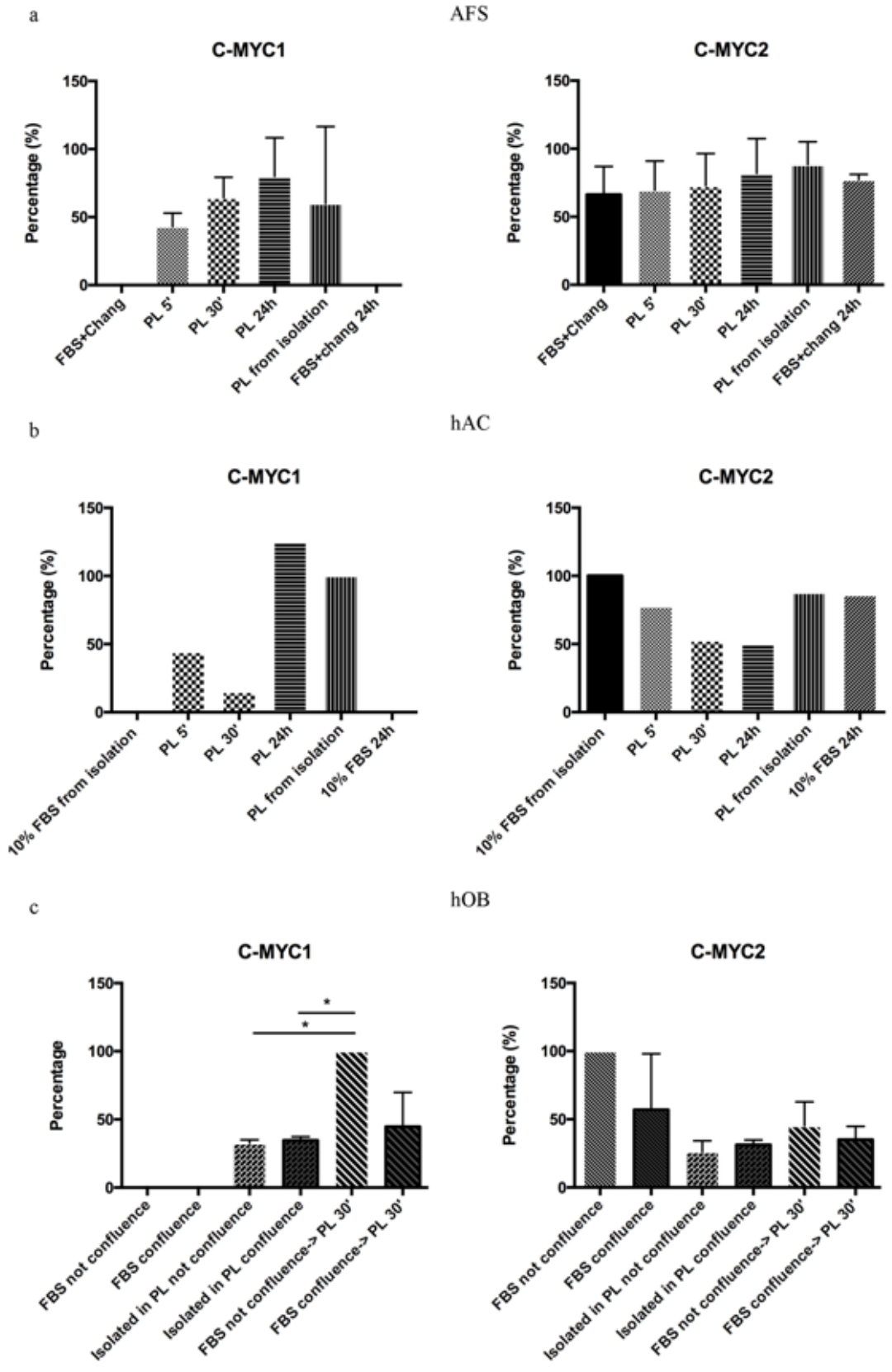

Figure 12: PL activates c-Myc1 isoform. Sub-confluent cells were treated with PL for multiple time intervals starting at 5 min. Western blot analysis of cell lysates AFS (a), hAC (b) and hOB (c). Tubulin was blotted as an internal control.

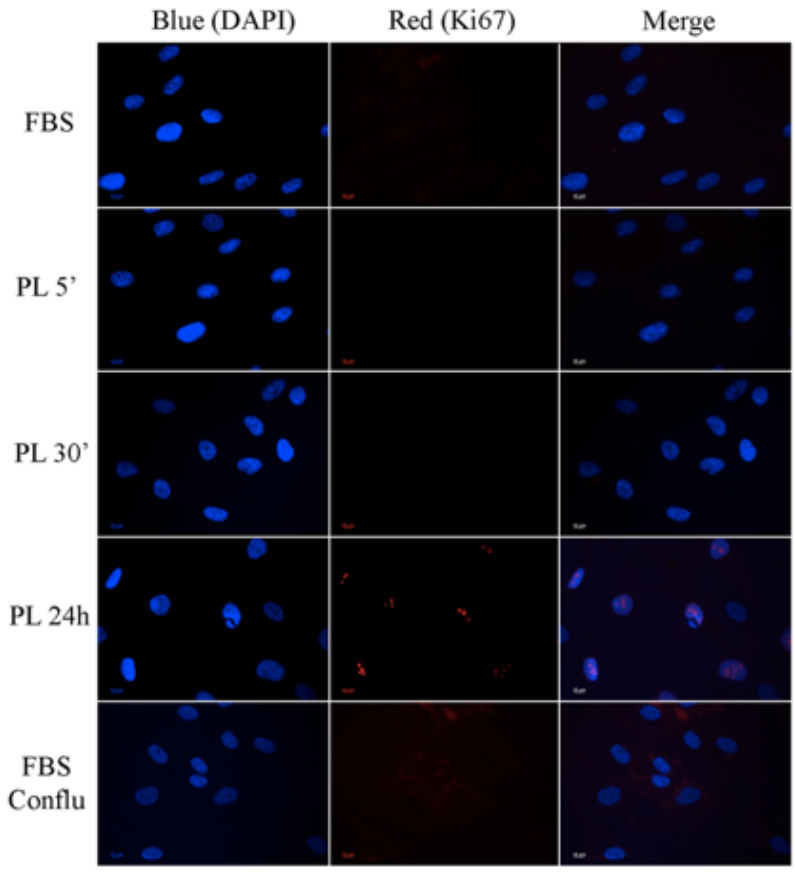

Figure 13: Immunofluorescent analysis to evaluate the expression of Ki67 protein in cells treated with PL at different time. In Red fluorescence corresponds to positivity for Ki67 nuclear marker; while blue fluorescence corresponds to the nuclei of the cells (DAPI); merge represent the union of the two dyes.

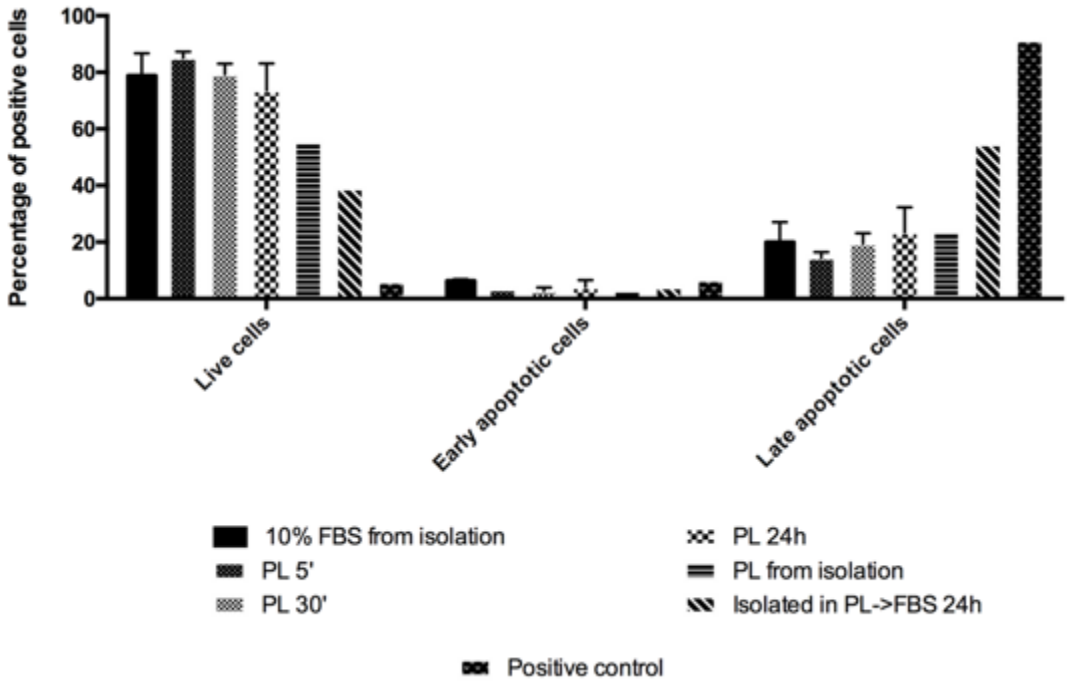

Figure 14: PL effect on the vitality of cells. Vybrant® Apoptosis Assay Kit with flow cytometry analysis was perform to evaluate if PL treatments induced apoptosis.

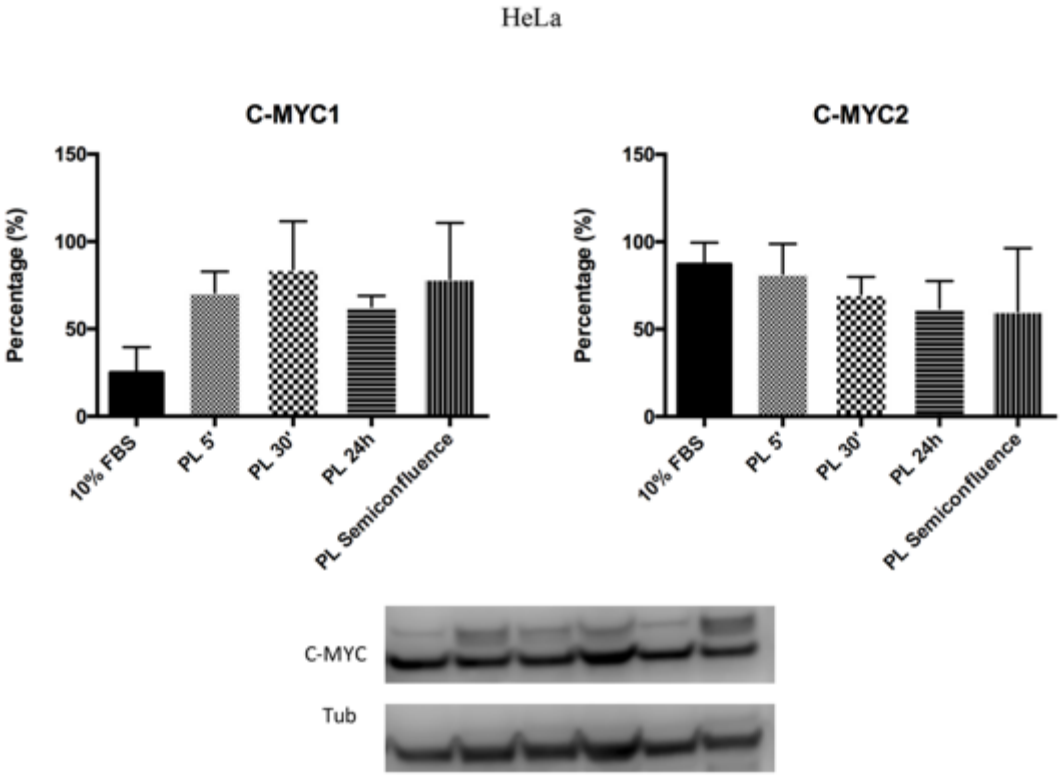

Figure 15: PL activates C-MYC1 isoform also in HeLa cells. Sub-confluent cells were treated with PL for multiple time intervals starting at 5 min. Western blot analysis of cell lysates was performed. Tubulin was blotted as an internal control.

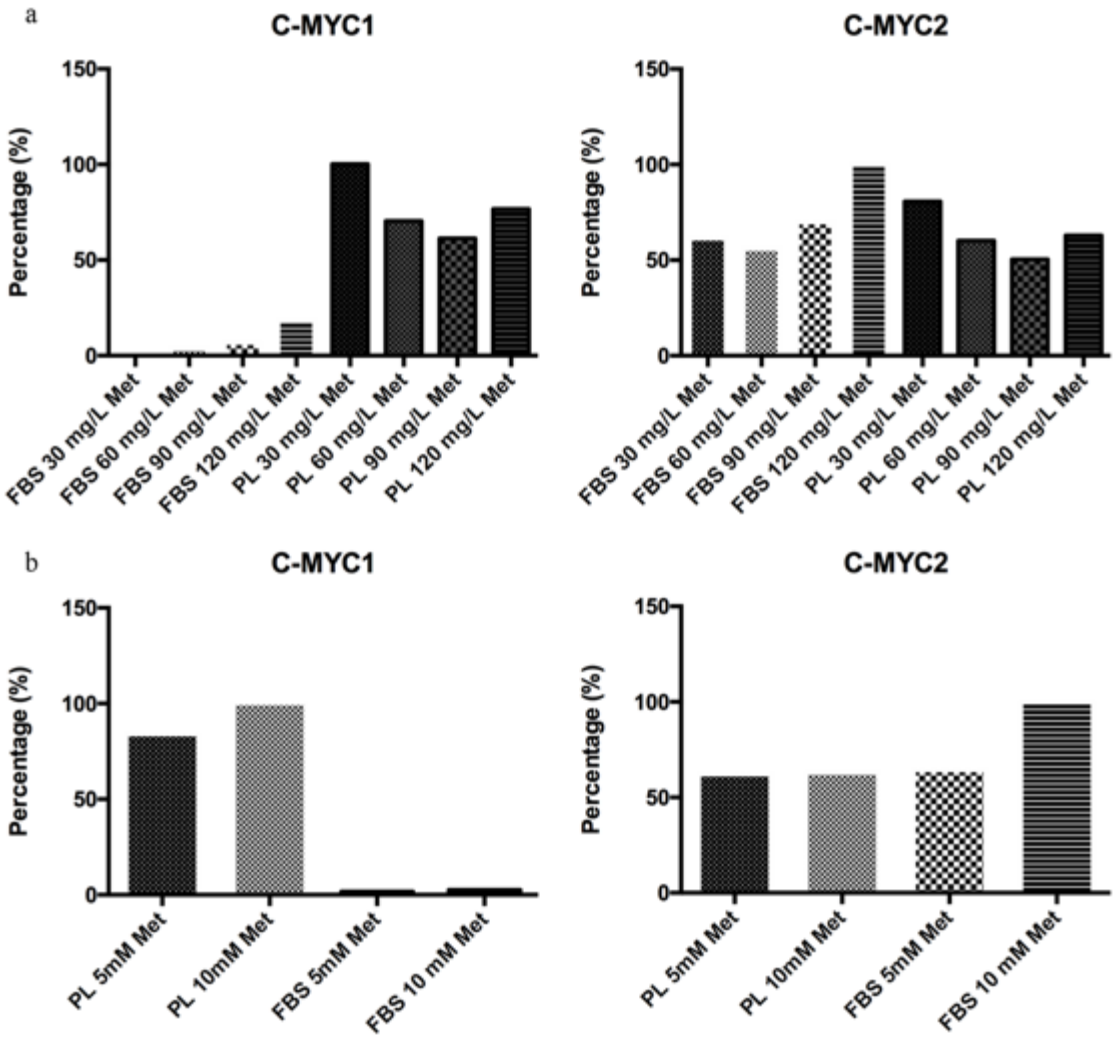

Figure 16: Activation of C-MYC1 isoform in presence of PL and methionine stimulation. Sub-confluent HeLa cells were treated with PL for multiple time intervals starting at 5 min. Western blot analysis was perform on cell lysate of cells treated with PL and different methionine concentration: 30-120 mg/L (a) and 5-10 mM (b). Tubulin was blotted as an internal control.

2. ELECTROSPUN SILK FIBROIN FIBERS FOR STORAGE AND CONTROLLED RELEASE OF HUMAN PLATELET LYSATE

ABSTRACT

Human platelet lysate (hPL) is a pool of growth factors and cytokines able to induce regeneration of different tissues. Despite its good potentiality as therapeutic tool for regenerative medicine applications, hPL has been only moderately exploited in this field. A more widespread use has been limited because of its rapid degradation at room temperature that decreases its functionality. Another limiting factor for its extensive use is the difficulty of handling the hPL gels. In this work, silk fibroin-based patches were developed to address several points: improving the handling of hPL, enabling its delivery in a controlled manner and facilitating its storage by creating a device ready to use with expanded shelf life. Patches of fibroin loaded with hPL were synthesized by electrospinning to take advantage of the fibrous morphology. The release kinetics of the material were characterized and tuned through the control of fibroin crystallinity. Cell viability assays performed in primary human dermal fibroblasts demonstrated that fibroin is able to preserve the hPL biological activity and prolong its shelf-life. The strategy of storing and preserving small active molecules within a naturally-derived, protein-based fibrous scaffold was successfully implemented, leading to the design of a biocompatible device, which can potentially simplify the storage and the application of the hPL on human patients, undergoing medical procedures such as surgery and wound care.

INTRODUCTION

Silk fibroin, a structural protein of the cocoons of the *Bombyx mori*, is widely studied for biomedical applications, such as tissue regeneration and drug delivery, because it is biocompatible, resorbable and can be fabricated in multiple formats [95–97]. The extraction of fibroin from the cocoons, a process known as regeneration, results in an aqueous solution that can be used to fabricate films, hydrogels, sponges, nanoparticles and fibers [95–102]. Silk fibroin self-assembles from the water solution into an amorphous state (called silk I) presenting α-helices, and a crystalline state (called silk II) with high β-sheets content [96,103,104]. The β-sheets characterizing silk II determine several of its physical and chemical properties, such as mechanical strength and refractive index [105,106]. Particularly interesting is the water stability provided by the β-sheet secondary structure: while silk I is soluble in water, highly crystalline silk II does not dissolve in pure water [107]. The transition from the amorphous state silk I to the crystalline silk II can be favored by using alcohols or via water vapor annealing [107–109]. The crystallization assisted by water vapor is slower, more controlled and it allows to obtain different crystallinity degrees by varying the treatment duration. Being a milder process, water vapor annealing can be applied even when sensitive molecules or cellular organelles are embedded in fibroin matrices [107,110–113]. Crystallinity manipulation of fibroin was used as a processing strategy to tune its biodegradability and to control the release of drugs. *In vitro* enzymatic degradation assays performed on fibroin fibrous scaffolds have shown a slower degradation rate when the scaffold presented high crystallinity [102,114,115]. *In vivo* studies confirmed the longer permanence of highly crystalline silk fibroin implants [116]. The control on the degradation is especially interesting in drug delivery applications, since controlling the rate of degradation enables the prolonged and sustained delivery of active factors during the entire course of the therapy. Investigations in vitro with highly crystalline silk fibroin matrices (>40% crystallinity) showed a slower release compared to the amorphous silk [117–121]. The ability of the silk fibroin in controlling the drug release was found also *in vivo* using chemotherapeutic agents, which were released in a sustained way and this kept their concentration under the toxic threshold [113,122]. Importantly, such controlled delivery can keep the overall drug concentration low within the patient's body, reducing the frequency of the treatment administration [123]. Within the context of regenerative medicine, the sustained release of growth factors from biodegradable polymeric matrices showed accelerated and improved wound healing and great potential for more complete cells differentiation in tissue engineering [124–126]. Also for chronic wounds, keeping the concentration of growth factors low and the release for longer time, can help their healing [127,128].

Human platelets lysate (hPL) is a potential therapeutic tool highly enriched with platelets-derived growth factors and cytokines. Although there are no publications reporting the exact and total content of single components of the hPL, many articles have described some of the growth factors included: platelet-derived growth factor B (PDGF-BB), fibroblasts growth factors (FGF), vascular endothelial growth factor (VEGF), epidermal growth factors (EGF) and transforming growth factor-β (TGF-β) [3,4,129]. Such growth factors are physiologically involved in regenerative and healing

processes. *In vitro* experiments have shown the hPL ability to support every stage of the wound healing, favoring cells growth, angiogenesis and stimulating the recruitment of white blood cells [18,130,131]. *In vivo* experiments showed its ability to support bone regeneration and the recovery of non-healing wounds [132,133]. hPL is commonly applied in the form of a gel, which can release the platelets-derived factors [15]. Despite these promising results, on-the-spot preparation, difficult handling and the need of storage at low temperature to preserve the activity of the factors are some of the technical and practical limitations that still hinder the hPL usage as therapeutic tool [134,135]. Therefore, there is a need of designing a device that could conjugate the sustained release of the allogenic hPL with an easier handling on a wound, while keeping the hPL factors well-preserved. This would allow a more effective use of the hPL molecules in the wound care management.

Herein, the hPL was encapsulated in silk fibroin electrospun fibers to exploit its tunable degradability and protective effect on sensitive molecules [111,136–142]. The electrospun format was chosen because the porosity granted by the micro and nanofibers facilitates both the absorption of exudate and an efficient gas exchange, while supporting cell proliferation and migration. All the above mentioned features successfully mimic the natural extracellular matrix, thus improving and sustaining the healing process of the wounds [143–146].

Silk fibroin fibers with a high content of hPL were fabricated, and their degradation and release kinetics were controlled via manipulation of the fibroin crystallinity. The release kinetics of the silk fibroin fibrous mats with different crystallinity degrees were characterized tracking the release of albumin [147,148] using an *in vitro* test that was developed to simulate in vivo degradation conditions. hPL released from silk fibroin fibers retained its ability to induce and sustain the viability of primary adult human dermal fibroblasts (HDFa) *in vitro*. Finally, the possibility to use silk fibroin for the preservation of hPL biological activity was proved even after thermal stress at 60 °C [140,142], demonstrating the improvement of the shelf-life of hPL, granted by the fibroin matrix. Such construct can be proposed as a valid, easy-to-fabricate and durable alternative to the platelet-rich plasma (PRP) gel in the wound care management.

MATERIALS AND METHODS

Materials

Sodium carbonate, sodium chloride, lithium bromide, poly (ethylene oxide) (PEO, Mw=1,000,000 g/mol), albumin conjugated with fluorescein isothiocyanate (FITC-albumin), phosphate buffer saline (PBS), Protease XIV (≥4 units/mg), paraformaldehyde (PFA), and bovine serum albumin (BSA) and Triton X-100 were purchased from Sigma Aldrich (MO, USA). Human dermal fibroblast from adult (HDFa), medium 106, low serum growth supplement kit, trypsin, trypsin neutralizer, Alexa Fluor™ 488 Phalloidin and ProLong™ Diamond Antifade Mountant with DAPI were purchased from ThermoFisher Scientific (MA, USA). Cell proliferation reagent WST-1 (2-(4-iodophenyl)-3-(4-nitophenyl)-5-(2,4-disulfophenyl)-2 H-tetrazolium monosodium salt) was purchased from Roche (Switzerland). Finally, hPL was gently granted by Bioregen s.r.l. (Italy).

Fibroin regeneration and hPL preparation

Fibroin was extracted from *Bombyx mori* cocoons according to the protocol previously described by Rockwood *et al.* [97]. Firstly, the cocoons were cut and boiled for 30 minutes in a water solution of 0.023M of Na_2CO_3; subsequently, the fibers were washed with MilliQ (18.3 MΩ) water and dried. Degummed fibroin, was solubilized in an aqueous solution of 9.3 M of lithium bromide at 60°C for 4 hours and dialyzed in a tube with a MWCO of 3500 kDa for 3 days against MilliQ water. Finally, regenerated fibroin was centrifuged twice at 9000 rpm, for 20 minutes at 4 °C. To quantify the fibroin concentration, 1 mL of regenerated fibroin solution was left to dry under an aspirating hood. Then, the dried film was weighted, obtaining the concentration of silk fibroin in the solution. The concentration was found to be in a range between 60 and 80 mg/mL.

hPL used in this work, provided by Bioregen s.r.l., was prepared according to the method described by Zaky et al. [3]. Briefly, PRP obtained from buffy coat samples from the whole blood of healthy donors was subjected to several freeze-thaw cycles in order to break the platelet membranes and to release their growth factors content. The supernatant hPL recovered was freeze-dried. It contained platelet growth factors with different size. To reduce or avoid the variability from batch to batch, each single batch was derived from 400 donors. hPL was standardized among batches by making sure PDGF-BB and VEGF concentrations were constant [4,129].

Fibers fabrication and water vapor treatment

To produce the fibers, a fibroin 60 mg/mL solution was used. To facilitate the electrospinning process and fabricate the fibers, PEO powder 25% (w/w_{silk}) was added to a 60 mg/mL aqueous solution of fibroin and stirred overnight. Generally, to electrospin silk fibroin, PEO is added because it adjusts the viscosity of the regenerate silk fibroin, as reported in previous works [149–152]. Once a homogeneous solution was obtained, FITC-albumin powder was added such to obtain a concentration of 2% (w/w_{silk}). To add hPL, a solution of it 7% (w/w_{silk}) was added to not diluted silk fibroin solution. Therefore, hPL solution needs to have an enough volume to dilute the silk

fibroin solution at 60mg/mL. The final concentration of the hPL in the electrospun fibers was 5% (w/w). The fibers were electrospun at 20°C in a controlled humidity environment (30% - 40% relative humidity) with a syringe pump (NE-1000, New Era Pump Systems, Inc., NY, USA) equipped with a blunt 19G needle, at a flow rate of 1 mL/h (Figure S1a). An aluminum, grounded collector was placed at 20cm from the needle, while a voltage of 18 kV was applied (EH40R2.5, Glassman High Voltage, Inc., US-NJ, USA). In the case of the hPL loaded fibers, the following parameters were set: a flow rate of 1.2 mL/h, a needle - collector distance of 30 cm, and a voltage of 23 kV. These parameters were optimized for the different compositions in order to have a continuous electrospinning process and to produce beads-free fibers.
The crystallinity degree of the silk fibroin fibrous mats was increased via water vapor annealing. The treatment was performed in a vacuum oven (VO500EA, MLS, Italy) at 40°C and 85-90% of relative humidity. Different treatment times were used for the different crystallization reported (Figure S1b), ranging from 10 minutes to 6 hours.

Fiber characterization

Morphology

Fiber morphology was characterized by scanning electron microscopy (SEM) using a JEOL JSM-6490LA microscope (JEOL Ltd., Japan) in high vacuum with an acceleration voltage of 15kV. The samples were previously coated with a 10-nm-thick gold layer with a Cressington 208HR high resolution sputter coater (Cressington Scientific Instrument Ltd, U.K.). Size analysis was performed with ImageJ software (NIH, USA). To evaluate the encapsulation of the FITC-albumin molecules, confocal imaging was performed with a laser scanning confocal microscope (A1R, Nikon, Japan). The lasers had wavelengths of 401 and 488 nm (Nikon, Japan).

Fibroin crystallinity characterization

Characterization of the fiber crystallinity was performed by Fourier transform infrared spectroscopy (FTIR). Samples were measured in Attenuated Total Reflectance (ATR) mode using MIRacle ATR accessory (PIKE Technologies, WI, USA) coupled to a Fourier Transform Infrared (FTIR) spectrometer (Equinox 70 FT-IR, Bruker, MA, USA). All the spectra were acquired in a spectral range from 4000 to 600 cm^{-1}, with a scanning resolution of 4 cm^{-1}, accumulating 64 scans.
The deconvolution of the fibroin amide I peak was performed as reported previously by Guzman-Puyol *et al.* and Hu *et al.* [153,154]. The software was PeakFit 4.11 [153] and the wavenumber positions of the different components were deduced by calculation of the second-order derivative [154]. The fitting of the different contributions was performed using Gaussian-shaped peaks, using a fixed width for each considered peak. The crystallinity content was obtained from the ratio between the areas of the β-sheets peaks and the total area of the amide I peak.

Drug release assessment and degradation of Electrospun silk fibroin

Electrospun silk fibroin unloaded (SF), loaded with FITC-albumin (SF-alb), loaded with hPL (SF-hPL) and loaded both with FITC-albumin and hPL (SF-alb-hPL) fibers, were weighted and placed in a 24 well-plate with 1 mL of PBS 0.04M at pH 7.4 and with 6.25 mU of Protease XIV in 0.04M PBS pH 7.4 at 37°C and gently stirred on a tilting plate for 5 months. At given time points, the total volume was taken out and substituted with fresh medium. The amount of FITC-albumin was determined by correlating the absorbance at 495 nm with a calibration curve measured by using the same media, after subtraction of a blank spectra obtained by measuring the SF and SF-hPL samples. The measurements were carried out using a UV-visible spectrophotometer (Cary 6000i-Varian, CA, USA) from 450 nm to 550 nm.

To characterize the effect of the enzymatic degradation on the samples, three SF-alb-hPL mats having different crystallinity (22%, 35% and 45%) were incubated at 37 °C for 1 month, either with PBS or in the presence of PBS containing the enzyme (6.25U/mg_{fibers}). The medium was completely replaced every day. Subsequently, the mats were washed with MilliQ water for 10 minutes five times, in order to remove traces of salt and enzyme. After the final timepoint, the samples were rinsed, dried and imaged by SEM.

Biological activity of the released hPL

Primary human dermal fibroblasts from an adult donor (HDFa) were seeded in medium 106, containing 2% v/v of fetal bovine serum (FBS), 1 μg/mL of hydrocortisone, 10 ng/mL human epidermal growth factor (hEGF), 3 ng/mL of basic fibroblast growth factor (bFGF), and 10 μg/mL of heparin. The cells were split every 7 days and seeded at a density of 4500 cells/cm^2 and grown at 37 °C in 5% CO_2 atmosphere. Medium was changed every day.

To assess the retained activity of the released hPL, 20 mg of SF and SF-hPL fibers, at 24% of crystallinity, were sterilized with UV treatment for 20 minutes for each side and incubated in 4 mL of serum-free culture medium for 24h at 37°C. The low crystallinity of the mats permits the dissolution of the matrix and the complete release of all the factors in 24h hours. The size of silk fibroin mats dissolved in the serum-free culture medium, was cut in order to release 250 μg/mL of hPL in the media. This concentration was chosen because, as observed in a dose-response experiment (Figure S5), it was found to be the minimum concentration able to increase the viability of the HDFa. Twenty-four hours before the treatment, cells were seeded at a density of 4500 cells/cm2 in complete culture medium. The day after, some cells were used to assess the viability before the treatment with the samples. This reading was labeled time point zero. The rest were washed with PBS and incubated according to the following conditions: SF extract, SF-hPL extracts, culture media containing the same hPL amount released from the SF-hPL, and serum-free culture media and complete culture media as controls. Cells viability was evaluated through the analysis of the cell metabolism, thanks to a colorimetric assay. WST-1 was directly added in culture medium with a 1:11 (v/v) ratio. After the addition of the WST-1, the cells were incubated for 3 hours, at 37°C with and 5% of CO2. The assay was performed after 1, 3, and 5 days of treatment, acquiring

the absorbance at 450 nm, through a multiwell plate reader (Multiskan™ GO Microplate Spectrophotometer, ThermoFisher scientific, MA, USA) and normalizing all the outcome signals with respect to the absorbance value at the zero-time point.

Improvement of hPL shelf-life

With the aim of mimicking a degradation process, an oven treatment at 60 °C was performed on SF and SF-hPL samples, lyophilized hPL and on aliquots of plain and hPL-containing serum-free culture media. Lyophilized hPL represents the common way for storage; hPL dissolved in serum-free culture media mimics the common "device" use to deliver hPL: the platelet gel; SF-hPL is the ready-to-use silk fibroin-based device. 60 °C were used because it is a temperature at which labile molecules, like hPL, are known to degrade and because it is a temperature used in previous works to test the improvement of stability granted by silk fibroin [140,142]. The electrospun mats were cut-down to be 20 mg in mass, containing 1 mg of hPL each. After the oven treatment and 20 minutes of UV sterilization cycle for each side, they were dissolved in 4 ml of serum free culture media for 24 h at 37 °C, to release the encapsulated hPL and prepare the extract for the following cell experiments. All the electrospun samples were 24% crystalline, so they fully dissolved during the 24 hours of incubation. For the control samples, lyophilized hPL was dissolved in the serum-free medium in order to have the same concentration of the electrospun samples (250 μg/ml). Three treatment time points were investigated: 24 hours, 48 hours and 72 hours. HDFa cells were seeded onto 96-well plates at a density of 4500 cells/cm2 and let attached overnight. The next morning, cells were treated with the prepared extracts from the thermally treated samples above listed. WST-1 viability assay was performed after 5 days, acquiring the absorbance at 450 nm and normalizing all the outcome signals with respect to the absorbance value of the negative control. The residual activity of the hPL was calculated from the ratio of the cell viability observed in the case of the thermally treated mats and the cell viability in the case of the untreated samples.

Cell morphology

To evaluate the morphology of the cells directly seeded onto the fibrous mats, electrospun silk fibroin fibers were collected on 14 mm coverslips and treated with water vapor, as previously described. After UV sterilization of the Electrospun silk fibroin fibers for 20 minutes, HDFa were seeded on SF and SF-hPL matrices and observed under the confocal microscope after 1, 3 and 5 days of growth. Cells were washed twice with PBS, fixed with PFA 4% for 10 minutes and treated with Triton X-100 0.1% in PBS for additional 10 minutes. Afterwards, the samples were incubated with a blocking solution of 1% BSA in PBS for 20 minutes and then stained with Alexa Fluor™ 488 Phalloidin (diluted 1:40 in 1% BSA) for 20 minutes. All the steps were performed at room temperature (RT). Finally, the cells were mounted on glass slides with ProLong™ Diamond Antifade Mountant containing DAPI for nuclear staining and stored at 4 °C.

Statistical analysis

The analysis of the fibers size was performed on three samples for each fibrous formulation (SF, SF-alb, SF-hPL and SF-alb-hPL) before and after the water vapor annealing. The average of size measurements (n = 400) was obtained along the respective standard errors.

Three samples of each fibrous sample and each condition (not treated, treated for 10 minutes and treated for 6 hours with water vapor) were used for FITR analysis, acquiring 5 spectra from each of them, which were averaged to obtain the final spectrum for the deconvolution. The same samples (three for each crystallinity degree and three for each fibers type) were used to investigate the release. The average of the release from the triplicates was obtained with the respective standard errors. The cell viability assays were repeated 3 times for each fibrous sample. The average with the respective standard error was obtained and statistical differences were assessed by the analysis of variance (ANOVA), followed by post-*hoc* Bonferroni correction. A value of $p \leq 0.05$ was considered statistically significant.

RESULTS

Fibers fabrication and characterization

In Figure 1 and Figure S2 electrospun mats of silk fibroin fibers (SF), FITC-albumin loaded silk fibroin fibers (SF-alb), hPL-loaded fibers (SF-hPL) and silk fibroin fibers with both FITC-albumin and hPL (SF-alb-hPL) are presented. The fibers were defect-free, showing a smooth morphology. Their average diameter was measured to be 370±3 nm, 330±2 nm, 360±3 nm, and 480±2 nm, respectively. After the water vapor treatment was performed, no statistically significant change in the average diameter was observed, with dimensions of 400±4 nm, 370±3 nm, 480±4 nm, and 530±8 nm, respectively.

Although different electrospinning parameters were used, the size and the morphology of the fibers did not significantly change with the addition of the FITC-albumin or hPL. Up to 5% (w/w) of hPL can be loaded in the fibers because above this amount, the process became less continuous and reproducible.

After the water vapor treatment, the surface of the single fibers resulted smooth, indicating that such treatment did not induce modifications on their surface. On the other hand, it induced the flattening of the fibers in all the formulations, an effect often associated with post treatment of fibroin fibers (Figure 1) [155,156].

FITC-albumin was used as a tracer to characterize the release kinetic of the hPL from the electrospun fibers, since albumin is one of the elements of hPL (Figure S2) [147,148]. The successful encapsulation was verified with a confocal microscope, through the FITC fluorescence determination (Figure 2). The distribution of the fluorescence signal appeared homogenous along the fibers and no differences were observed when the hPL was added to the system (Figure 2).

Silk fibroin's secondary structure (i.e. the formation of β–sheets domains) is important to tailor the release kinetics from the electrospun samples. To characterize it together with the modifications induced by water vapor annealing, the amide I peak was analyzed by FT-IR and reported in Figure 3 [107]. The peak of the non-treated fibrous mats was centered at 1651 cm^{-1}. After 10 minutes of water vapor treatment, the spectra showed a change in the peak shape, with a shoulder at 1628 cm^{-1}, while a further shift to 1624 cm^{-1} was noticed after 6 hours treatment. These changes can be associated to an increase in the β-sheets formation, as reported previously by Hu et al. [154].

The crystallinity degree was calculated for each sample through the deconvolution of the amide I peak. As expected, non-treated electrospun fibers showed a β-sheets content ranging from 21% to 24%. On the other hand, fibers treated for 10 minutes presented a crystallinity degree of 34-36%, while those undergoing water vapor annealing for 6 hours reached up to 44-46% of crystalline phase.

Drug release assessment

To precisely assess the release kinetics for all the crystallinities explored, a release medium with proteolytic enzymes was developed in order to simulate the *in vivo* enzymatic degradation. Protease XIV was used as proteolytic enzyme. Such protease is commonly used as enzyme for comparing the degradation properties of the silk fibroin [157,158]. The quantity of the protease was selected, after testing several concentrations, to ensure that the time of degradation of the fibroin in the release medium would has the same kinetics reported in literature for the biodegradation in vivo. To select the protease concentration, 6.25 mU/mg_{fibers} and 250 mU/mg_{fibers} were tested (Figure S3). The 6.25 mU/mg_{fibers} was chosen because it resulted in a degradation time of 10 months, comparable to previous data reported in literature on the silk fibroin biodegradation *in vivo.* [116,159]

Figure 3 shows the release profiles of FITC-albumin from the fibrous mats, with different crystallinity, over a period of 5 months. The results are summarized in Table I. The study was performed on both SF-alb and SF-alb-hPL mats. In both cases, the fibers presenting the lowest crystallinity were totally dissolved within 1 hour and all the encapsulated FITC-albumin was completely released. During the initial burst, the samples with about 30% crystallinity released 41±2% - 48±2% of the loaded FITC-albumin. A strikingly different behavior in this initial phase was observed for the samples with 45% of crystallinity, which released only 6±0.2% - 10±0.7% of the total loaded FITC-albumin. After the initial burst, the release continued with a slower rate for all the samples. For example, after 25 days SF-alb samples with 33% of crystallinity showed a release of 90±0.3%, while samples with crystallinity of 46% released 38±1% of the total FITC-albumin (Figure 3d). Similarly (Figure 3e), for the SF-alb-hPL samples, a release of 80±2 % was observed from the mats with 35% of crystallinity, while a release of 46±1% was observed from the 44% crystalline mats. As shown in Figure S3, this sustained phase of the release was absent in all the samples when the Protease XIV was not used during the experiment, and a plateau at the end of the burst was observed.

In Figure 4, SEM images show the fibers morphology of SF-alb-hPL mats with different crystallinity incubated with and without the enzyme for 1 month. The morphology of the fibers without the enzyme was preserved, unlike those incubated with the enzyme, confirming the destructive activity of the Protease XIV towards the fibroin. The loss of the fibers' morphology was higher when the crystallinity was low. The effect of slower degradation of silk fibroin by Protease XIV caused by the increased crystallinity was observed also by Gil et al. [158]. They attributed this effect to the slower diffusion of the enzyme in the amorphous fibroin phase. In fact, after its crystallization, supramolecular interactions in the amorphous silk fibroin increases, such to create a more organized structure, which retards the passage of the enzyme through the crystalline domains. The results in Figure 4 are in agreement with the model they proposed by them, confirming also that this crystalline dependent degradation drove the second phase of the release.

Biological activity of released hPL

To verify the activity of the hPL encapsulated in the fibers, low crystalline SF and SF-hPL samples were incubated in serum-free culture media for 24h. The Protease XIV was not used, since the sample completely dissolved in the media thanks to their low crystallinity. Figure 6a shows the viability of HDFa cells treated with media containing the dissolved fibers. As control samples, cells were seeded in FBS-free media (labeled as negative control), in FBS-free media in which lyophilized hPL was dissolved at the same concentration (labeled hPL), or in media with FBS (labeled FBS). The amount of hPL in the control was the same as the one released from SF-hPL fibers (250 μg/mL). This concentration, from the results showed in Figure S5, resulted sufficient to observe an increase in HDFa viability. The absorbance values of all the days were normalized to the absorbance values relative to the zero-time point. After the first day of treatment, cells cultivated in media with hPL (hPL and SF-hPL samples) had the same increase in the viability ($p>0.05$) and showed a two-fold increase in the viability when compared to the negative control. This higher viability can be associated to the cell proliferation induced by the hPL, as reported before [160]. These trends were confirmed after 3 and 5 days. Silk fibroin produced no effects on the cells viability, confirming that the increase in this parameter was due the hPL released from the fibroin fibers. Therefore, these results proved that the growth factors released from the SF-hPL were still active and that they could increase and sustain cells viability of the HDFa cells for up to 5 days.

Cell morphology

To evaluate the role of the hPL in cell adhesion and morphology, HDFa were seeded on the SF and SF-hPL mats for 5 days. Intermediate crystalline fibrous mats (about 30% crystallinity) were used, in order to avoid their dissolution and allow the cells to attach. As showed in Figure 6b and c, the cells attached onto SF mats mostly showed a rounded morphology, while, when seeded onto SF-hPL fibers the cells appeared more elongated. Moreover, the presence of the hPL in the fibers seemed to accelerate cellular adhesion processes. Control samples on flat films with the same composition of the SF-hPL fibers, shown in Figure S7, confirmed that the elongated morphology is caused by the hPL encapsulated in the fibers.

hPL shelf-life

To test if the activity of hPL growth factors can be preserved via encapsulation in silk fibroin fibers, an accelerated stability test was performed, inducing a thermal stress at 60 °C [140,142]. Three conditions were tested: lyophilized hPL, hPL dissolved in serum-free medium and SF-hPL. As shown in Figure 7, the activity of the free hPL in solution was reduced to 66±3% after 1 day of thermal treatment and it decreased to 41±2% after 3 days. The lyophilized hPL, showed an activity of 76±2% after 3 days of treatment. On the other hand, the activity of the hPL released from the SF-hPL mats, thermally treated for 3 days, was 88±6%. It resulted statistically more active than the lyophilized hPL ($p<0.05$) and the dissolved hPL ($p<0.0001$), demonstrating the ability of silk

fibroin to preserve the functionality of the encapsulated molecules even at temperatures that are expected to denature the labile hPL components.

DISCUSSION

Silk fibroin electrospun fibers, were fabricated from the aqueous solution of fibroin, using PEO to facilitate the process, following a strategy adopted in previous works [149–152]. This procedure proved to be effective even for high loading of hPL. To have well-formed submicron fibers, the parameters were adjusted to account for the presence of meta-stable, complex composition of hPL. Since albumin is a component of the hPL (as reported in literature and confirmed by us in Figure S2g), the fluorescently tagged FITC-albumin was encapsulated in the fibers and used as a tracker because of its easier detection [148]. The homogeneous encapsulation of FITC-albumin in SF-alb and SF-alb-hPL suggested a homogeneous loading of hPL in the electrospun mats as well. In addition, the confirmation of the hPL encapsulation was demonstrated with the *in vitro* experiments. Through the water vapor treatment, a fine control on the fibroin crystallinity was ensured, enabling the tuning of the release time of FITC-albumin from the electrospun samples (SF-alb and SF-alb-hPL) over a large range of time scales. As suggested by previous works [117,118], in the release of FITC-albumin from the electrospun mats two different phases were distinguished: a first burst release, that might be relative to the dissolution of part of the fibers, with a quick diffusion, and a second slower and more sustained release that could involves the enzymatic degradation of the fibers, as observed in the SEM images in Figure 4. This hypothesis is supported by the experiments showed in Figure S3, where in the absence of a proteolytic enzyme, the release was inhibited after the first 24 hours.

The degradation mechanism of silk fibroin depends on its crystallinity [157]. Thus, at low crystallinity (<20 %) a fast dissolution is the main pathway for degradation, while, when the crystalline phase is increased (>40 %), the main pathway accountable for the degradation is the proteolysis, being the dissolution is responsible only for 4% of the mass [114,116–118,157–159,161]. Therefore, considering that the release of drugs from silk fibroin matrices is intertwined with the material's integrity, for amorphous silk, the release is dictated by the dissolution of the material, while for silk with high β-sheets content the kinetic depends on the molecular weight of the drug. A schematic depicting these two mechanisms is reported in Figure 5. The outcomes reported in Figure 3 and Figure S4 suggested that, even for highly loaded samples (SF-alb-hPL), the release was mostly dictated by the fibroin matrix and its crystallinity degree.

In a previous work by Hines and Kaplan [117,118], the release of small molecules from silk fibroin films was characterized. Two sequential steps were hypothesized: an initial release controlled by the diffusion of the molecules within the fibroin matrix, followed by a second step in which the release from the silk fibroin film was supposed to be controlled by the degradation of the polymeric matrix. The results of this study support our proposed model in which, after the initial burst, the degradation of the silk fibroin matrix plays an important role in determining the rate of release. We show here, for the first time, that this degradation-dependent release, hypothesized by Hines and Kaplan, is able to support a sustained release. When enzyme degradation is not present, the molecules would remain entrapped in the fibroin matrix, whereas, by adding Protease XIV, the demolition of the crystalline domain induces the release of the FITC-albumin.

Hines and Kaplan also demonstrated that the release kinetic of a drug depends on its molecular weight [117], while Nultsch and others [162] showed the effect of the molecules charge (or their isoelectric points, IP) on the release rate [163–166]. Thus, for hPL proteins with molecular weight and IP similar to albumin, the release kinetic during the burst phase (0 h to 24 h), the degradation phase (24 h to 7 days) and the sustained degradation (8 days to exhaustion) are reported in Table Ib. The rates have been obtained from the graph in Figure 3. These results showed how the release of drugs can be tuned from few hours for the low crystalline silk fibroin (< 24 % crystallinity), up to 20 days for the intermediate crystalline samples (between 25 % and 35 % crystallinity), and a sustained release for up to 100 days for the highly crystalline silk fibroin (> 36% crystallinity). The main growth factors of hPL have molecular weight slightly lower than albumin (between 22 and 44 kDa) and IP higher than albumin (8-9 and 4,7 in hPL growth factors and albumin, respectively). The lower molecular weight is expected to facilitate the diffusion, while the higher IP is expected to retard it, making the exact release of the growth factors difficult to predict. Nevertheless, since the crystallinity of silk fibroin provide a general mechanism to tune the kinetic of the release, growth factors wouldl be released slowly from highly crystalline silk fibroin than from low crystalline silk fibroin. Further studies are needed to precisely assess the release kinetic of the different components of hPL, because of the diversity of protein size and the possible formation of aggregates.

Viability assays performed on the HDFa cells, reported in Figure 6, demonstrated that the labile growth factors and cytokines present in hPL are still active after all the fabrication steps. Moreover, HDFa cells seeded onto SF-hPL fibers were able to successfully attach on the matrix, acquiring an elongated morphology which was kept during all the 5 days of growth (Figure 6b, c and Figure S6). As shown by Barsotti et al. [130] and Anitua et al. [160], platelets-derived proteins induced similar changes on dermal fibroblast. This morphology was hypothesized to be associated to cell polarization, a complex process involved in cell migration and wound closure [18].

The preservation of the hPL growth factors activity is of crucial importance not only in the short term of usage, when applied as wound management device, but also in the long term of storage after the fabrication. Nowadays, the general usage of the platelets-derived factors is in a gel form, which needs to be prepared immediately before the treatment [15]. This procedure is time consuming, difficult and only accessible to qualified operators. Thus, the possibility of having a hPL-encapsulated device as a ready-to-use patch should simplify the operations. Given the meta-stability of the growth factors, an improved device should be able to protect and preserve the biological activity of the hPL proteins in the long term. Fibroin is known to be able to preserve growth factors and enzymes, and to stabilize blood [107,110–112,119,136–142,167]. As highlighted in Figure 7, hPL released from SF-hPL patches was able to increase cell viability after 3 days of thermal stress, demonstrating the protective role of the fibroin towards the hPL proteins. These results show that the SF-hPL device, in its ready-to-use form, has a stability that is even better than the lyophilized form of hPL. This entails the possibility that SF-hPL devices could be prepared in advance, simplifying their conservation and facilitating their use.

In summary we show here that hPL was successfully encapsulated with high loading efficiency into electrospun silk fibroin fibers up to 5% (w/w) of the total mass of the fibers. The release kinetics from the silk fibroin fibers, characterized using FITC-albumin, were shown to be tunable by controlling silk fibroin's crystallinity using a simple and mild water vapor treatment. All the steps involved in the release dissolution of the matrix, diffusion rate and degradation of the fibers have been shown to be affected by the fibroin crystallinity, with samples with the highest crystallinity having the smaller dissolution and the slower diffusion and degradation.
Encapsulated hPL retained its biological activity, sustaining the HDFa cell growth *in vitro* for up to 5 days. Interestingly, hPL treated cells appeared to acquire a more polarized morphology, typical of migrating cells that are involved in the wound closure. Finally, the accelerated stability test revealed the maintained bioactivity of the growth factor pool, confirming silk fibroin's ability of preserving sensible molecules. hPL in the fibroin patches has an extended shelf life and will not require particular storage conditions. The proposed engineered fibers could facilitate the use of hPL for wound healing and in medical procedures in which hPL gels are currently used. Electrospun patches are readily applicable to the wound site, similarly to a gauze, could have a pre-determined release kinetic and could be prepared and store as ready-to-use devices thanks to the preservation of the hPL activity and the prolonged shelf life granted by the silk matrix.
A more precise knowledge of the growth factors' releases and their biological activity *in vitro* and *in vivo*, could lead to the exploit of the facile usage, tunable degradation and sustained release in different applications from wound healing to regenerative medicine.

This work is presented in the publication submitted to *Acta Biomaterialia*:

Electrospun silk fibroin fibers for storage and controlled release of human platelet lysate
Cataldo Pignatelli, Giovanni Perotto, ***Marta Nardini****, Maddalena Mastrogiacomo, Ilker S. Bayer, Ranieri Cancedda and Athanassia Athanassiou*

FIGURES

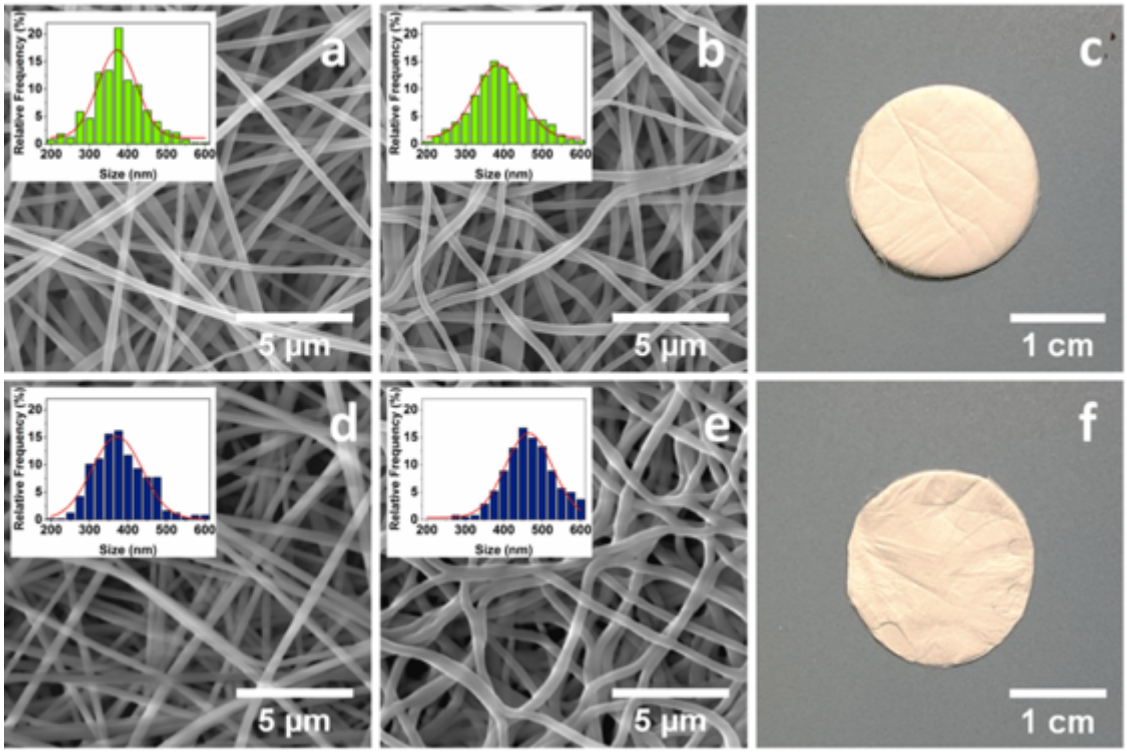

Figure 1: SEM images of SF (a and b) and SF-hPL (d and e) fibers mats obtained by electrospinning. The fibers morphology is characterized before (a and d) and after (b and e) the water vapor treatment. The insets show the corresponding size distributions. Photos of the obtained electrospun SF (c) and SF-hPL (d) fibrous mats.

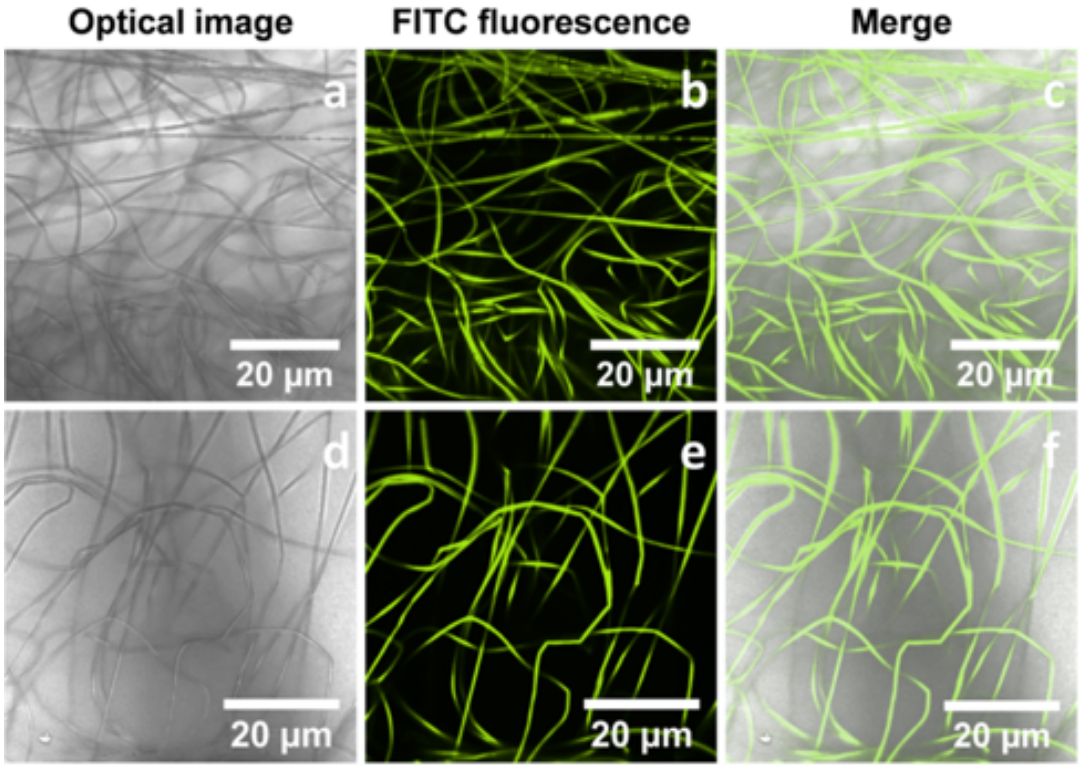

Figure 2: Confocal microscope images of SF-alb (a, b and c), and SF-alb-hPL (d, e and f).

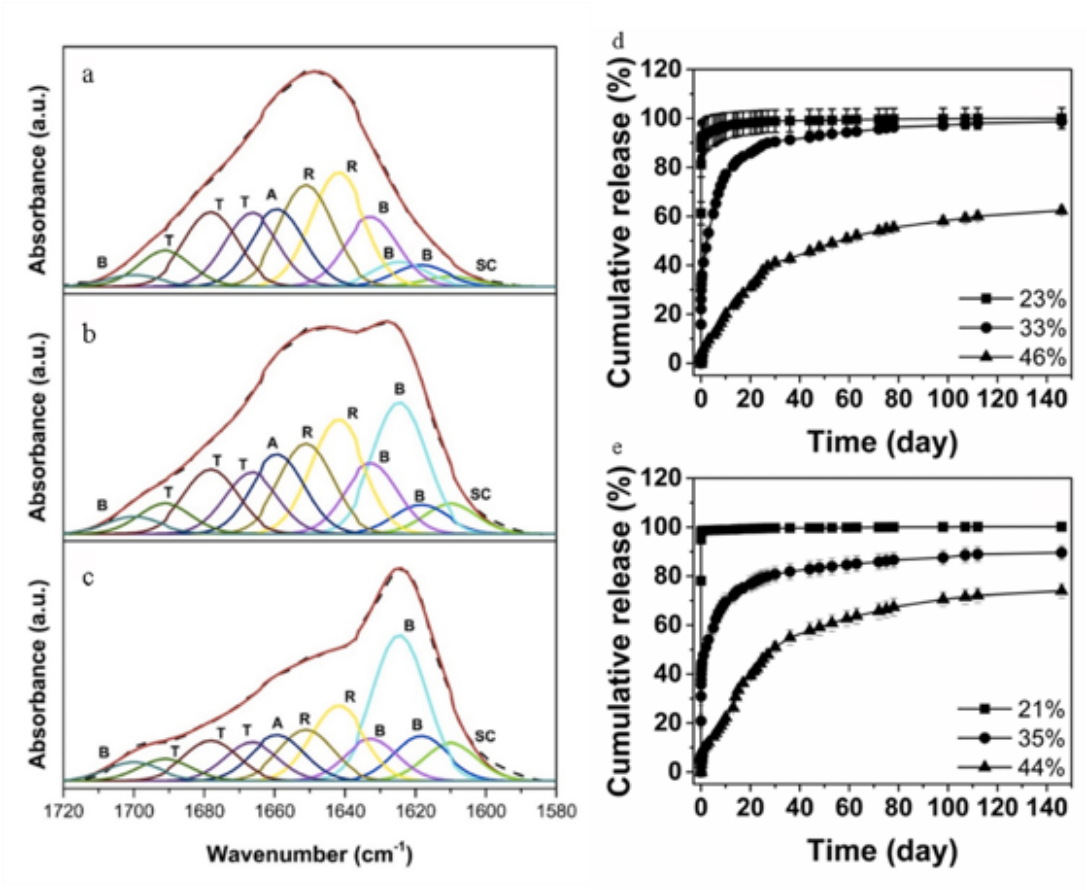

Figure 3: Deconvoluted FT-IR spectra of the amide I band of non-treated fibers (a), fibers treated for 10 minutes (b), and fibers treated for 6 hours (c). The crystallinity content for these samples are 21%, 34%, and 45%, respectively. SC = side chains; B = β-sheets; R = random coils; A = α-helices; T = turns.
FITC-albumin release kinetics: (d) SF-alb and (e) SF-alb-hPL electrospun fibers. The percentages indicate the crystallinity of the fibrous mats. The release medium contained Protease XIV, to simulate the in-vivo degradation.

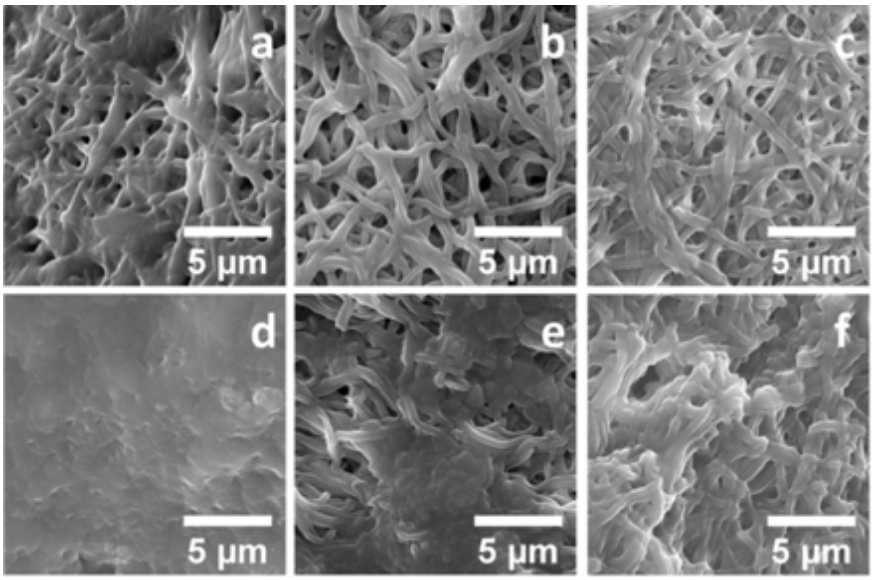

Figure 4: SEM images of SF-alb-hPL mats with different crystallinity. Micrographs a, b and c depict fiber morphology for the mats with crystallinity of 22%, 35% and 45% respectively, incubated in PBS for 1 month. Micrographs d, e and f, show the resulting morphology of mats at equal crystallinity after incubation with protease XIV (6.25mU/mg_{fibers}).

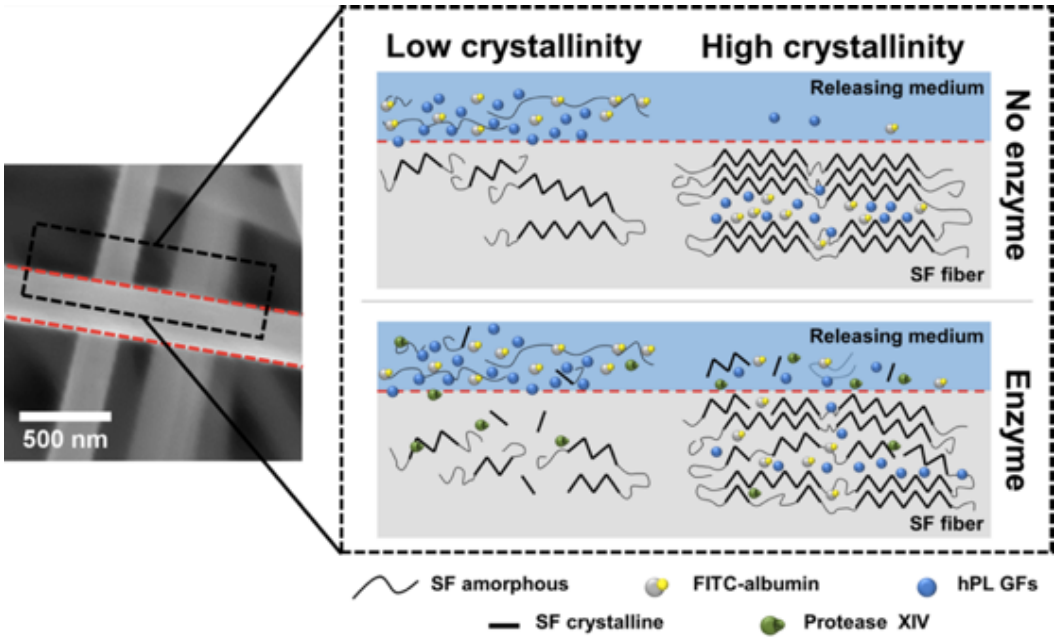

Figure 5: Proposed mechanism of controlled release from silk fibroin fibrous mats, considering the different silk fibroin crystallinity degree and the presence of the enzymatic activity. Low crystalline samples completely dissolved during the burst release, while the highly crystalline samples featured a reduced release due to the presence of the crystalline domains which impaired the diffusion of the FITC-albumin molecules. After the burst release, for the highly crystalline mats, when the enzyme degradation is not present, the molecules would remain entrapped in the fibroin matrix, whereas, by adding an enzyme, the degradation of the crystalline domain induces the release of the FITC-albumin and the other molecules embedded in it. Therefore, crystallinity also appeared to affect this second release step, since the silk fibroin crystalline domains constitute a physical barrier that limits the accessibility of the cleavage sites, leading to a slower degradation rate of the fibers during the release process. This leads to a crystallinity-dependent release.

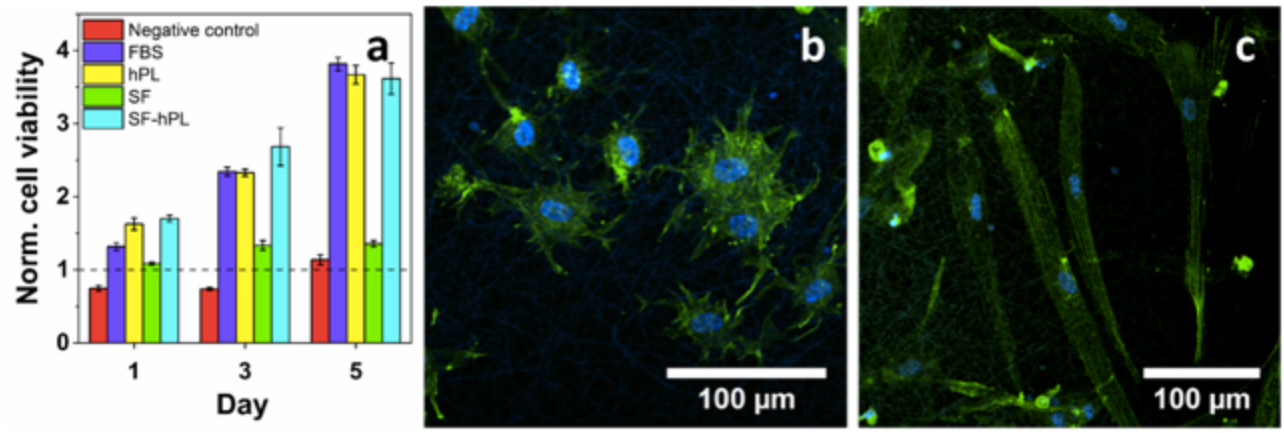

Figure 6: a) Viability of HDFa cells treated either with 250 µg/mL of hPL or with the extracts of SF and SF-hPL fibers. The values were normalized with respect to the absorbance value of the cells before the treatments, which is showed as a dashed line in the graph; the cells in presence of the hPL (SF-hPL and hPL) have a significative increase in their viability ($p<0.0001$); for all the they, the cells cultivated in presence of the hPL released from the fibers (SF-hPL) had no significative difference ($p>0.05$) with those grown with hPL in the medium (hPL); b) and c) Confocal images of HDFa cells seeded onto the SF and SF-hPL fibrous mats at 5 days of culture. F-actin is stained with the Alexa-fluor phalloidin (green), while nuclei are stained with DAPI (blue).

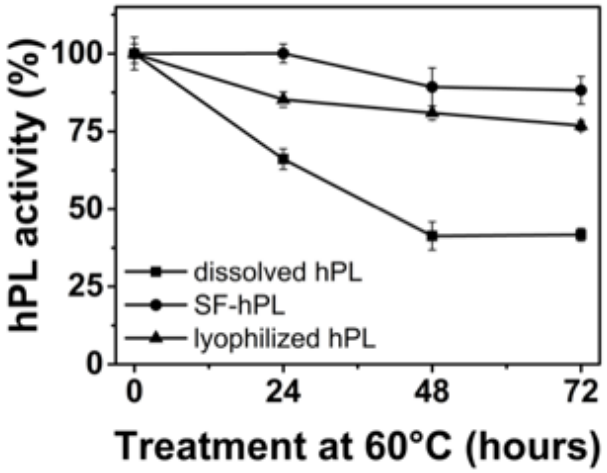

Figure 7: hPL activity of dissolved hPL, lyophilized hPL and hPL released from SF-hPL matrices after the accelerated stability test. The activity of the hPL released from the fibers after 3 days of thermal treatment had statistically more activity than the lyophilized hPL ($p<0.05$) and dissolved hPL ($p<0.0001$).

TABLES

a

Samples	*Crystallinity*	*Burst release 0-24 h*	*Sustained release 1-25 d*	*Sustained release 26-146 d*
SF-Alb	23%	100%	-	
	33%	41%	90%	100%
	46%	6%	38%	62%
SF-Alb-hPL	21%	100%	-	-
	35%	48%	80%	90%
	44%	10%	46%	74%

b

	Releasing rate of FITC-albumin		
	High crystallinity	Intermediate crystallinity	Low crystallinity
Burst 24h (%/h)	0.4	2	4
1-7 day (%/d)	1	2	-
8-20 days (%/d)	1.5	0.8	-
21-exhaustion (%/d)	0.4	0.1	-

Table I: (a) Summary of the release kinetics of FITC-albumin from SF-alb and SF-alb-hPL samples reported in Figure 3. (b) FITC-albumin releasing rate from silk fibroin fibrous mats at different crystallinity. The rates derive from the graph in Figure 3.

SUPPLEMENTARY MATERIAL

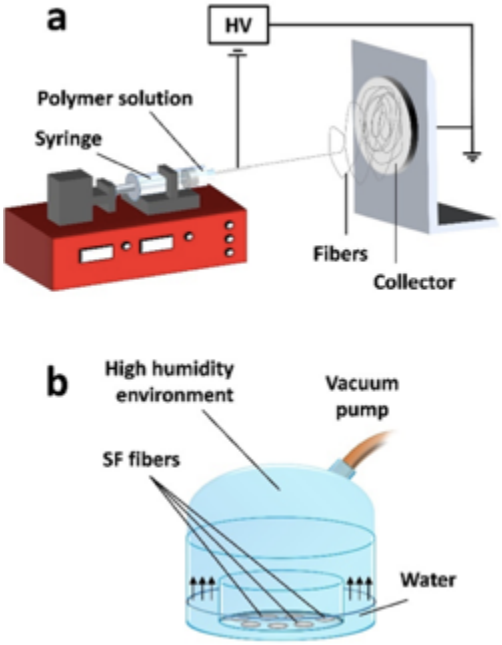

Figure S1: (a) Electrospinning set-up used to fabricate the different silk fibroin fibers mats. (b) Schematic of the water vapor treatment set-up used to increase the fibroin crystallinity.

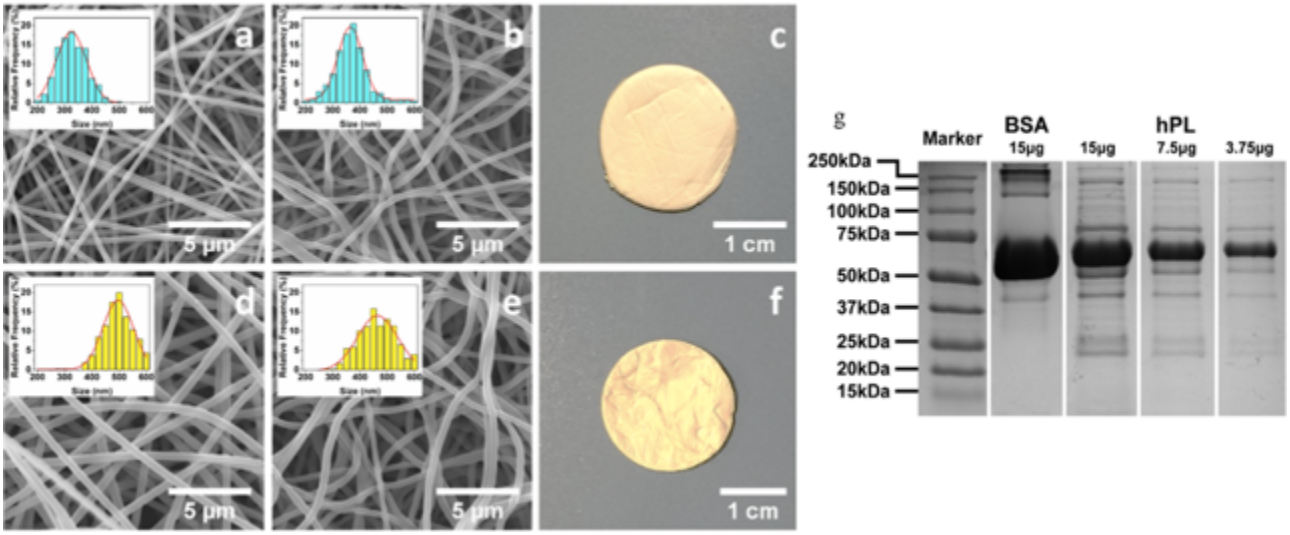

Figure S2: SEM images of SF-alb (a and b) and SF-alb-hPL (d and e) fibrous mats obtained via electrospinning. The fiber morphology is characterized before (a and d) and after (b and e) the water vapor treatment. Insets show the correspondent distribution of the fibers dimensions. Photo of the obtained electrospun SF-alb (c) and SF-alb-hPL (d) fibrous mats. (g) SDS-page of a BSA standard and hPL at different concentration.

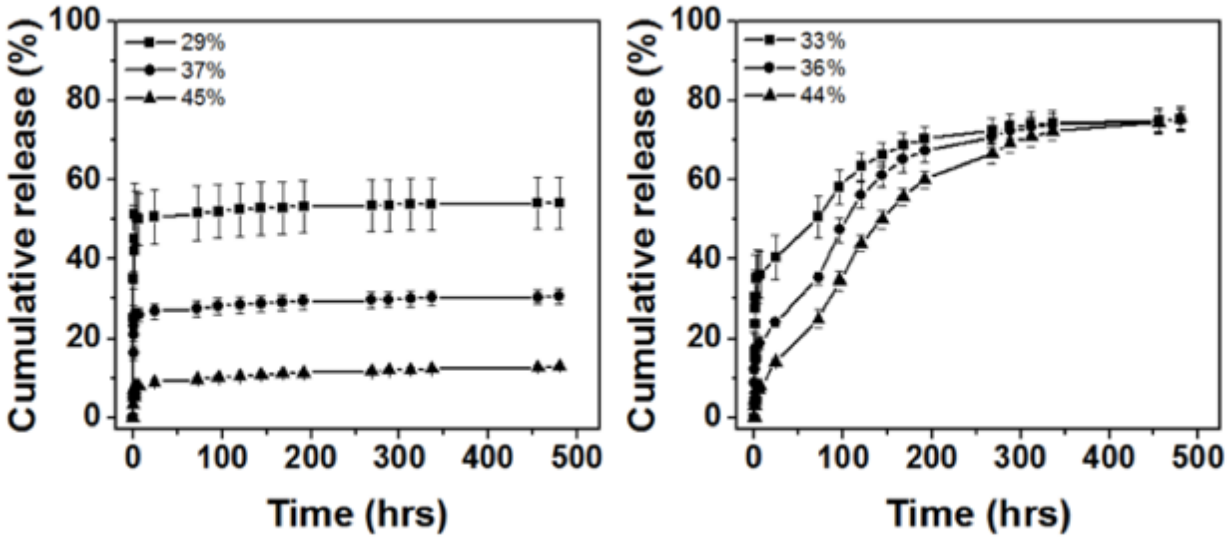

Figure S3: FITC-albumin released from electrospun mats in PBS buffer (left) and in PBS containing 0.25 U/mg_{fibers} of protease XIV (right). The percentages indicate the crystallinity of the electrospun mats used in the experiments.

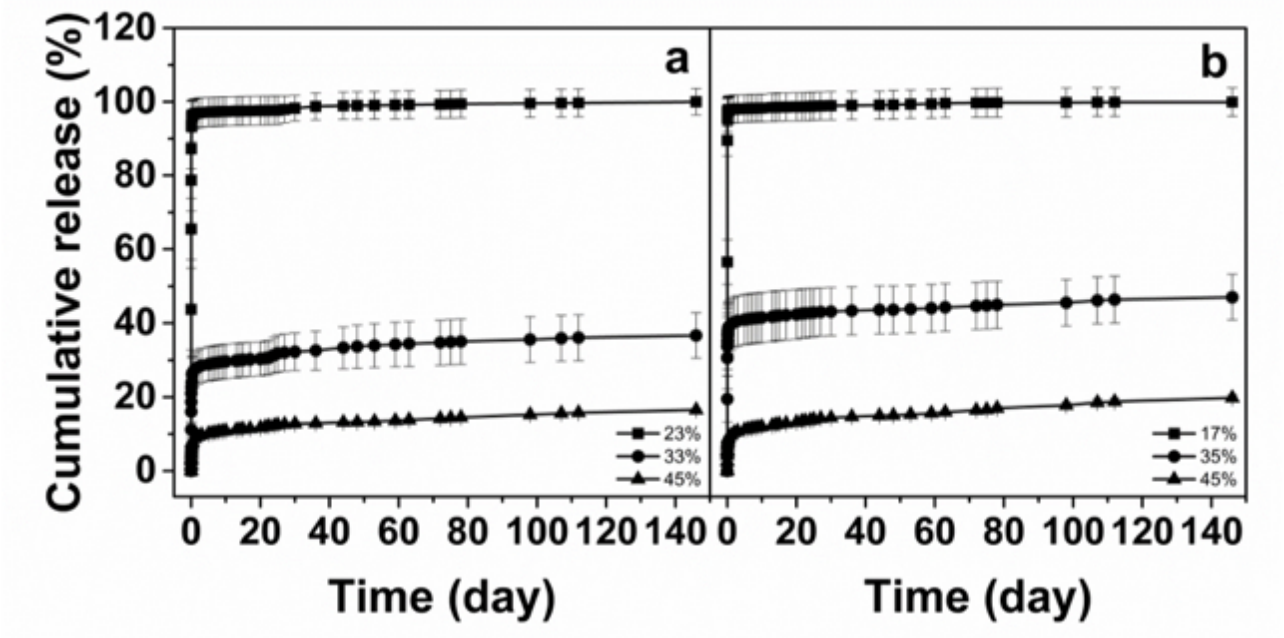

Figure S4: FITC-albumin released in PBS buffer from electrospun mats loaded with FITC-albumin (a) and loaded with both FITC-albumin and hPL (b). The percentages indicate the crystallinity of the electrospun mats used in the experiments.

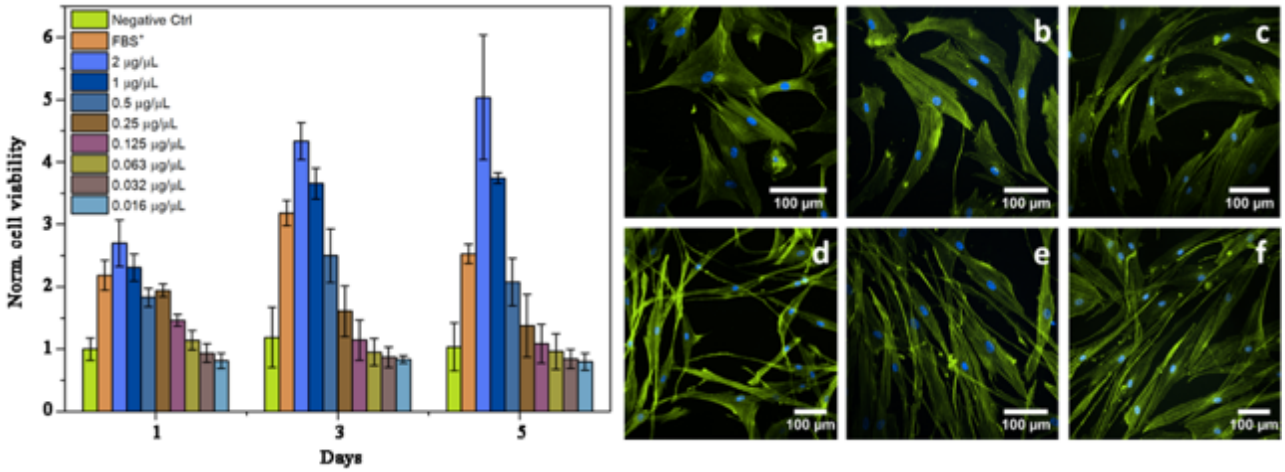

Figure S5: The graph shows HDFa cell viability upon treatment with different concentrations of hPL. On the left confocal images depicting HDFa cells seeded on glass coverslips for (a) 1, (b) 3, and (c) 5 days; HDFa cells seeded on glass coverslips and treated with hPL-containing media for (d) 1, (e) 3, and (f) 5 days. F-actin is stained with the Alexa-fluor phalloidin (green), while nuclei are stained with DAPI (blue).

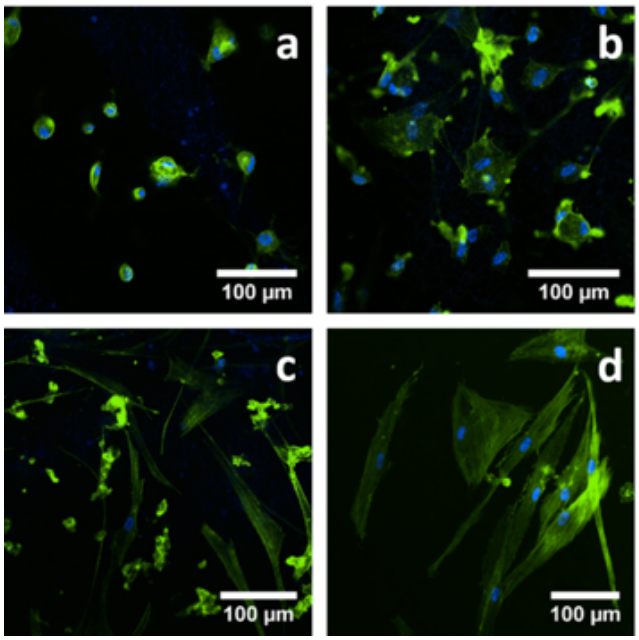

Figure S6: Confocal images depicting HDFa cells seeded on silk fibroin mats for (a) 1 and (b) 3 days; HDFa seeded on SF-hPL mats for 1 (c) and 3 (d) days; F-actin is stained with the Alexa-fluor phalloidin (green), while nuclei are stained with DAPI (blue).

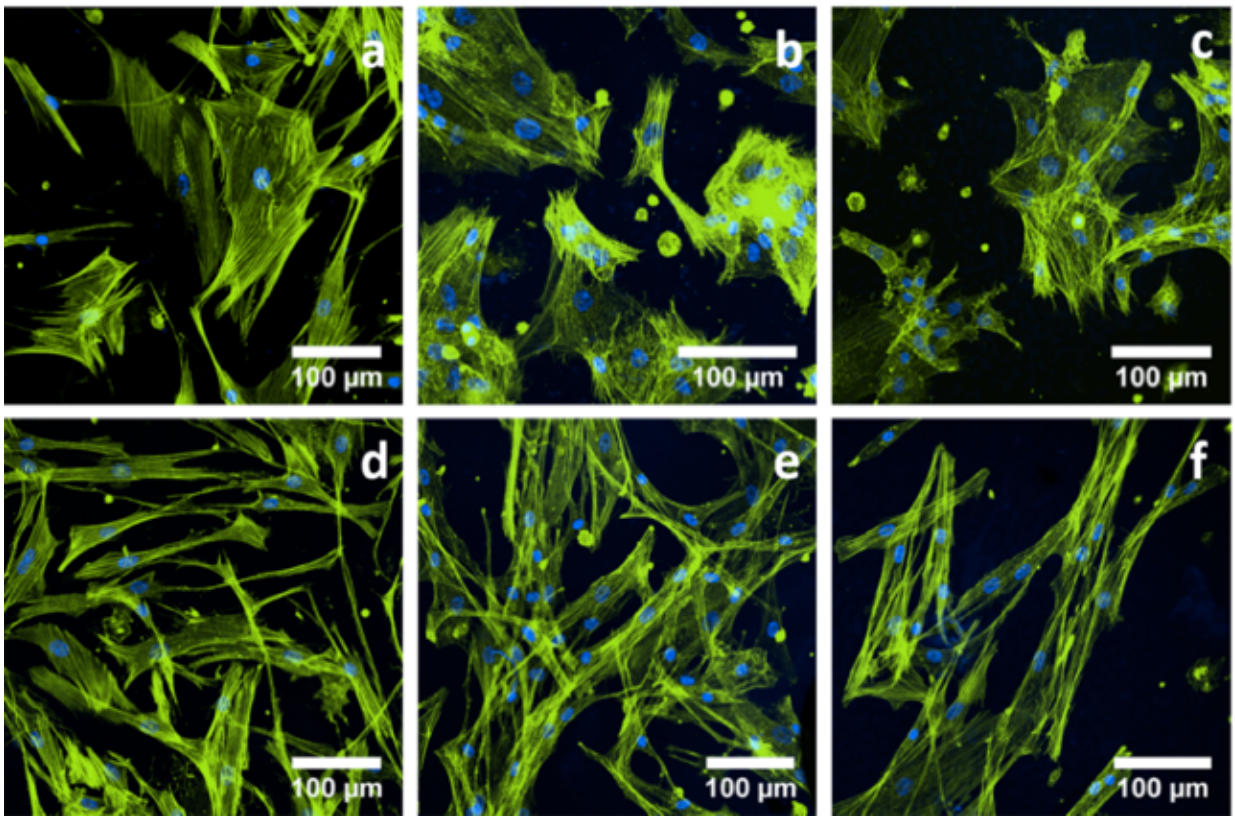

Figure S7: In a and d, confocal images of HDFa cells seeded on glass coverslips respectively without and with hPL. In b and c HDFa seeded respectively on film of silk fibroin and silk fibroin/PEO, respectively; in e and f HDFa, respectively on film of silk fibroin/hPL and silk fibroin/PEO/hPL, respectively. The images were acquired after 3 days of culture. F-actin is stained with the Alexa-fluor phalloidin (green), while nuclei are stained with DAPI (blue).

3. SERICIN, ALGINATE AND PLATELET LYSATE COMBINED IN A BIOMEMBRANE FOR THE TREATMENT OF SKIN ULCERS.

ABSTRACT

Chronic skin wounds with different etiophatology heavily compromise the patients' life quality and represent a high and constantly growing cost for National Health Services. Platelet derivatives (PL) has been used in clinical practice for reparative treatments of these pathologies, given their capacity to activate cell recruitment, proliferation, differentiation, as well as to regulate angiogenesis. We here report the development of a sericin/alginate sponge-like membrane as a new delivery system of PL.

Sericin (SS), alginate (Alg) and PL were solubilized in distilled water and cast into freeze-dried molds. An *in vitro* test was performed to quantify the growth factor release from sponge/PL membrane by ELISA kit. The *in vitro* capability of SS and PL, contained in our membrane, to induce proliferation and protective effects against oxidative stress was performed on BMSCs and human fibroblast (hFB) with MTT assay. *In vivo* efficacy of sponge/PL was evaluated by skin mouse model. The lesions were treated with sponge membranes, with or without PL, and covered by Tegaderm™. The animals were sacrificed at different times (3, 7, 14 and 21 days and a histological investigation was performed.

In vitro results indicated that the release of growth factors and the biodegradation of sponge membrane occurred within 48 hours, a time optimized to burst the healing process. The presence of SS contributes and support the effect of PL by controlling the release of growing factors.

The proliferation effects and the protection against the oxidative stress of our membrane, monitored on BMSC cells and hFB, was prevalently due to the presence of PL.

This *in vivo* analyses showed how Alg:SS:PL membrane led to a faster regeneration of the skin respect to the control one (Alg:SS). The inflammation phase occurred faster in treated lesion to evolve rapidly in the formation of granulation tissue and forming new collagen. These concatenation of events showed a non-complete resolution of the healing process in control lesions, but a burst of chronic inflammation probably induced by the presence of platelet derivatives as reported in several papers.

In this context we have studied and characterized a biomembrane composed of sericin, alginate in combination with a powerful inductor of cell proliferation, PL, that lead to complete skin regeneration. The SS contribute and support the effect of PL by its controlling its release into the lesion.

INTRODUCTION

Skin wound healing requires the recruitment and activity of different cell types, such as native immune response cells, endothelial progenitors, keratinocytes, and fibroblasts.

Platelet derived products, such as platelet gel, PRP or PL, have been used in the clinical practice for various reparative treatments since 1986 [133] to promote or facilitate the wound healing process. Wound treated with PL gel recovered more quickly in all patients, leading to a reduction of hospital stay and of the related cost. No adverse reactions were observed and all patients treated with platelet gel reported a significant pain relief, thus bettering their quality of life [168]. A recent review highlighted the positive effects of platelet-rich fibrin (a platelet concentrate produced without the use of non-coagulating factors) on wound healing of various soft tissue defects in medicine and dentistry [169].

Silk sericin (SS) is a globular and water-soluble protein with a molecular weight up to 200 kDa that, together with fibroin, constitutes the silk cocoon. In the past years, SS was considered a waste product of textile industry because, during the silk production, sericin is eliminated from the fibroin filaments by a degumming process.

The protein component is made of 17 amino acids, even if there are some differences depending on the variety of cocoon [170]. Generally, it is composed by 78% of polar amino acids (especially serine and aspartic acid) and by 22 % of non-polar amino acids [171].

The antioxidant flavonoids are able to protect cocoons from the oxidative stress and to inhibit the action of tyrosine. Ethanoic extracts of silk cocoons showed an antioxidant activity approximately double than that of vitamin E. The antioxidant activity of SS is due to its amino acid sequence, which allows to eliminate the free radicals and the reactive oxygen species (ROS) [172] and increases the antioxidant activity of enzymes, such as the superoxide dismutase and the glutathione peroxidase [171]. The large amount of hydroxyl groups contributes to this activity chelating trace elements such as iron, zinc and copper. Other amino acids, such as L-alanine and L-glycine showed cytoprotective properties on hepatocytes and kidney tubule cells [173].

It has been shown that treatment with SS inhibited apoptosis induced by UVB and the hydrogen peroxide formation, suggesting a role of SS in preventing mitochondrial damage [174].

The SS has often been added to the culture media not only for its ability to protect cells from oxidative stresses, but also for its mitogen effects, which occur according to yet unidentified mechanisms and which differ depending on the considered cell line [171].

Several studies reported that SS supports and enhances the cell growth of insect cells [175] and mammalian cells [171]. Sahu et al. [176] investigated the potential of sericin as growth supplement in serum-free culture medium on murine fibrosarcoma cell line.

The mitogen effect of SS on mammalian cells allowed its use also in regenerative medicine, as it could sustain the proliferation of keratinocytes and fibroblasts during the skin wound healing process[177]. The local administration of a SS cream on a skin lesion in a murine model significantly improved healing, when compared to a physiological solution or a cream without sericin [178].

Composite hydrogels, based on poly (γ-glutamic acid) and SS were used as wound dressing. These hydrogels promoted *in vivo* the granulation and capillary formation, as they maintained a moist healing environment, protected the wound from bacterial infection, absorbed excess exudates and promoted the reconstruction of the damaged tissue [179].

SS was also employed for treatment of burn-wounds, to prevent infections and reduce scars [180].

The treatment of wounds should remove exudate, if present, in order to prevent infections. For this reason, to date, wounds are often treated with dressings based on alginate, which has excellent biocompatibility and ability to adsorb exudate [181]. Alginates are water-soluble linear polysaccharides which are the major component of marine brown algae. They are widely used for tissue engineering because of their simplicity to create hydrogels in the presence of bivalent cations. In fact, alginate is constituted by two monomers: β-D-mannuronic acid (M) and α-L-glucuronic acid (G) linked by α1-4 binding. Due to their structure, G domains establish ionic bonds with divalent cations, such as calcium and magnesium, thus forming a hydrophilic gel [182]. High G alginates form much more rigid gels, while high M alginates form much softer and flexible hydrogels [183].

Moreover, alginate dressings do not have any side effects, even if, sometimes, a burning sensation could be experienced by the patient as result of the rapid movement of fluid from the soft tissue into the dressing matrix [183].

The combination of PL, alginate and SS led to the bird of highly effective bioactive devices for the treatment of chronic skin defects.

MATERIALS AND METHODS

Membrane fabrication

The sericin was obtained from cocoons of *Bombyx mori* belonging to the Orgosolo strain. They were degummed in an autoclave at 120 °C for 1 hour [172]. The resulting sericin solution was allowed to cool to RT and then spray dried using Büchi Mini Spray Dryer B-290. The sericin powder obtained was stored at -18 °C until use.

Alginate is a commercial product provided by Sigma (MO, USA).

Sericin and alginate powders were solubilized in water. At this point, two types of membranes were produced: Treated membranes obtained by addition of Platelet Lysate (PL) to the aqueous solution of sericin/alginate and control membranes to which PL was not added. The composition of the different of membranes synthesized is showed in the table below.

Type of membrane	Alginate (%)	Sericin (%)	PL (%)	Name
Control	50	50	0	Alg:SS
Control	100	0	0	Alg
Treated	25	25	50	Alg:SS:PL
Treated	50	0	50	Alg:PL

The membranes were fabricated in two different formulations, microspheres and sponges. The obtained solution was placed into special moulds (wells of 24 multi-wells), frozen and lyophilized to obtain circular sponges. To obtain the microspheres, the solution was spray dried one more time after the addition of PL.

With both membrane formulations s, we performed preliminary *in vivo* tests to determine which membrane was easy to handle. Preliminary results guided our experiments toward the use of sponge formulation according also to our interest to develop a patch for skin repair.

Kinetic release of membranes

Dosage of proteins and growth factors released by membranes was performed on the released product obtained from membranes. The membranes were allocated in transwells: 300 μL of physiological solution was placed on the bottom of the plate and 100 μL directly inside of transwell to allow the dissolution of membrane and release of protein content.

Approximately 350 μL of the physiological solution were collected at 30 min, 2, 4, 24, 48, 96, 120 and 144 hours and approximately 350 μL of fresh solution were added to each well after each collection..The harvested solution was aliquoted and stored at -20 °C for further analysis.

The total protein content was determined with BCA (Pierce™ BCA Protein Assay Kit) assay in all samples. Vascular Endothelial Growth Factor (VEGF), Platelet Derived Growth Factor (PDGF-BB) and Transforming Growth Factor Beta (TGF-beta) were evaluated in all samples by ELISA assays

(Human PDGF-BB ELISA kit, RayBiotech Inc; Human VEGF ELISA kit, Invitrogen; Human TGF-beta 1 Duo set ELISA R&D Systems) according to the manufacturer's instructions. All the measurements were performed on three different preparations. By these analyses we studied the kinetic release of different factors, determining the percentage of factors released respect to the quantity uploaded of platelet lysate.

Fourier transform infrared (FTIR) spectroscopy

Fourier transform infrared spectroscopy was performed on both bioactive membranes and single components (silk sericin, platelet lysate and sodium alginate). Samples were analyzed using a Spectrum One Perkin-Elmer spectrophotometer (Perkin Elmer, Wellesley, MA, USA) equipped with a MIRacleTM ATR device (Pike Technologies, Madison, WI, USA). The IR spectra in transmittance mode where obtained in the spectral region of 4000-650 cm^{-1}, with a resolution of 4 cm^{-1}. Measurements were carried out at least in triplicate.

Cell cultures

Human bone marrow stromal cells (BMSC) were obtained by treating femoral heads of patients undergoing orthopaedic surgery for hip rupture, who have previously signed an informed consent. The bone marrow was washed 5 times with PBS 1X. The obtained liquid was centrifuged at 1500 rpm for 10 minutes. The supernatant was discarded while the pellet was recovered and re-suspended in the appropriate volume of α-MEM (Lonza, Belgium) to obtain 50-100 nucleated cells per square in Burker's chamber. Counting was carried out using a nuclear dye (0.1% methyl violet in 0.1M citric acid). After counting, the cells were plated at a consonant density and allowed to adhere. Only BMSC adhere to the bottom of the plate and therefore they were selected by washing the plates with PBS 1X. The cells were cultivated in α-MEM supplemented with 10% FBS or 5% of PL, 100 UI/mL penicillin, 100 μg/mL streptomycin and 2 mM L-glutamine. Once the cells reached confluence, they were detached using 0.05% trypsin-0.01% EDTA, counted and plated at a density of 7 x 10^4 cells per 6 cm Ø Petri dish for cellular expansion.

Human fibroblast cells (hFB) were obtained from human skin fragment derived from discarded samples of patients undergoing reconstructive mastoplasty surgery, who have previously signed an informed consent. The skin was separated from the fat layer below. The extracted pieces were disinfected by immersion in 70% ethanol followed by two washes in sterile 1X PBS. To extract cells, the tissue fragments were transferred into a 10 cm Ø tissue culture dish using sterile scalpel avoiding the transfer of excess of PBS with the sample. The tissue was cut using two scalpels into ~1 mm pieces that were transfered to the centre of a sterile 10 cm Ø Petri dish. A sterile slide was put over the tissue exercising a pressure over the skin fragments. Then, α-MEM (Lonza, Belgium) supplemented with 10% FBS or 5% of platelet derivatives, 100 UI/mL penicillin, 100 μg/mL streptomycin and 2 mM L-glutamine was added. The fibroblasts start to exit the tissue fragments within 7 days.

Once the cells reached confluence, they were detached using 0.05% trypsin-0.01% EDTA, counted and plated at a density of 7 x 10^4 cells per 6 cm Ø Petri dish cellular expansion.

Proliferation assay

Cell viability was assayed performed to test the biocompatibility of sericin alone or in combination with PL, since alginatehas been already reported in literature to be biocompatible [184]. Thiazolyl blue staining (MTT) was performed on BMSC and hFB grown in serum free medium or in medium containing SS PL or SS and PL in combination. BMSC and hFB at a density of 1 x10^3 cells per well were plated in a 96-well plate in 10% FBS. The day after, the cells were washed with PBS to remove the FBS and exposed to the different treatments.

Cell proliferation was assayed 0, 24, 48 and 72 hours after treatment. At each time point, cells were incubated with MTT for 3 hours, then the MTT solution was removed and 100 µL of absolute ethanol was added per well to solubilize the formazan product. The reduction of MTT to formazan was quantified by reading the absorbance at 570 nm and 670 nm by spectrophotometry.

All tested conditions are summarized in the table below:

Condition	Serum Free	5% PL	1% Sericin
1	√	-	-
2	-	-	√
3	-	√	-
4	-	√	√

Oxidative stress induction and anti-oxidant assay

BMSC and hFB were seeded as described above and grow on medium contained SF, PL or a combination of both. Oxidative stress was induced by treating the cells with 3 mM H_2O_2 for 24 h. The antioxidant capacity of sericin was evaluated by MTT assay as described above.

The MTT reading was performed after 24, 48 and 72 hours after treatments.

The treatments applied are summarized in the table below.

Condition	5% PL	3 mM H_2O_2	1% Sericin
1	-	√	-
2	-	√	√
3	√	√	-
4	√	√	√

***In vivo* analysis-mouse wound healing model**

In vivo tests were performed to determine the efficiency of our membranes. C57/BL6 wt mice were anesthetized with xylazine/ketamine. Once anesthetized, the mice were depilated on the dorsal surface with depilatory cream, so that mouse hair did not affect the evaluation of the wound closure. A full-thickness wound was performed with a circular 6mm punch. An empty sponge (control) or a sponge loaded with PL (treated) was then applied over the wound Next, a transparent patch (Tegaderm) was applied over the lesions to protect the wound from any contact with external agents. After finishing the surgical procedure, mice were returned to their cages and kept under red light to compensate for the hypothermic effect of the anesthesia. Every two days the wounds were photographed.

The mice treated with membranes containing sericin were euthanized with carbon dioxide 2,3,7,14 and 21 days after surgery, while the mice treated with membrane containing only alginate were euthanized after 3,7 and 14 days.

Histological analysis

All harvested samples were fixed with 4% paraformaldehyde at RT for 24 hours and paraffin embedded for tissue sectioning. 5 μm thickness sections were prepared and stained by hematoxylin-eosin and trichrome blue staining. The evaluation of different parameters was performed following guidelines provided from Abramov et al. [185] in collaboration with Prof.ssa Grillo and Dr. Mastracci of the Department of Pathological Anatomy of Ospedale Policlinico San martino (Genova).

Statistical analysis

All in vitro experiments were conducted in duplicate on different primary cell cultures. Statistical analyses were performed using the two-way ANOVA provided by the Graphpad Software (www.graphpad.com). All *in vivo* experiments were conducted in triplicate for the membranes of Alg:PL and seven time for Alg:SS:PL membranes at time 3-7 and 14 days, instead, was conducted in triplicate for 2 and 21 days. Statistical analyses were carry out using Mann-Whitney test to evaluate in the best possible way, the differences between treated and control lesions.

RESULTS

Characterization of the sponges

We performed a deep characterization of the biomembrane, evaluating the growth factors released in term of kinetic analysis and quantization of total content of proteins to determine the efficiency of this new typology of membrane.

First, we compared the total protein content in both membranes based on Alg:PL and Alg:SS:PL.

The histogram in figure 1 shows the release of the proteins for both membranes with the same trend but different protein content. The differences in term of total proteins released were attributed to the presence of sericin in one of the two sponges, that is a protein.

Considering that the membranes were loaded with the same quantity of PL (50% w/w), standardized for the equal platelet count, we evaluate the release by the measurements of the principal growth factors contained in PL, PDGF-BB, VEGF and TGF-β, as reported in literature [3] using ELISA tests.

In the Figure 2 a, b and c is showed the released product of VEGF, PDGF-BB and TGF-β respectively in both membranes. The statistical analysis demonstrated that VEGF is released in the similar way (not statistically significant), whereas the PDGF-BB and TGFb are released differently for both membranes (Fig. 2 b-c).

Growth factors kinetic release from sponges

To evaluate the kinetic release of the three principal growth factors released from both membranes, (Alg:SS:PL and Alg:PL), we performed the analysis as described in material and methods. The harvested samples were analysed for the total amount of PDGF-BB, VEGF and TGF-β respectively as represented in Figure 3 and reported each value in term of percentage, like the maximum capability of the sponge to release a specific growth factor. For each time point, we estimated the ability of the membranes to release the factors in term of percentage.

PDGF-BB kinetic release showed statistical differences between the Alg:PL and Alg:SS:PL membranes during time (Fig. 3b). The same behaviour is registered for TGF-β (Fig. 3c), but not for VEGF (Fig. 3a).

Considering the different curves of released PDGF-BB, VEGF and TGF-β, we underlined that in Alg:SS:PL membrane the PDGF-BB showed a burst in the first 4 hours to which follows a gradual release to reaches a plateau during next hours. Instead for the membrane composed of Alg:PL we observed a growing release during time and any burst was evident.

FTIR analyses of single component and membranes

FTIR spectrum of silk sericin (Figure 4a) showed a peak between 1800-1600 cm^{-1} and characteristics of the stretching vibration of C=O groups. Peaks at 3500-3000 cm^{-1} are associated with N-H stretching vibrations. At 1513 cm^{-1} it was possible to show an amide II absorption band; while C=O symmetry stretching was observed at about 1400 cm^{-1} (1397 cm^{-1}). FTIR peaks of

lyophilized silk sericin considered for this study was similar to those obtained by other researchers [172,186,187].

Sodium alginate FTIR spectrum (Figure 4a) presented absorption bands around 1590 cm^{-1}, 1402 cm^{-1}, and 1291 cm^{-1} that are correlated to stretching vibrations of asymmetric and symmetric bands of carboxylate anions. A not well resolute band at about 3400 cm-1 is characteristic of –OH stretching vibrations. Similar spectra, presenting the same characteristic absorption bands, were obtained by Khurana et al. [188] and Rao et al. [189].

FTIR analysis of PL (Figure 4a) showed the characteristics peaks of proteins, as reported by Barth [190]. The NH stretching vibration of amide A and B gives rise two to bands at 3277 and 3061 cm^{-1}, respectively. Absorption band at 1641 cm-1 is correlated to C=O stretching vibration of amide I, while peaks at 1540 and 1451 cm^{-1} are related to the amide II bending and stretching vibrations (NH and CN groups, respectively). Contributions of amide III-correlated NH bending vibration are visible in the 1400-1200 cm^{-1} region.

After analysis of single components, FTRI was performed on alginate, sericin and platelet lysate-based membrane (Figure 4 b) demonstrating the simultaneous presence of absorption bands related to OH stretching vibration of alginate chains and to NH stretching vibration of platelet lysate (3400-3000 cm^{-1} region). In the region 1600-1100 cm^{-1} peaks are principally correlated to the amides of platelet lysate (1538, 1402, 1121 cm^{-1}). An interaction between two components was observed by the shift of absorption bands of sodium alginate, from 1595 to 1590 cm^{-1}, and of platelet lysate, from 1294 to 1305 cm^{-1}. FTIR spectrum of Alg:SS:PL membrane was superimposable to the spectrum of control membrane (Alg:PL) though a peak at 1639 cm^{-1}, attributable to the presence of sericin, was well-visible. Moreover, the addiction of silk sericin to bioactive membrane induced the interaction between functional groups of protein chains; in particular, it was possible to observe the presence of a well-defined peak at 1241 cm^{-1}, not visible in platelet lysate and sericin spectra, owing to C-N stretching vibrations in the amide III linkage.

Biocompatibility of the membranes

To evaluate the biological efficiency of alginate and sericin based biomembranes we tested the capacity of cells to proliferate under the stimulation with sericin. In literature it has been already demonstrated that the alginate is inert in terms of biocompatibility [191], but it plays an important mechanical role [192,193] because it can form hydrogels simulating extracellular matrices of living tissues [191].

Sericin effect on a BMSC and hFB cells is evaluated in term of cell proliferation: as reported in the Figure 5 a, in BMSC the sericin alone sustained the vitality of the cells without statistically significant differences respect to the medium alone (SF). However, when sericin was in combination with PL, cell proliferation was significantly increased compared to SF condition at successive time points ($p=0,0199$ at 24 hours, $p=0,0001$ at 48 hours and $p<0,0001$ at 72 hours).

Also in hFB (Figure 5 b), sericin alone maintained the cell vitality with statistically significant difference at all time points ($p<0,0001$) and when in combination with PL, cell proliferation is

increased and the difference from SF condition is statistically significant on progressive time points ($p=0,0245$ at 24 hours, $p<0,0001$ at 48 hours and $p<0,0001$ at 72 hours).

Protection against oxidative stress due to membrane

In literature it has been reported that the SS plays a role in protection of cells against oxidative stress [172]. To support the choose of SS in our membranes, we performed experiments of oxidative stress on BMSC and hFB administering to the cells a dose of hydrogen peroxide (3mM) that previously has been demonstrated to be toxic.

We noticed (Figure 6a and b) that the cells treated with only 1% of sericin, the same amount contained into the membrane, is not sufficient to protect cells from oxidative stress if compared with only hydrogen peroxide in the medium ($p\geq0.9999$ for BMSC and hFB for all the time points examinated). Sericin is more efficient in combination with PL against H_2O_2 for BMSC cells and hFB ($p=0,0044$ for BMSC and $p=0,0016$ for hFB at 24 hours, $p<0,0001$ at 48 hours and $p<0,0001$ at 72 hours for both types of cells). Considering that the PL showed a protective effect from H_2O_2 when was supplemented alone in the medium, we suggest that the real contribution to this protective effect of the Alg:SS:PL membrane in both types of cells was due to the PL.

Sponge effect in excisional wound healing mouse model

To evaluate the effect of the membranes in vivo, we used excisional wound healing mouse model in C57/BL6 mice. A full-thickness skin lesions were created in the back of the animals and a membrane was applied. For each animal we applied two membranes: one without PL as control and one with PL as treatment. First, we performed the *in vivo* experiment using sponges composed of Alg:SS, Alg, Alg:PL and Alg:SS:PL to evaluate if there were differences among the different compositions.

The in vivo results were obtained from histological analysis of the samples recovered from the animals at different time of implant (2,3,7,14 and 21 days).

In Figure 7 different steps of the wound healing process is reported as histological images comparing the Alg:SS:PL and Alg:SS membranes. Hematoxilin-eosin staining showed the closure of the lesion in the treatment (Alg:SS:PL) and control (Alg:SS) at 3 weeks, highlighting a more organized tissue similar to healthy skin of the mouse in the treatment. At 3 days the inflammation is evident but completely substituted from the granulation tissue at 1 week. The results of histological analysis were based not only on macroscopic investigation but also on the evaluation of the parameters providing from Abramov et al. [185]: 1) inflammation is considered as acute inflammation defined by presence of neutrophils and chronic inflammation by presence of plasma and monocytic cells; 2) granulation tissue as granulation tissue amount and as granulation tissue fibroblast maturation where the degree of maturation of the granulation tissue was determined by the shape of fibroblast and their alignment; 3) collagen deposition according to the amount of more or less mature collagen fibers; 4) reepithelization based on the degree of closure of the lesion and 5) neovascularization on the number of counted vessels.

Preliminary *in vivo* tests on three animals per group, demonstrated that the membranes containing Alg without SS didn't show any different effect in the closure of the skin lesions respect to the the membranes containing SS (data not shown).

In this respect we increased the animal number per group, comparing the Alg:SS and Alg:SS:PL membranes to focus the attention on the role of PL and SS. All evaluations were reported in the plot as difference between the treatment and control membranes. As reported in Figure 8 (a) acute inflammation was more evident in the control respect to the treatment after two days, whereas (b) the chronic inflammation was clearly more evident in the treatment. In the following times there is no statistically significant difference between the control and the treatment for both acute and chronic inflammation. At 21 days chronic inflammation appeared evident only in the control.

The parameter concerning the granulation tissue is evaluated as (c) granulation tissue amount and (d) granulation tissue fibroblast maturation. All these parameters showed an increment in the treatment respect to the control after 3 days statistically significant respect to 7 days. (e) The collagen deposition was more evident in the treatment respect to the control and no statistically significant difference was at different time of implant.

(f) The reepithelization occurred faster in treated wound showing no difference between treatment and control until 7 days. At 14 days an increment of the reepithelization in the treatment was evident.

In term of neovascularization (g) any difference was noticed between the two lesions until 14 days where the control lesion showed a prevalence of vessels. This could be due to the delay in the wound healing process in the control animal in which, at the same time during the treatment, the reepithelization occurred.

DISCUSSION

Autologous platelet-derived products, such as Platelet Rich Plasma gel, have been used in the clinical practice for various regenerative treatments [10–13].

Many studies have been conducted to evaluate the effectiveness of PRP gel for the treatment of chronic and diabetic ulcers [2,194,195]. The PRP gel is derived from blood by the combination of PRP and a fibrin rich matrix extracted from plasma, which in presence of thrombin and calcium generates a growth factor enriched membrane [27,196,197]. Released growth factors activate a cascade of signals that lead to the tissue repair [197]. The platelets are widely recognized as having a critical role in primary hemostasis and thrombosis and experimental and clinical evidences identified these enucleated cells as relevant modulators of other physiopathological processes including inflammation and tissue regeneration. These phenomena are mediated through the release of growth factors, cytokines and extracellular matrix modulators that sequentially promote (i) revascularization of damaged tissue through the induction of migration, proliferation, differentiation and stabilization of endothelial cells in new blood vessels; (ii) restoration of damaged connective tissue through migration, proliferation and activation of fibroblasts; and (iii) proliferation and differentiation of mesenchymal stem cells into tissue-specific cell types. For these reasons, PRP derivatives are used in regenerative medicine for the treatment of several clinical conditions including ulcers, burns, muscle repair, bone diseases and tissue recovery following surgery. The benefits of PRP administration are associated with an economical advantage, taking into consideration that PRP administration does not require complex equipment or training for its execution [198]. For these reasons, many studies have been focused on the controlled release of platelet growth factors in the regenerative process studying the kinetic of release and the activated molecular mechanisms [71,72,199].

In regenerative medicine the concept of biomaterial as scaffold to guide the cells into the site of tissue regeneration, it has also been used to control the release of the growth factors [200–202]. In this context we have considered a new tool to repair damaged tissue by the combination of platelet derivates and biomaterial based on Sericin, a silk protein. Silk sericin, a protein fiber, is derived from spider or some lepidoptera, from which they can be obtained fine fabrics. Primarily it can be collect from cocoons of silkworm of the *Bombix mori* specie.

SS is a globular and water-soluble protein that has attracted much interest in the last years. In fact, this protein showed to effectively sustain the proliferation of different mammalian and insect cell lines and, thanks to its free-radical-scavenging activity, to protect them from the oxidative stress [203]. Due to its mitogen effect on mammalian cells, SS was also used for the improvement of the healing process. This protein has been found to have no immunogenicity and it is now utilized in biomedical applications [204]. An increasing number of studies have focused on the usefulness of sericin in biomedical applications because it has several biological activities, such as anti-oxidation, anti-bacterium, anti-coagulation and promotion of cell growth and differentiation [205–207]. In the field of regenerative medicine, owing to its biodegradability, easy availability, and hydrophilicity with many polar side groups, sericin is mostly copolymerized, crosslinked, or blended with other

polymers to form various scaffolds in order to help obtain improved properties for relevant biomedical applications [208–210] such as skin regeneration.

During the wound healing process, to facilitate the tissue regeneration and prevent infections, wounds must be kept in a moist state, without excess of exudate. For this purpose, alginate, a natural and biocompatible polymer, was introduced as component of the membrane with SS and PL because of its absorbance and ability to form a gel [181]. In our work a membrane based on Alginate, sericin and platelet derivatives was developed for ulcer care and designed to control the release of platelet factors in the skin lesion. First, several combinations of three components were tested in term of release of growth factors (data not shown), choosing finally a ratio 25:25:50 of Alg:SS:PL. This composition was used to develop a device for skin regeneration. The growth factor release study was performed in the membranes containing PL monitoring PDGF-BB, VEGF and TGF-β factors; the protein content in the membrane composed of ALg:SS:PL was higher than the control membrane based only on Alg:PL due to the presence of sericin. The release kinetic studied by ELISA assay showed a different trend for the three factors monitored, VEGF and TGF-β were released for the 50% in the first two hours, as an initial burst, from gel formation to follow a gradual release in the next 6 days until a plateau, for both typologies of membranes, with and without SS. PDGF-BB resulted to be released with the same trend of VEGF and TGF-β in the Alg:SS:PL membrane, whereas its release from Alg:PL membrane appeared more slowly and no initial burst occurred. In the hypothesis that this was related to a different affinity of growth factors to sericin an FTRI analysis was performed to understand the interaction among different components of the membrane. Fourier-transform infrared spectroscopy (FTIR) is a technique used to obtain an infrared spectrum of absorption or emission of a material allowing the study the interaction among the molecules. Thus, FTIR analysis showed that the addiction of silk sericin to bioactive membrane induced the interaction between functional groups of protein chains; the comparison of absorption spectra of the components showed a in particular the presence of a new well-defined peak, not visible in platelet lysate and sericin spectra, owing to C-N stretching vibrations in the amide III linkage.

Considering the role of the sericin in the tissue regeneration, the effect of SS and PL was evaluated in cell proliferation and in oxidative stress condition of mesenchymal stem cell derived from bone marrow and skin fibroblasts. The dose of SS and PL supplemented to the culture medium simulated the same amount and ratio in which they are mixed in the membrane. The sericin has no effect on cell proliferation even if it is not toxic to cells because it allowed them to grow better than in serum free condition. Sericin in combination with PL favored the proliferation, but much of this effect has been attributed to PL. This behavior was reproduced in BMSC and fibroblast cells. This result is in line with the data published from other authors in the ability of SS to maintain cell vitality [211,212]. Regarding the protection of SS against oxidative stress induced by H2O2, our experiments showed that sericin alone was not sufficient to protect the cell vitality. But SS in combination with PL guaranteed the cell vitality also in oxidative stress culture conditions. This

effect was ascribable to the PL that alone showed the same effect. The BMSC and fibroblast had the same behavior [172,213].

These findings lead us to consider a key role of the PL as a good inductor of cell proliferation and protector from oxidative stress condition and the SS a good modulator of its release. To be more sure of our hypothesis derived from *in vitro* experimental data, a wide study *in vivo* in mouse skin regeneration model was performed. Membranes based on Alg:SS:PL and Alg:SS were applied on the back of mouse where a critical skin lesion was created. The samples recovered at different time from the application on the cute were histologically analyzed.

This analysis showed that Alg:SS:PL membrane led to a faster regeneration of the skin respect to the control one (Alg:SS). The inflammation phase occurred faster in treated lesion to evolve rapidly in the formation of granulation tissue and forming new collagen. This concatenation of events showed a non-complete resolution of the healing process in control lesions, but a burst of chronic inflammation in the treated wounds, probably induced by the presence of platelet derivatives as reported previously in several studies [32]. Also the reepithelization phase occurred in 14 days in treated lesion respect to the neovascularization that delayed in the control lesion. This is associated with the inflammation, collagen deposition, granulation tissue formation parameters that led to conclude that there is a faster resolution of the wound healing process in the treated lesion.

In conclusion this work propose a handle membrane composed of biomaterial (alginate and sericin) that are biocompatible and have particular mechanical properties [171,184,214,215] in combination with a powerful inductor of cell proliferation, PL, that lead to complete skin regeneration. The SS contribute and support the effect of PL by its controlling its release into the lesion.

This work is in preparation:

Sericin, alginate and platelet lysate combined in a biomembrane for the treatment of skin ulcers.

Nardini M., Perteghella S., Cancedda R., Torre M.L., Mastrogiacomo M.

FIGURES

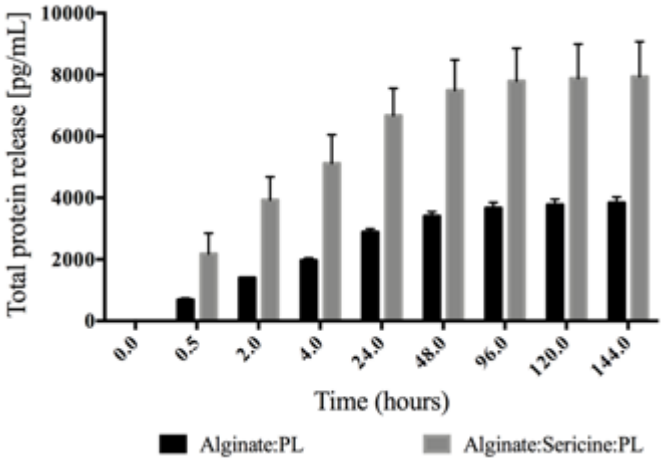

Figure 1: Proteins release during time from our membrane. There is not a statistical analysis because the two membrane cannot be compared in terms of protein because the presence of sericin in one of the two membranes.

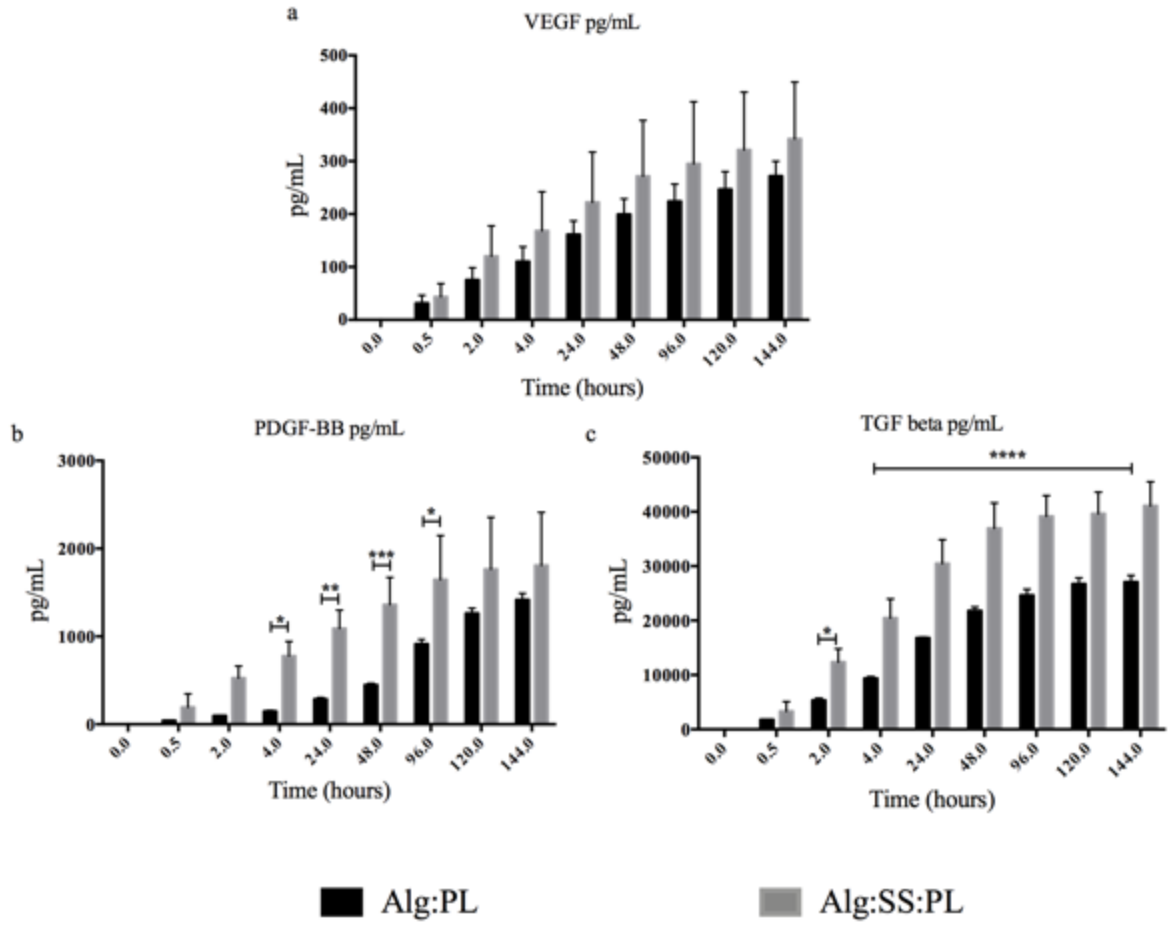

Figure 2: Release of the principal growth factors contained in PL from Alg:PL and Alg:SS:PL membranes overtime. No statistical differences were observed in released VEGF (a); the release of PDGF-BB was higher

form Alg:SS:PL membranes starting from 4 h until 96h (b); (c) TGF-β was higher released from Alg:SS:PL membranes starting from 2 h until the end of the experiment (144 hours). * p<0.05, **<0.01, ***p<0,0001.

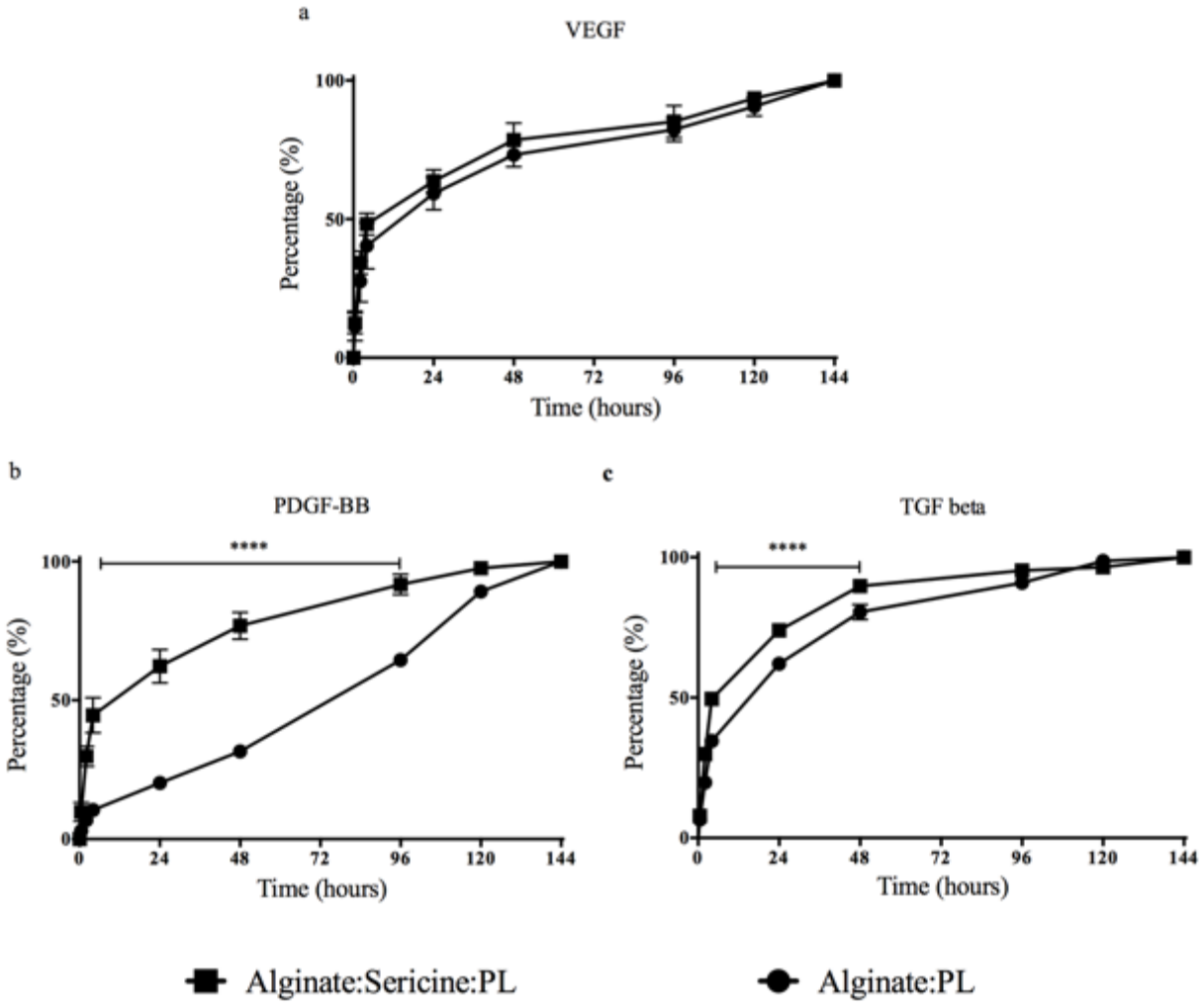

Figure 3: The curves represent the kinetic of the release of three different factors expressed as percentage of the maximum release; VEGF (a) without statistical differences, PDGF-BB (b) with a statistical difference between the two membrane from 2 to 96 hours (p<0,0001) and TGF beta (c) with statistical difference from 2 to 48 hours (p<0,0001).

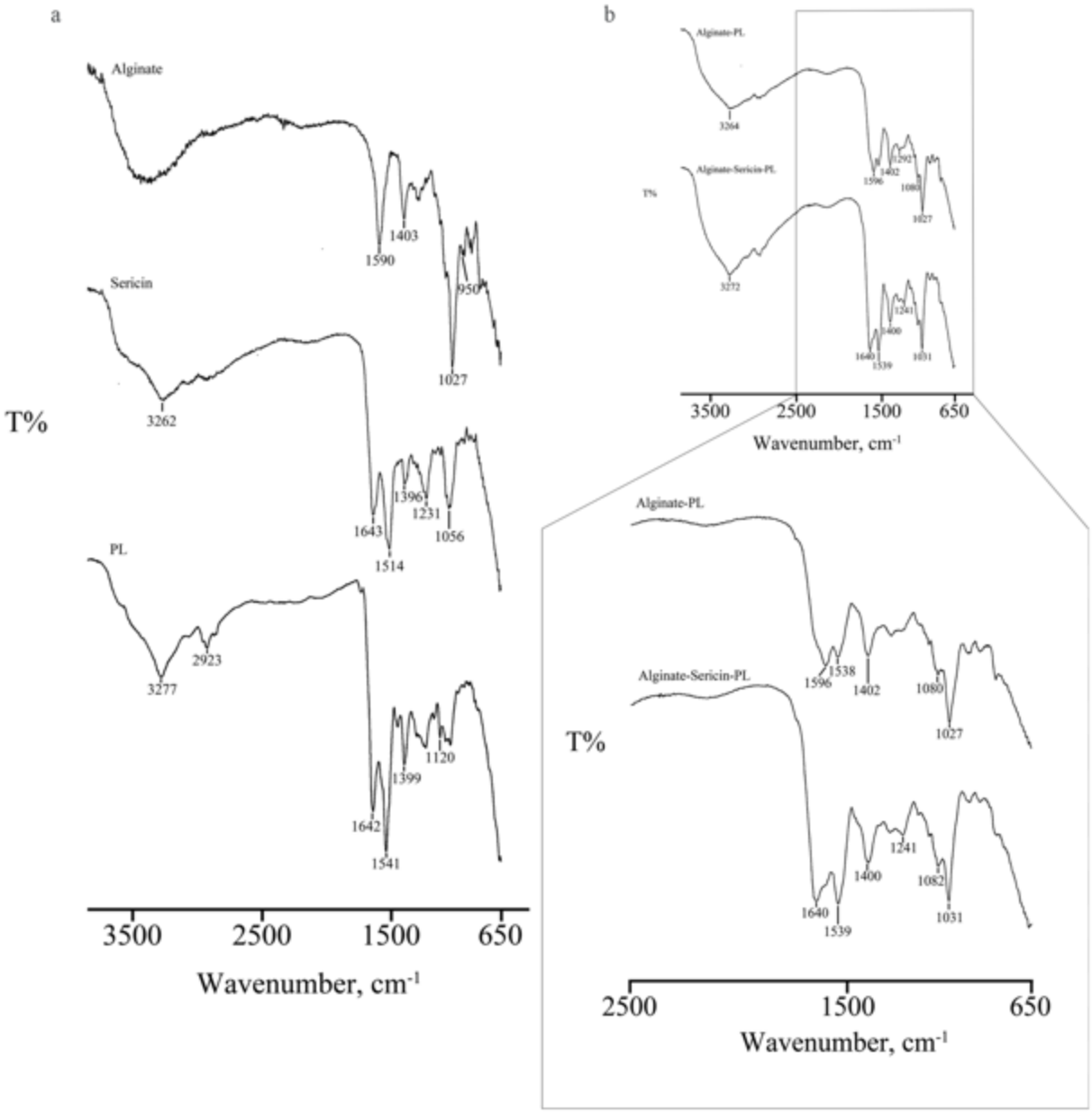

Figure 4: Fourier transform infrared (FTIR) spectroscopy was performed on both single components (silk sericin, PL and sodium alginate) (a) and bioactive membranes (b) The IR spectra where obtained in the spectral region of 4000-650 cm^{-1}.

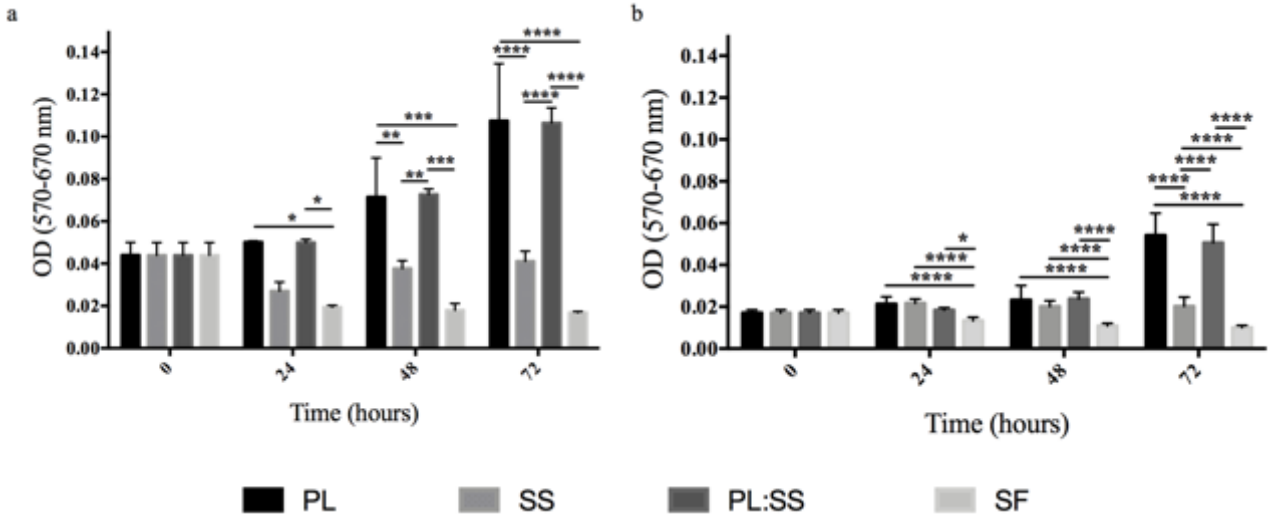

Figure 5: The two graphs show the cells viability in presence of sericin. We perform the experiments with two different cell types BMSC (a) and hFB (b). * $p<0.05$, ** $p<0.01$ and *** $p<0.0001$.

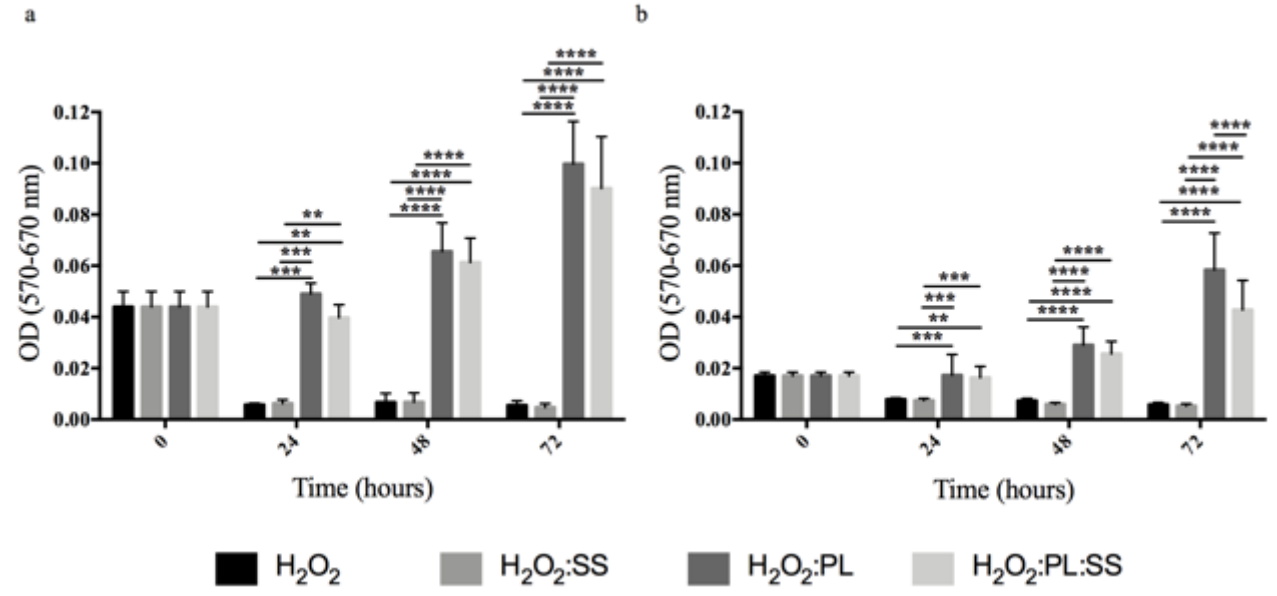

Figure 6: The two graphs show the cells viability after oxidative stress induced by H_2O_2 (3mM) and treatment with sericin. We perform the experiments with two different cell types BMSC (a) and hFB (b). * $p<0.05$, ** $p<0.01$ and *** $p<0.0001$.

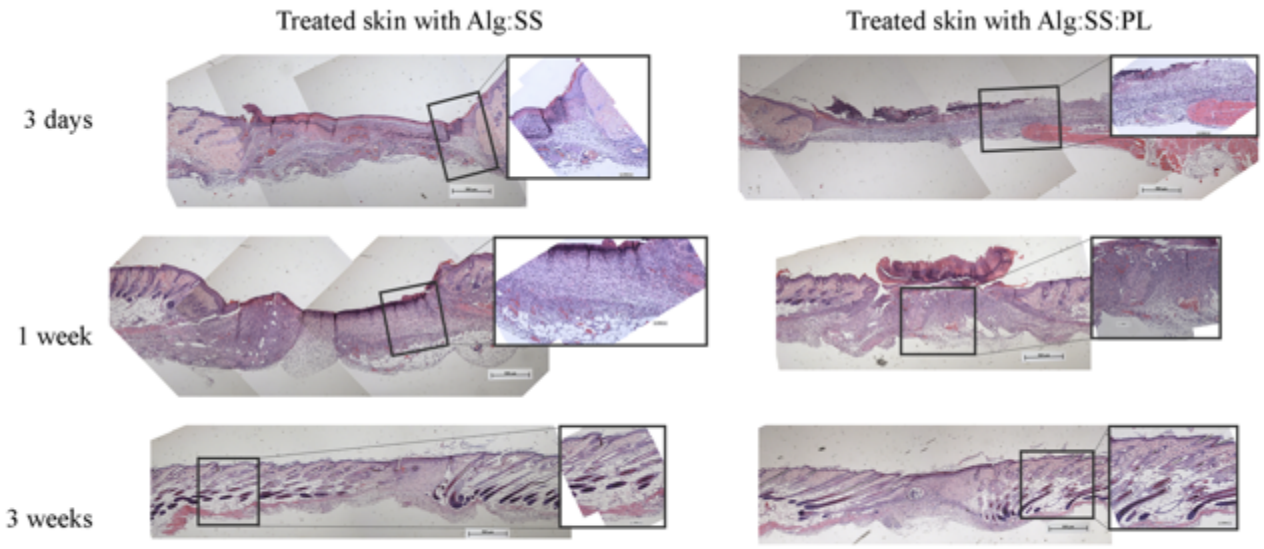

Figure 7: Histological analysis of treated (Alg:SS:PL) and untreated (Alg:SS) lesions. Images were acquired at 5x magnification (5mm scale bar) and 20x magnification (1mm scale bar). The sections were cut at 5 μm thickness and stained with haematoxylin-eosin.

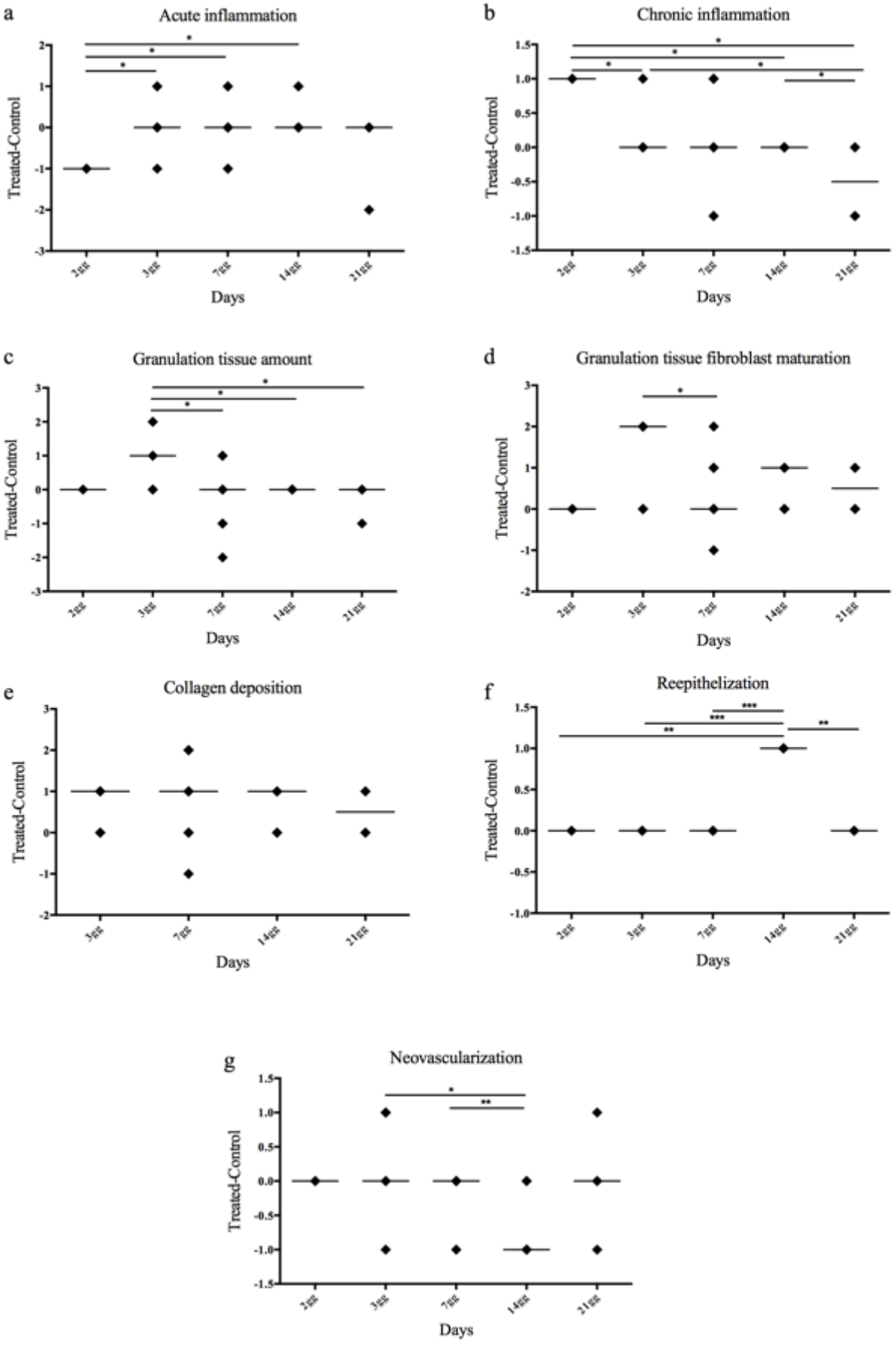

Figure 8: Statistical analyses of histological evaluations following the parameters provided by Abramov et al. [185].

REFERENCES

1. Polak, R.; Dill, D.; Abrahamson, M. J.; Pojednic, R. M.; Phillips, E. M. Innovation in diabetes care: improving consumption of healthy food through a "chef coaching" program: a case report. *Glob. Adv. Health Med.* **2014**, *3*, 42–8, doi:10.7453/gahmj.2014.059.
2. Greer, N.; Foman, N. A.; MacDonald, R.; Dorrian, J.; Fitzgerald, P.; Rutks, I.; Wilt, T. J. Advanced wound care therapies for nonhealing diabetic, venous, and arterial ulcers: a systematic review. *Ann. Intern. Med.* **2013**, *159*, 532–42, doi:10.7326/0003-4819-159-8-201310150-00006.
3. Zaky, S. H.; Ottonello, A.; Strada, P.; Cancedda, R.; Mastrogiacomo, M. Platelet lysate favours *in vitro* expansion of human bone marrow stromal cells for bone and cartilage engineering. *J. Tissue Eng. Regen. Med.* **2008**, *2*, 472–481, doi:10.1002/term.119.
4. Muraglia, A.; Todeschi, M. R.; Papait, A.; Poggi, A.; Spanò, R.; Strada, P.; Cancedda, R.; Mastrogiacomo, M. Combined platelet and plasma derivatives enhance proliferation of stem/progenitor cells maintaining their differentiation potential. *Cytotherapy* **2015**, *17*, 1793–806, doi:10.1016/j.jcyt.2015.09.004.
5. van der Valk, J.; Mellor, D.; Brands, R.; Fischer, R.; Gruber, F.; Gstraunthaler, G.; Hellebrekers, L.; Hyllner, J.; Jonker, F. H.; Prieto, P.; Thalen, M.; Baumans, V. The humane collection of fetal bovine serum and possibilities for serum-free cell and tissue culture. *Toxicol. In Vitro* **2004**, *18*, 1–12.
6. Gstraunthaler, G. Alternatives to the use of fetal bovine serum: serum-free cell culture. *ALTEX* **2003**, *20*, 275–81.
7. Jochems, C. E. A.; van der Valk, J. B. F.; Stafleu, F. R.; Baumans, V. The use of fetal bovine serum: ethical or scientific problem? *Altern. Lab. Anim. 30*, 219–27.
8. Shih, D. T.-B.; Burnouf, T. Preparation, quality criteria, and properties of human blood platelet lysate supplements for ex vivo stem cell expansion. *N. Biotechnol.* **2015**, *32*, 199–211, doi:10.1016/j.nbt.2014.06.001.
9. Maver, T.; Maver, U.; Kleinschek, K. S.; Ra????an, I. M.; Smrke, D. M. Advanced therapies of skin injuries. *Wien. Klin. Wochenschr.* **2015**, *127*, 187–198, doi:10.1007/s00508-015-0859-7.
10. Gkini, M. A.; Kouskoukis, A. E.; Tripsianis, G.; Rigopoulos, D. Study of Platelet - Rich Plasma Injections in the Treatment of Androgenetic Alopecia Through an One - Year Period. **2015**, *7*, 213–219, doi:10.4103/0974.
11. Geremicca, W.; Fonte, C.; Vecchio, S. Blood components for topical use in tissue regeneration: evaluation of corneal lesions treated with platelet lysate and considerations on repair mechanisms. *Blood Transfus.* **2010**, *8*, 107–12, doi:10.2450/2009.0091-09.
12. Pak, J.; Chang, J.-J.; Lee, J. H.; Lee, S. H. Safety reporting on implantation of autologous adipose tissue-derived stem cells with platelet-rich plasma into human articular joints. *BMC Musculoskelet. Disord.* **2013**, *14*, 337, doi:10.1186/1471-2474-14-337.

13. Vos, R. J. De; Weir, A.; Schie, H. T. M. Van; Weinans, H.; Page, P. Platelet-Rich Plasma Injection for Chronic Achilles Tendinopathy. **2010**, *303*.
14. Wang, Z.; Qian, Y.; Li, L.; Pan, L.; Njunge, L. W.; Dong, L.; Yang, L. Evaluation of emulsion electrospun polycaprolactone/hyaluronan/epidermal growth factor nanofibrous scaffolds for wound healing. *J. Biomater. Appl.* **2015**, doi:10.1177/0885328215586907.
15. Spanò, R.; Muraglia, A.; Todeschi, M. R.; Nardini, M.; Strada, P.; Cancedda, R.; Mastrogiacomo, M. Platelet-rich plasma-based bioactive membrane as a new advanced wound care tool. *J. Tissue Eng. Regen. Med.* **2017**, doi:10.1002/term.2357.
16. Patterson, J.; Martino, M. M.; Hubbell, J. A. Biomimetic materials in tissue engineering. **2010**, *13*, 1–2, doi:10.1016/S1369-7021(10)70013-4.
17. Junker, J. P. E.; Kamel, R. A.; Caterson, E. J.; Eriksson, E. Clinical Impact Upon Wound Healing and Inflammation in Moist, Wet, and Dry Environments. *Adv. wound care* **2013**, *2*, 348–356, doi:10.1089/wound.2012.0412.
18. Backly, R. El; Ulivi, V.; Tonachini, L.; Cancedda, R.; Descalzi, F.; Mastrogiacomo, M. Wound Healing of Human Keratinocytes Associated with a Strong Proinflammatory Response. *Tissue Eng. Part A* **2011**, *17*, 1787–1800, doi:10.1089/ten.tea.2010.0729.
19. Broughton, G.; Janis, J. E.; Attinger, C. E. The basic science of wound healing. *Plast. Reconstr. Surg.* **2006**, *117*, 12S–34S, doi:10.1097/01.prs.0000225430.42531.c2.
20. Jespersen, J. Pathophysiology and clinical aspects of fibrinolysis and inhibition of coagulation. Experimental and clinical studies with special reference to women on oral contraceptives and selected groups of thrombosis prone patients. *Dan. Med. Bull.* **1988**, *35*, 1–33.
21. Robson, M. C.; Steed, D. L.; Franz, M. G. Wound healing: biologic features and approaches to maximize healing trajectories. *Curr. Probl. Surg.* **2001**, *38*, 72–140, doi:10.1067/msg.2001.111167.
22. Lawrence, W. T. Physiology of the acute wound. *Clin. Plast. Surg.* **1998**, *25*, 321–40.
23. Hart, J. Inflammation 1: its role in the healing of acute wounds. *J. Wound Care* **2002**, *11*, 205–209, doi:10.12968/jowc.2002.11.6.26411.
24. Toy, L. W. Matrix metalloproteinases: their function in tissue repair. *J. Wound Care* **2005**, *14*, 20–22, doi:10.12968/jowc.2005.14.1.26720.
25. Velnar, T.; Bailey, T.; Smrkolj, V. The wound healing process: an overview of the cellular and molecular mechanisms. *J. Int. Med. Res. 37*, 1528–42.
26. Hunt, T. K.; Hopf, H.; Hussain, Z. Physiology of wound healing. *Adv. Skin Wound Care 13*, 6–11.
27. Gurtner, G. C.; Werner, S.; Barrandon, Y.; Longaker, M. T. Wound repair and regeneration. *Nature* **2008**, *453*, 314–321, doi:10.1038/nature07039.
28. Witte, M. B.; Barbul, A. General principles of wound healing. *Surg. Clin. North Am.* **1997**, *77*, 509–28.
29. Ramasastry, S. S. Acute wounds. *Clin. Plast. Surg.* **2005**, *32*, 195–208,

doi:10.1016/j.cps.2004.12.001.

30. Das, S.; Baker, A. B. Biomaterials and Nanotherapeutics for Enhancing Skin Wound Healing. *Front. Bioeng. Biotechnol.* **2016**, *4*, 82, doi:10.3389/fbioe.2016.00082.
31. Andreu, V.; Mendoza, G.; Arruebo, M.; Irusta, S. Smart Dressings Based on Nanostructured Fibers Containing Natural Origin Antimicrobial, Anti-Inflammatory, and Regenerative Compounds. *Mater. (Basel, Switzerland)* **2015**, *8*, 5154–5193, doi:10.3390/ma8085154.
32. Papait, A.; Cancedda, R.; Mastrogiacomo, M.; Poggi, A. Allogeneic platelet-rich plasma affects monocyte differentiation to dendritic cells causing an anti-inflammatory microenvironment, putatively fostering wound healing. *J. Tissue Eng. Regen. Med.* **2017**, doi:10.1002/term.2361.
33. Ayache, S.; Panelli, M. C.; Byrne, K. M.; Slezak, S.; Leitman, S. F.; Marincola, F. M.; Stroncek, D. F. Comparison of proteomic profiles of serum, plasma, and modified media supplements used for cell culture and expansion. *J. Transl. Med.* **2006**, *4*, 40, doi:10.1186/1479-5876-4-40.
34. Kocaoemer, A.; Kern, S.; Klüter, H.; Bieback, K. Human AB serum and thrombin-activated platelet-rich plasma are suitable alternatives to fetal calf serum for the expansion of mesenchymal stem cells from adipose tissue. *Stem Cells* **2007**, *25*, 1270–8, doi:10.1634/stemcells.2006-0627.
35. Cavari, S.; Ruggiero, M.; Vannucchi, S. Antiproliferative effects of heparin on normal and transformed NIH/3T3 fibroblasts. *Cell Biol. Int.* **1993**, *17*, 781–6, doi:10.1006/cbir.1993.1140.
36. Khorana, A. A.; Sahni, A.; Altland, O. D.; Francis, C. W. Heparin inhibition of endothelial cell proliferation and organization is dependent on molecular weight. *Arterioscler. Thromb. Vasc. Biol.* **2003**, *23*, 2110–5, doi:10.1161/01.ATV.0000090671.56682.D7.
37. Tiozzo, R.; Reggiani, D.; Cingi, M. R.; Bianchini, P.; Osima, B.; Calandra, S. Effect of heparin derived fractions on the proliferation and protein synthesis of cells in culture. *Thromb. Res.* **1991**, *62*, 177–88.
38. Vannucchi, S.; Pasquali, F.; Fiorelli, G.; Bianchini, P.; Ruggiero, M. Effect of heparin on proliferation and signalling in BC3H-1 muscle cells. Evidence for specific binding sites. *FEBS Lett.* **1990**, *263*, 137–41.
39. Mishra-Gorur, K.; Castellot, J. J. Heparin rapidly and selectively regulates protein tyrosine phosphorylation in vascular smooth muscle cells. *J. Cell. Physiol.* **1999**, *178*, 205–215, doi:10.1002/(SICI)1097-4652(199902)178:2<205::AID-JCP10>3.0.CO;2-9.
40. Gilotti, A. C.; Nimlamool, W.; Pugh, R.; Slee, J. B.; Barthol, T. C.; Miller, E. A.; Lowe-Krentz, L. J. Heparin responses in vascular smooth muscle cells involve cGMP-dependent protein kinase (PKG). *J. Cell. Physiol.* **2014**, *229*, 2142–52, doi:10.1002/jcp.24677.
41. Papathanasopoulos, A.; Kouroupis, D.; Henshaw, K.; McGonagle, D.; Jones, E. A.; Giannoudis, P. V Effects of antithrombotic drugs fondaparinux and tinzaparin on in vitro proliferation and osteogenic and chondrogenic differentiation of bone-derived mesenchymal stem cells. *J. Orthop. Res.* **2011**, *29*, 1327–35, doi:10.1002/jor.21405.

42. Handschin, A. E.; Trentz, O. A.; Hoerstrup, S. P.; Kock, H. J.; Wanner, G. A.; Trentz, O. Effect of low molecular weight heparin (dalteparin) and fondaparinux (Arixtra) on human osteoblasts in vitro. *Br. J. Surg.* **2005**, *92*, 177–83, doi:10.1002/bjs.4809.
43. Andress, D. L. Heparin modulates the binding of insulin-like growth factor (IGF) binding protein-5 to a membrane protein in osteoblastic cells. *J. Biol. Chem.* **1995**, *270*, 28289–96.
44. Hemeda, H.; Kalz, J.; Walenda, G.; Lohmann, M.; Wagner, W. Heparin concentration is critical for cell culture with human platelet lysate. *Cytotherapy* **2013**, *15*, 1174–1181, doi:10.1016/j.jcyt.2013.05.006.
45. Seeger, F. H.; Rasper, T.; Fischer, A.; Muhly-Reinholz, M.; Hergenreider, E.; Leistner, D. M.; Sommer, K.; Manavski, Y.; Henschler, R.; Chavakis, E.; Assmus, B.; Zeiher, A. M.; Dimmeler, S. Heparin Disrupts the CXCR4/SDF-1 Axis and Impairs the Functional Capacity of Bone Marrow-Derived Mononuclear Cells Used for Cardiovascular Repair. *Circ. Res.* **2012**, *111*, 854–862, doi:10.1161/CIRCRESAHA.112.265678.
46. Bottio, T.; Pittarello, G.; Bonato, R.; Fagiolo, U.; Gerosa, G. Life-threatening anaphylactic shock caused by porcine heparin intravenous infusion during mitral valve repair. *J. Thorac. Cardiovasc. Surg.* **2003**, *126*, 1194–5, doi:10.1016/S0022.
47. Huang, Q.; Xu, T.; Wang, G.-Y.; Huang, J.-F.; Xia, H.; Yin, R.; Tang, A.; Fu, W.-L. Species-specific identification of ruminant components contaminating industrial crude porcine heparin using real-time fluorescent qualitative and quantitative PCR. *Anal. Bioanal. Chem.* **2012**, *402*, 1625–1634, doi:10.1007/s00216-011-5590-2.
48. Mojica-Henshaw, M. P.; jacobson, P.; Morris, J.; Kelley, L.; Pierce, J.; Boyer, M.; Reems, J.-A. Serum-converted platelet lysate can substitute for fetal bovine serum in human mesenchymal stromal cell cultures. *Cytotherapy* **2013**, *15*, 1458–1468, doi:10.1016/j.jcyt.2013.06.014.
49. Copland, I. B.; Garcia, M. A.; Waller, E. K.; Roback, J. D.; Galipeau, J. The effect of platelet lysate fibrinogen on the functionality of MSCs in immunotherapy. *Biomaterials* **2013**, *34*, 7840–7850, doi:10.1016/j.biomaterials.2013.06.050.
50. Rauch, C.; Feifel, E.; Amann, E.-M.; Spötl, H. P.; Schennach, H.; Pfaller, W.; Gstraunthaler, G. Alternatives to the use of fetal bovine serum: human platelet lysates as a serum substitute in cell culture media. *ALTEX* **2011**, *28*, 305–16.
51. Stute, N.; Holtz, K.; Bubenheim, M.; Lange, C.; Blake, F.; Zander, A. R. Autologous serum for isolation and expansion of human mesenchymal stem cells for clinical use. *Exp. Hematol.* **2004**, *32*, 1212–1225, doi:10.1016/j.exphem.2004.09.003.
52. Kobayashi, T.; Watanabe, H.; Yanagawa, T.; Tsutsumi, S.; Kayakabe, M.; Shinozaki, T.; Higuchi, H.; Takagishi, K. Motility and growth of human bone-marrow mesenchymal stem cells during ex vivo expansion in autologous serum. *J. Bone Joint Surg. Br.* **2005**, *87*, 1426–33, doi:10.1302/0301-620X.87B10.16160.
53. Pisciotta, A.; Riccio, M.; Carnevale, G.; Beretti, F.; Gibellini, L.; Maraldi, T.; Cavallini, G. M.; Ferrari, A.; Bruzzesi, G.; De Pol, A. Human Serum Promotes Osteogenic Differentiation

of Human Dental Pulp Stem Cells In Vitro and In Vivo. *PLoS One* **2012**, *7*, e50542, doi:10.1371/journal.pone.0050542.

54. Shetty, P.; Bharucha, K.; Tanavde, V. Human umbilical cord blood serum can replace fetal bovine serum in the culture of mesenchymal stem cells. *Cell Biol. Int.* **2007**, *31*, 293–8, doi:10.1016/j.cellbi.2006.11.010.
55. Jung, J.; Moon, N.; Ahn, J.-Y.; Oh, E.-J.; Kim, M.; Cho, C.-S.; Shin, J.-C.; Oh, I.-H. Mesenchymal Stromal Cells Expanded in Human Allogenic Cord Blood Serum Display Higher Self-Renewal and Enhanced Osteogenic Potential. *Stem Cells Dev.* **2009**, *18*, 559–572, doi:10.1089/scd.2008.0105.
56. Anselme, K.; Broux, O.; Noel, B.; Bouxin, B.; Bascoulergue, G.; Dudermel, A.-F.; Bianchi, F.; Jeanfils, J.; Hardouin, P. *In Vitro* Control of Human Bone Marrow Stromal Cells for Bone Tissue Engineering. *Tissue Eng.* **2002**, *8*, 941–953, doi:10.1089/107632702320934047.
57. Yamaguchi, M.; Hirayama, F.; Wakamoto, S.; Fujihara, M.; Murahashi, H.; Sato, N.; Ikebuchi, K.; Sawada, K.; Koike, T.; Kuwabara, M.; Azuma, H.; Ikeda, H. Bone marrow stromal cells prepared using AB serum and bFGF for hematopoietic stem cells expansion. *Transfusion* **2002**, *42*, 921–7.
58. Le Blanc, K.; Samuelsson, H.; Lönnies, L.; Sundin, M.; Ringdén, O. Generation of Immunosuppressive Mesenchymal Stem Cells in Allogeneic Human Serum. *Transplantation* **2007**, *84*, 1055–1059, doi:10.1097/01.tp.0000285088.44901.ea.
59. Shahdadfar, A.; Frønsdal, K.; Haug, T.; Reinholt, F. P.; Brinchmann, J. E. In vitro expansion of human mesenchymal stem cells: choice of serum is a determinant of cell proliferation, differentiation, gene expression, and transcriptome stability. *Stem Cells* **2005**, *23*, 1357–66, doi:10.1634/stemcells.2005-0094.
60. Tateishi, K.; Ando, W.; Higuchi, C.; Hart, D. A.; Hashimoto, J.; Nakata, K.; Yoshikawa, H.; Nakamura, N. Comparison of human serum with fetal bovine serum for expansion and differentiation of human synovial MSC: potential feasibility for clinical applications. *Cell Transplant.* **2008**, *17*, 549–57.
61. Turnovcova, K.; Ruzickova, K.; Vanecek, V.; Sykova, E.; Jendelova, P. Properties and growth of human bone marrow mesenchymal stromal cells cultivated in different media. *Cytotherapy* **2009**, *11*, 874–885, doi:10.3109/14653240903188947.
62. Tanaka, Y.; Ogasawara, T.; Asawa, Y.; Yamaoka, H.; Nishizawa, S.; Mori, Y.; Takato, T.; Hoshi, K. Growth factor contents of autologous human sera prepared by different production methods and their biological effects on chondrocytes. *Cell Biol. Int.* **2008**, *32*, 505–14, doi:10.1016/j.cellbi.2007.12.012.
63. dos Santos, V. T. M.; Mizukami, A.; Orellana, M. D.; Caruso, S. R.; da Silva, F. B.; Traina, F.; de Lima Prata, K.; Covas, D. T.; Swiech, K. Characterization of Human AB Serum for Mesenchymal Stromal Cell Expansion. *Transfus. Med. Hemotherapy* **2017**, *44*, 11–21, doi:10.1159/000448196.
64. Balk, S. D.; Whitfield, J. F.; Youdale, T.; Braun, A. C. Roles of calcium, serum, plasma, and folic acid in the control of proliferation of normal and Rous sarcoma virus-infected chicken

fibroblasts. *Proc. Natl. Acad. Sci. U. S. A.* **1973**, *70*, 675–9.

65. Ross, R.; Glomset, J.; Kariya, B.; Harker, L. A platelet-dependent serum factor that stimulates the proliferation of arterial smooth muscle cells in vitro. *Proc. Natl. Acad. Sci. U. S. A.* **1974**, *71*, 1207–10.
66. Gospodarowicz, D.; Ill, C. R. Do plasma and serum have different abilities to promote cell growth? *Proc. Natl. Acad. Sci. U. S. A.* **1980**, *77*, 2726–30.
67. Mizuno, N.; Shiba, H.; Ozeki, Y.; Mouri, Y.; Niitani, M.; Inui, T.; Hayashi, H.; Suzuki, K.; Tanaka, S.; Kawaguchi, H.; Kurihara, H. Human autologous serum obtained using a completely closed bag system as a substitute for foetal calf serum in human mesenchymal stem cell cultures. *Cell Biol. Int.* **2006**, *30*, 521–4, doi:10.1016/j.cellbi.2006.01.010.
68. Gajdusek, C.; DiCorleto, P.; Ross, R.; Schwartz, S. M. An endothelial cell-derived growth factor. *J. Cell Biol.* **1980**, *85*, 467–72.
69. Ross, R.; Nist, C.; Kariya, B.; Rivest, M. J.; Raines, E.; Callis, J. Physiological quiescence in plasma-derived serum: influence of platelet-derived growth factor on cell growth in culture. *J. Cell. Physiol.* **1978**, *97*, 497–508, doi:10.1002/jcp.1040970325.
70. Rutherford, R. B.; Ross, R. Platelet factors stimulate fibroblasts and smooth muscle cells quiescent in plasma serum to proliferate. *J. Cell Biol.* **1976**, *69*, 196–203.
71. Nguyen, V. T.; Cancedda, R.; Descalzi, F. Platelet lysate activates quiescent cell proliferation and reprogramming in human articular cartilage: Involvement of hypoxia inducible factor 1. *J. Tissue Eng. Regen. Med.* **2017**, doi:10.1002/term.2595.
72. Ruggiu, A.; Ulivi, V.; Sanguineti, F.; Cancedda, R.; Descalzi, F. The effect of Platelet Lysate on osteoblast proliferation associated with a transient increase of the inflammatory response in bone regeneration. *Biomaterials* **2013**, *34*, 9318–9330, doi:10.1016/j.biomaterials.2013.08.018.
73. Xiao, Q.; Claassen, G.; Shi, J.; Adachi, S.; Sedivy, J.; Hann, S. R. Transactivation-defective c-MycS retains the ability to regulate proliferation and apoptosis. *Genes Dev.* **1998**, *12*, 3803–8.
74. Hann, S. R. MYC cofactors: molecular switches controlling diverse biological outcomes. *Cold Spring Harb. Perspect. Med.* **2014**, *4*, a014399, doi:10.1101/cshperspect.a014399.
75. Hann, S. R.; King, M. W.; Bentley, D. L.; Anderson, C. W.; Eisenman, R. N. A non-AUG translational initiation in c-myc exon 1 generates an N-terminally distinct protein whose synthesis is disrupted in Burkitt's lymphomas. *Cell* **1988**, *52*, 185–95.
76. Hann, S. R.; Eisenman, R. N. Proteins Encoded by the Human c-myc Oncogene: Differential Expression in Neoplastic Cells. *Mol. Cell. Biol.* **1984**, *4*, 2486–2497.
77. Spotts, G. D.; Patel, S. V; Xiao, Q.; Hann, S. R. Identification of Downstream-Initiated c-Myc Proteins Which Are Dominant-Negative Inhibitors of Transactivation by Full-Length c-Myc Proteins. **1997**, *17*, 1459–1468.
78. Benassayag, C.; Montero, L.; Colombié, N.; Gallant, P.; Cribbs, D.; Morello, D. Human c-Myc isoforms differentially regulate cell growth and apoptosis in Drosophila melanogaster. *Mol. Cell. Biol.* **2005**, *25*, 9897–909, doi:10.1128/MCB.25.22.9897-9909.2005.

79. Hann, S. R.; Sloan-Brown, K.; Spotts, G. D. Translational activation of the non-AUG-initiated c-myc 1 protein at high cell densities due to methionine deprivation. *Genes Dev.* **1992**, *6*, 1229–1240, doi:10.1101/gad.6.7.1229.
80. Hann, S. R.; Dixit, M.; Sears, R. C.; Sealy, L. The alternatively initiated c-Myc proteins differentially regulate transcription through a noncanonical DNA-binding site. *Genes Dev.* **1994**, *8*, 2441–2452, doi:10.1101/gad.8.20.2441.
81. Capelli, C.; Gotti, E.; Morigi, M.; Rota, C.; Weng, L.; Dazzi, F.; Spinelli, O.; Cazzaniga, G.; Trezzi, R.; Gianatti, A.; Rambaldi, A.; Golay, J.; Introna, M. Minimally manipulated whole human umbilical cord is a rich source of clinical-grade human mesenchymal stromal cells expanded in human platelet lysate. *Cytotherapy* **2011**, *13*, 786–801, doi:10.3109/14653249.2011.563294.
82. Zerega, B.; Cermelli, S.; Bianco, P.; Cancedda, R.; Cancedda, F. D. Parathyroid hormone [PTH(1-34)] and parathyroid hormone-related protein [PTHrP(1-34)] promote reversion of hypertrophic chondrocytes to a prehypertrophic proliferating phenotype and prevent terminal differentiation of osteoblast-like cells. *J. Bone Miner. Res.* **1999**, *14*, 1281–9, doi:10.1359/jbmr.1999.14.8.1281.
83. Ryan, K. M.; Birnie, G. D. Myc oncogenes : the enigmatic family. **1996**, *721*, 713–721.
84. Obaya, A. J.; Mateyak, M. K.; Sedivy, J. M. Mysterious liaisons: the relationship between c-Myc and the cell cycle. *Oncogene* **1999**, *18*, 2934–41, doi:10.1038/sj.onc.1202749.
85. Meyer, N.; Penn, L. Z. Reflecting on 25 years with MYC. *Nat. Rev. Cancer* **2008**, *8*, 976–90, doi:10.1038/nrc2231.
86. Nie, Z.; Hu, G.; Wei, G.; Cui, K.; Yamane, A.; Resch, W.; Wang, R.; Green, D. R.; Tessarollo, L.; Casellas, R.; Zhao, K.; Levens, D. c-Myc is a universal amplifier of expressed genes in lymphocytes and embryonic stem cells. *Cell* **2012**, *151*, 68–79, doi:10.1016/j.cell.2012.08.033.
87. Bieback, K.; Hecker, A.; Kocaömer, A.; Lannert, H.; Schallmoser, K.; Strunk, D.; Klüter, H. Human Alternatives to Fetal Bovine Serum for the Expansion of Mesenchymal Stromal Cells from Bone Marrow. *Stem Cells* **2009**, *27*, 2331–2341, doi:10.1002/stem.139.
88. Pawitan, J. A. Platelet rich plasma in xeno-free stem cell culture: the impact of platelet count and processing method. *Curr. Stem Cell Res. Ther.* **2012**, *7*, 329–35.
89. Oreffo, R. O.; Virdi, A. S.; Triffitt, J. T. Modulation of osteogenesis and adipogenesis by human serum in human bone marrow cultures. *Eur. J. Cell Biol.* **1997**, *74*, 251–61.
90. Koellensperger, E.; von Heimburg, D.; Markowicz, M.; Pallua, N. Human serum from platelet-poor plasma for the culture of primary human preadipocytes. *Stem Cells* **2006**, *24*, 1218–25, doi:10.1634/stemcells.2005-0020.
91. Simões, I. N.; Boura, J. S.; dos Santos, F.; Andrade, P. Z.; Cardoso, C. M. P.; Gimble, J. M.; da Silva, C. L.; Cabral, J. M. S. Human mesenchymal stem cells from the umbilical cord matrix: Successful isolation and ex vivo expansion using serum-/xeno-free culture media. *Biotechnol. J.* **2013**, *8*, 448–458, doi:10.1002/biot.201200340.
92. TODARO, G. J.; GREEN, H. Quantitative studies of the growth of mouse embryo cells in

culture and their development into established lines. *J. Cell Biol.* **1963**, *17*, 299–313.

93. Vogel, A.; Raines, E.; Kariya, B.; Rivest, M. J.; Ross, R. Coordinate control of 3T3 cell proliferation by platelet-derived growth factor and plasma components. *Proc. Natl. Acad. Sci. U. S. A.* **1978**, *75*, 2810–4.
94. Currie, G. A. Platelet-derived growth-factor requirements for in vitro proliferation of normal and malignant mesenchymal cells. *Br. J. Cancer* **1981**, *43*, 335–43.
95. Altman, G. H.; Diaz, F.; Jakuba, C.; Calabro, T.; Horan, R. L.; Chen, J.; Lu, H.; Richmond, J.; Kaplan, D. L. Silk-based biomaterials. *Biomaterials* **2003**, *24*, 401–416, doi:10.1016/S0142-9612(02)00353-8.
96. Vepari, C.; Kaplan, D. L. Silk as a Biomaterial. *Prog. Polym. Sci.* **2007**, *32*, 991–1007, doi:10.1016/j.progpolymsci.2007.05.013.
97. Rockwood, D. N.; Preda, R. C.; Yücel, T.; Wang, X.; Lovett, M. L.; Kaplan, D. L. Materials fabrication from Bombyx mori silk fibroin. *Nat. Protoc.* **2011**, *6*, 1612–1631, doi:10.1038/nprot.2011.379.
98. Kundu, B.; Rajkhowa, R.; Kundu, S. C.; Wang, X. *Silk fibroin biomaterials for tissue regenerations*; 2013; Vol. 65; ISBN 1872-8294 (Electronic)n0169-409X (Linking).
99. Wenk, E.; Merkle, H. P.; Meinel, L. Silk fibroin as a vehicle for drug delivery applications. *J. Control. Release Off. J. Control. Release Soc.* **2011**, *150*, 128–141, doi:10.1016/j.jconrel.2010.11.007.
100. Mitropoulos, A. N.; Perotto, G.; Kim, S.; Marelli, B.; Kaplan, D. L.; Omenetto, F. G. Synthesis of Silk Fibroin Micro- and Submicron Spheres Using a Co-Flow Capillary Device. *Adv. Mater.* **2014**, *26*, 1105–1110, doi:10.1002/adma.201304244.
101. Seib, F. P.; Jones, G. T.; Rnjak-Kovacina, J.; Lin, Y.; Kaplan, D. L. pH-Dependent Anticancer Drug Release from Silk Nanoparticles. *Adv. Healthc. Mater.* **2013**, *2*, 1606–1611, doi:10.1002/adhm.201300034.
102. Catto, V.; Farè, S.; Cattaneo, I.; Figliuzzi, M.; Alessandrino, A.; Freddi, G.; Remuzzi, A.; Tanzi, M. C. Small diameter electrospun silk fibroin vascular grafts: Mechanical properties, in vitro biodegradability, and in vivo biocompatibility. *Mater. Sci. Eng. C* **2015**, *54*, 101–111, doi:10.1016/J.MSEC.2015.05.003.
103. Zhou, C. Z.; Confalonieri, F.; Medina, N.; Zivanovic, Y.; Esnault, C.; Yang, T.; Jacquet, M.; Janin, J.; Duguet, M.; Perasso, R.; Li, Z. G. Fine organization of Bombyx mori fibroin heavy chain gene. *Nucleic Acids Res.* **2000**, *28*, 2413–9.
104. Lu, Q.; Hu, X.; Wang, X.; Kluge, J. A.; Lu, S.; Cebe, P.; Kaplan, D. L. Water-insoluble silk films with silk I structure. *Acta Biomater.* **2010**, *6*, 1380–1387, doi:10.1016/j.actbio.2009.10.041.
105. Wang, M.; Jin, H. J.; Kaplan, D. L.; Rutledge, G. C. Mechanical properties of electrospun silk fibers. *Macromolecules* **2004**, *37*, 6856–6864, doi:10.1021/ma048988v.
106. Perotto, G.; Zhang, Y.; Naskar, D.; Patel, N.; Kaplan, D. L.; Kundu, S. C.; Omenetto, F. G. The optical properties of regenerated silk fibroin films obtained from different sources. *Appl.*

Phys. Lett. **2017**, *111*, 103702, doi:10.1063/1.4998950.

107. Hu, X.; Shmelev, K.; Sun, L.; Gil, E.-S.; Park, S.-H.; Cebe, P.; Kaplan, D. L. Regulation of silk material structure by temperature-controlled water vapor annealing. *Biomacromolecules* **2011**, *12*, 1686–96, doi:10.1021/bm200062a.
108. Motta, A.; Maniglio, D.; Migliaresi, C.; Kim, H.-J.; Wan, X.; Hu, X.; Kaplan, D. L. Silk fibroin processing and thrombogenic responses. *J. Biomater. Sci. Polym. Ed.* **2009**, *20*, 1875–97, doi:10.1163/156856208X399936.
109. Floren, M.; Bonani, W.; Dharmarajan, A.; Motta, A.; Migliaresi, C.; Tan, W. Human mesenchymal stem cells cultured on silk hydrogels with variable stiffness and growth factor differentiate into mature smooth muscle cell phenotype. *Acta Biomater.* **2016**, *31*, 156–166, doi:10.1016/j.actbio.2015.11.051.
110. Mitropoulos, A. N.; Marelli, B.; Perotto, G.; Amsden, J.; Kaplan, D. L.; Omenetto, F. G. Towards the fabrication of biohybrid silk fibroin materials: entrapment and preservation of chloroplast organelles in silk fibroin films. *RSC Adv.* **2016**, *6*, 72366–72370, doi:10.1039/C6RA13228F.
111. Pritchard, E. M.; Dennis, P. B.; Omenetto, F.; Naik, R. R.; Kaplan, D. L. Review physical and chemical aspects of stabilization of compounds in silk. *Biopolymers* **2012**, *97*, 479–98, doi:10.1002/bip.22026.
112. Kluge, J. A.; Li, A. B.; Kahn, B. T.; Michaud, D. S.; Omenetto, F. G.; Kaplan, D. L. Silk-based blood stabilization for diagnostics. *Proc. Natl. Acad. Sci. U. S. A.* **2016**, *113*, 5892–7, doi:10.1073/pnas.1602493113.
113. Seib, F. P.; Kaplan, D. L. Doxorubicin-loaded silk films: Drug-silk interactions and in vivo performance in human orthotopic breast cancer. *Biomaterials* **2012**, *33*, 8442–8450, doi:10.1016/j.biomaterials.2012.08.004.
114. Kim, J. H.; Park, C. H.; Lee, O.-J.; Lee, J.-M.; Kim, J. W.; Park, Y. H.; Ki, C. S. Preparation and in vivo degradation of controlled biodegradability of electrospun silk fibroin nanofiber mats. *J. Biomed. Mater. Res. A* **2012**, *100*, 3287–3295, doi:10.1002/jbm.a.34274.
115. Kim, U.-J.; Park, J.; Joo Kim, H.; Wada, M.; Kaplan, D. L. Three-dimensional aqueous-derived biomaterial scaffolds from silk fibroin. *Biomaterials* **2005**, *26*, 2775–2785, doi:10.1016/j.biomaterials.2004.07.044.
116. Wang, Y.; Rudym, D. D.; Walsh, A.; Abrahamsen, L.; Kim, H.-J.; Kim, H. S.; Kirker-Head, C.; Kaplan, D. L. In vivo degradation of three-dimensional silk fibroin scaffolds. *Biomaterials* **2008**, *29*, 3415–28, doi:10.1016/j.biomaterials.2008.05.002.
117. Hines, D. J.; Kaplan, D. L. Mechanisms of Controlled Release from Silk Fibroin Films. *Biomacromolecules* **2011**, *12*, 804–812, doi:10.1021/bm101421r.
118. Hines, D. J.; Kaplan, D. L. Characterization of Small Molecule Controlled Release From Silk Films. *Macromol. Chem. Phys.* **2013**, *214*, 280–294, doi:10.1002/macp.201200407.
119. Hofmann, S.; Wong Po Foo, C. T.; Rossetti, F.; Textor, M.; Vunjak-Novakovic, G.; Kaplan, D. L.; Merkle, H. P.; Meinel, L. Silk fibroin as an organic polymer for controlled drug delivery. *J. Control. Release* **2006**, *111*, 219–227, doi:10.1016/j.jconrel.2005.12.009.

120. Coburn, J. M.; Na, E.; Kaplan, D. L. Modulation of vincristine and doxorubicin binding and release from silk films. *J. Control. Release* **2015**, *220*, 229–238, doi:10.1016/j.jconrel.2015.10.035.
121. Wang, X.; Wenk, E.; Matsumoto, A.; Meinel, L.; Li, C.; Kaplan, D. L. Silk microspheres for encapsulation and controlled release. *J. Control. Release* **2007**, *117*, 360–370, doi:10.1016/j.jconrel.2006.11.021.
122. Chiu, B.; Coburn, J.; Pilichowska, M.; Holcroft, C.; Seib, F. P.; Charest, A.; Kaplan, D. L. Surgery combined with controlled-release doxorubicin silk films as a treatment strategy in an orthotopic neuroblastoma mouse model. *Br. J. Cancer* **2014**, *111*, 708–715, doi:10.1038/bjc.2014.324.
123. Boateng, J. S.; Matthews, K. H.; Stevens, H. N. E.; Eccleston, G. M. Wound Healing Dressings and Drug Delivery Systems: A Review. *J. Pharm. Sci.* **2008**, *97*, 2892–2923, doi:10.1002/jps.21210.
124. Buckley, A.; Davidson, J. M.; Kamerath, C. D.; Wolt, T. B.; Woodward, S. C. Sustained release of epidermal growth factor accelerates wound repair. *Proc. Natl. Acad. Sci. U. S. A.* **1985**, *82*, 7340–4.
125. Sheridan, M. H.; Shea, L. D.; Peters, M. C.; Mooney, D. J. Bioabsorbable polymer scaffolds for tissue engineering capable of sustained growth factor delivery. *J. Control. Release* **2000**, *64*, 91–102.
126. Putney, S. D.; Burke, P. A. Improving protein therapeutics with sustained-release formulations. *Nat. Biotechnol.* **1998**, *16*, 153–157, doi:10.1038/nbt0298-153.
127. Bennett, N. T.; Schultz, G. S. Growth factors and wound healing: Part II. Role in normal and chronic wound healing. *Am. J. Surg.* **1993**, *166*, 74–81.
128. Morimoto, N.; Yoshimura, K.; Niimi, M.; Ito, T.; Aya, R.; Fujitaka, J.; Tada, H.; Teramukai, S.; Murayama, T.; Toyooka, C.; Miura, K.; Takemoto, S.; Kanda, N.; Kawai, K.; Yokode, M.; Shimizu, A.; Suzuki, S. Novel Collagen/Gelatin Scaffold with Sustained Release of Basic Fibroblast Growth Factor: Clinical Trial for Chronic Skin Ulcers. *Tissue Eng. Part A* **2013**, *19*, 1931–1940, doi:10.1089/ten.tea.2012.0634.
129. Muraglia, A.; Ottonello, C.; Spanò, R.; Dozin, B.; Strada, P.; Grandizio, M.; Cancedda, R.; Mastrogiacomo, M. Biological activity of a standardized freeze-dried platelet derivative to be used as cell culture medium supplement. *Platelets* **2014**, *25*, 211–220, doi:10.3109/09537104.2013.803529.
130. Barsotti, M. C.; Losi, P.; Briganti, E.; Sanguinetti, E.; Magera, A.; Al Kayal, T.; Feriani, R.; Di Stefano, R.; Soldani, G. Effect of platelet lysate on human cells involved in different phases of wound healing. *PLoS One* **2013**, *8*, 1–11, doi:10.1371/journal.pone.0084753.
131. Yang, H. S.; Shin, J.; Bhang, S. H.; Shin, J. Y.; Park, J.; Im, G. Il; Kim, C. S.; Kim, B. S. Enhanced skin wound healing by a sustained release of growth factors contained in platelet-rich plasma. *Exp. Mol. Med.* **2011**, *43*, 622–9, doi:10.3858/emm.2011.43.11.070.
132. El Backly, R. M.; Zaky, S. H.; Muraglia, A.; Tonachini, L.; Brun, F.; Canciani, B.; Chiapale, D.; Santolini, F.; Cancedda, R.; Mastrogiacomo, M. A Platelet-Rich Plasma-Based

Membrane as a Periosteal Substitute with Enhanced Osteogenic and Angiogenic Properties: A New Concept for Bone Repair. *Tissue Eng. Part A* **2013**, *19*, 152–165, doi:10.1089/ten.tea.2012.0357.

133. Knighton, D. R.; Ciresi, K. F.; Fiegel, V. D.; Austin, L. L.; Butler, E. L. Classification and treatment of chronic nonhealing wounds. Successful treatment with autologous platelet-derived wound healing factors (PDWHF). *Ann. Surg.* **1986**, *204*, 322–30.
134. Anitua, E.; Aguirre, J. J.; Algorta, J.; Ayerdi, E.; Cabezas, A. I.; Orive, G.; Andia, I. Effectiveness of autologous preparation rich in growth factors for the treatment of chronic cutaneous ulcers. *J. Biomed. Mater. Res. B. Appl. Biomater.* **2008**, *84*, 415–21, doi:10.1002/jbm.b.30886.
135. Fekete, N.; Gadelorge, M.; Fürst, D.; Maurer, C.; Dausend, J.; Fleury-Cappellesso, S.; Mailänder, V.; Lotfi, R.; Ignatius, A.; Sensebé, L.; Bourin, P.; Schrezenmeier, H.; Rojewski, M. T. Platelet lysate from whole blood-derived pooled platelet concentrates and apheresis-derived platelet concentrates for the isolation and expansion of human bone marrow mesenchymal stromal cells: production process, content and identification of active comp. *Cytotherapy* **2012**, *14*, 540–554, doi:10.3109/14653249.2012.655420.
136. Putthanarat, S.; Eby, R. K.; Naik, R. R.; Juhl, S. B.; Walker, M. A.; Peterman, E.; Ristich, S.; Magoshi, J.; Tanaka, T.; Stone, M. O.; Farmer, B. L.; Brewer, C.; Ott, D. Nonlinear optical transmission of silk/green fluorescent protein (GFP) films. *Polymer (Guildf).* **2004**, *45*, 8451–8457, doi:DOI 10.1016/j.polymer.2004.10.014.
137. Kikuchi, J.; Mitsui, Y.; Asakura, T.; Hasuda, K.; Araki, H.; Owaku, K. Spectroscopic investigation of tertiary fold of staphylococcal protein A to explore its engineering application. *Biomaterials* **1999**, *20*, 647–654, doi:10.1016/S0142-9612(98)00220-8.
138. Lu, S.; Wang, X.; Lv, Q.; Hu, X.; Uppal, N.; Kaplan, D. L. Stabilization of Enzymes in Silk Films. *Biomacromolecules* **2009**, *10*, 1032–1042, doi:10.1021/bm800956n.Stabilization.
139. Wu, Y.; Shen, Q.; Hu, S. Direct electrochemistry and electrocatalysis of heme-proteins in regenerated silk fibroin film. *Anal. Chim. Acta* **2006**, *558*, 179–186, doi:10.1016/j.aca.2005.11.031.
140. Zhang, J.; Pritchard, E.; Hu, X.; Valentin, T.; Panilaitis, B.; Omenetto, F. G.; Kaplan, D. L. Stabilization of vaccines and antibiotics in silk and eliminating the cold chain. *Proc. Natl. Acad. Sci. U. S. A.* **2012**, *109*, 11981–6, doi:10.1073/pnas.1206210109.
141. Li, A. B.; Kluge, J. A.; Guziewicz, N. A.; Omenetto, F. G.; Kaplan, D. L. Silk-based stabilization of biomacromolecules. *J. Control. Release* **2015**, *219*, 416–430, doi:10.1016/j.jconrel.2015.09.037.
142. Tseng, P.; Perotto, G.; Napier, B.; Riahi, P.; Li, W.; Shirman, E.; Kaplan, D. L.; Zenyuk, I. V.; Omenetto, F. G. Silk Fibroin-Carbon Nanotube Composite Electrodes for Flexible Biocatalytic Fuel Cells. *Adv. Electron. Mater.* **2016**, *2*, 1600190, doi:10.1002/aelm.201600190.
143. Zahedi, P.; Rezaeian, I.; Ranaei-Siadat, S.-O.; Jafari, S.-H.; Supaphol, P. A review on wound dressings with an emphasis on electrospun nanofibrous polymeric bandages. *Polym. Adv.*

Technol. **2010**, *21*, 77–95, doi:10.1002/pat.1625.

144. Abrigo, M.; McArthur, S. L.; Kingshott, P. Electrospun nanofibers as dressings for chronic wound care: advances, challenges, and future prospects. *Macromol. Biosci.* **2014**, *14*, 772–792, doi:10.1002/mabi.201300561.
145. Hajiali, H.; Summa, M.; Russo, D.; Armirotti, A.; Brunetti, V.; Bertorelli, R.; Athanassiou, A.; Mele, E. Alginate–lavender nanofibers with antibacterial and anti-inflammatory activity to effectively promote burn healing. *J. Mater. Chem. B* **2016**, *4*, 1686–1695, doi:10.1039/C5TB02174J.
146. Romano, I.; Summa, M.; Heredia-Guerrero, J. A.; Spanò, R.; Ceseracciu, L.; Pignatelli, C.; Bertorelli, R.; Mele, E.; Athanassiou, A. Fumarate-loaded electrospun nanofibers with anti-inflammatory activity for fast recovery of mild skin burns. *Biomed. Mater.* **2016**, *11*, 41001, doi:10.1088/1748-6041/11/4/041001.
147. Wolfe, P.; Sell; Sa; Ericksen, J.; Simpson, D.; Bowlin The Creation of Electrospun Nanofibers from Platelet Rich Plasma. *J Tissue Sci Eng* **2011**, *24172*, 1072157–7552, doi:10.4172/2157-7552.1000107.
148. Shanskii, Y. D.; Sergeeva, N. S.; Sviridova, I. K.; Kirakozov, M. S.; Kirsanova, V. A.; Akhmedova, S. A.; Antokhin, A. I.; Chissov, V. I. Human platelet lysate as a promising growth-stimulating additive for culturing of stem cells and other cell types. *Bull. Exp. Biol. Med.* **2013**, *156*, 146–51.
149. Jin, H.-J.; Fridrikh, S. V; Rutledge, G. C.; Kaplan, D. L. Electrospinning Bombyx mori silk with poly(ethylene oxide). *Biomacromolecules 3*, 1233–9.
150. Chutipakdeevong, J.; Ruktanonchai, U. R.; Supaphol, P. Process optimization of electrospun silk fibroin fiber mat for accelerated wound healing. *J. Appl. Polym. Sci.* **2013**, *130*, 3634–3644, doi:10.1002/app.39611.
151. Gil, E. S.; Panilaitis, B.; Bellas, E.; Kaplan, D. L. Functionalized Silk Biomaterials for Wound Healing. *Adv. Healthc. Mater.* **2013**, *2*, 206–217, doi:10.1002/adhm.201200192.
152. Schneider, A.; Wang, X. Y.; Kaplan, D. L.; Garlick, J. A.; Egles, C. Biofunctionalized electrospun silk mats as a topical bioactive dressing for accelerated wound healing. *Acta Biomater.* **2009**, *5*, 2570–2578, doi:10.1016/j.actbio.2008.12.013.
153. Guzman-Puyol, S.; Heredia-Guerrero, J. A.; Ceseracciu, L.; Hajiali, H.; Canale, C.; Scarpellini, A.; Cingolani, R.; Bayer, I. S.; Athanassiou, A.; Mele, E. Low-Cost and Effective Fabrication of Biocompatible Nanofibers from Silk and Cellulose-Rich Materials. *ACS Biomater. Sci. Eng.* **2016**, *2*, 526–534, doi:10.1021/acsbiomaterials.5b00500.
154. Hu, X.; Kaplan, D.; Cebe, P. Determining Beta-Sheet Crystallinity in Fibrous Proteins by Thermal Analysis and Infrared Spectroscopy. *Macromolecules* **2006**, *39*, 6161–6170, doi:10.1021/ma0610109.
155. Meinel, A. J.; Kubow, K. E.; Klotzsch, E.; Garcia-Fuentes, M.; Smith, M. L.; Vogel, V.; Merkle, H. P.; Meinel, L. Optimization strategies for electrospun silk fibroin tissue engineering scaffolds. *Biomaterials* **2009**, *30*, 3058–3067, doi:10.1016/j.biomaterials.2009.01.054.

156. Min, B. M.; Jeong, L.; Lee, K. Y.; Park, W. H. Regenerated silk fibroin nanofibers: Water vapor-induced structural changes and their effects on the behavior of normal human cells. *Macromol. Biosci.* **2006**, *6*, 285–292, doi:10.1002/mabi.200500246.
157. Seib, F. P.; Kaplan, D. L. Silk for drug delivery applications: Opportunities and challenges. *Isr. J. Chem.* **2013**, *53*, 756–766, doi:10.1002/ijch.201300083.
158. Gil, E. S.; Park, S.-H.; Hu, X.; Cebe, P.; Kaplan, D. L. Impact of sterilization on the enzymatic degradation and mechanical properties of silk biomaterials. *Macromol. Biosci.* **2014**, *14*, 257–69, doi:10.1002/mabi.201300321.
159. Zhou, J.; Cao, C.; Ma, X.; Hu, L.; Chen, L.; Wang, C. In vitro and in vivo degradation behavior of aqueous-derived electrospun silk fibroin scaffolds. **2010**, doi:10.1016/j.polymdegradstab.2010.05.025.
160. Anitua, E.; Pino, A.; Orive, G. Plasma rich in growth factors promotes dermal fibroblast proliferation, migration and biosynthetic activity. *J. Wound Care* **2016**, *25*, 680–687, doi:10.12968/jowc.2016.25.11.680.
161. Li, M.; Ogiso, M.; Minoura, N. Enzymatic degradation behavior of porous silk fibroin sheets. *Biomaterials* **2003**, *24*, 357–365, doi:10.1016/S0142-9612(02)00326-5.
162. Nultsch, K.; Germershaus, O. Silk fibroin degumming affects scaffold structure and release of macromolecular drugs. *Eur. J. Pharm. Sci.* **2017**, *106*, 254–261, doi:10.1016/j.ejps.2017.06.012.
163. Carlin, C. R.; Knowles, B. B. Identity of human epidermal growth factor (EGF) receptor with glycoprotein SA-7: evidence for differential phosphorylation of the two components of the EGF receptor from A431 cells. *Proc. Natl. Acad. Sci. U. S. A.* **1982**, *79*, 5026–30, doi:10.1074/jbc.M403114200.Epidermal.
164. Mullen, L. M.; Best, S. M.; Brooks, R. A.; Ghose, S.; Gwynne, J. H.; Wardale, J.; Rushton, N.; Cameron, R. E. Binding and Release Characteristics of Insulin-Like Growth Factor-1 from a Collagen–Glycosaminoglycan Scaffold. *Tissue Eng. Part C Methods* **2010**, *16*, 1439–1448, doi:10.1089/ten.tec.2009.0806.
165. Heldin, C. H.; Johnsson, a; Ek, B.; Wennergren, S.; Rönnstrand, L.; Hammacher, a; Faulders, B.; Wasteson, a; Westermark, B. Purification of human platelet-derived growth factor. *Methods Enzymol.* **1987**, *147*, 3–13.
166. Vuorela-Vepsalainen, P.; Alfthan, H.; Orpana, A.; Alitalo, K.; Stenman, U. H.; Halmesmaki, E. Vascular endothelial growth factor is bound in amniotic fluid and maternal serum. *Hum Reprod* **1999**, *14*, 1346–1351.
167. Lu, Q.; Wang, X.; Hu, X.; Cebe, P.; Omenetto, F.; Kaplan, D. L. Stabilization and Release of Enzymes from Silk Films. *Macromol. Biosci.* **2010**, *10*, 359–368, doi:10.1002/mabi.200900388.
168. Mazzucco, L.; Medici, D.; Serra, M.; Panizza, R.; Rivara, G.; Orecchia, S.; Libener, R.; Cattana, E.; Levis, A.; Betta, P. G.; Borzini, P. The use of autologous platelet gel to treat difficult-to-heal wounds: a pilot study. *Transfusion* **2004**, *44*, 1013–8, doi:10.1111/j.1537-

2995.2004.03366.x.

169. Miron, R. J.; Fujioka-Kobayashi, M.; Bishara, M.; Zhang, Y.; Hernandez, M.; Choukroun, J. Platelet-Rich Fibrin and Soft Tissue Wound Healing: A Systematic Review. *Tissue Eng. Part B. Rev.* **2017**, *23*, 83–99, doi:10.1089/ten.TEB.2016.0233.
170. Wang, Y. J.; Zhag, Y. Q. Three-Layered Sericins around the Silk Fibroin Fiber from Bombyx mori; Cocoon and their Amino Acid Composition. *Adv. Mater. Res.* **2011**, *175–176*, 158–163, doi:10.4028/www.scientific.net/AMR.175-176.158.
171. Cao, T.-T.; Zhang, Y.-Q. Processing and characterization of silk sericin from Bombyx mori and its application in biomaterials and biomedicines. *Mater. Sci. Eng. C* **2016**, *61*, 940–952, doi:10.1016/j.msec.2015.12.082.
172. Chlapanidas, T.; Faragò, S.; Lucconi, G.; Perteghella, S.; Galuzzi, M.; Mantelli, M.; Avanzini, M. A.; Tosca, M. C.; Marazzi, M.; Vigo, D.; Torre, M. L.; Faustini, M. Sericins exhibit ROS-scavenging, anti-tyrosinase, anti-elastase, and in vitro immunomodulatory activities. *Int. J. Biol. Macromol.* **2013**, *58*, 47–56, doi:10.1016/j.ijbiomac.2013.03.054.
173. Li, Y.; Ji, D.; Lin, T.; Zhong, S.; Hu, G.; Chen, S. Protective effect of sericin peptide against alcohol-induced gastric injury in mice. *Chin. Med. J. (Engl).* **2008**, *121*, 2083–7.
174. Dash, R.; Mandal, M.; Ghosh, S. K.; Kundu, S. C. Silk sericin protein of tropical tasar silkworm inhibits UVB-induced apoptosis in human skin keratinocytes. *Mol. Cell. Biochem.* **2008**, *311*, 111–119, doi:10.1007/s11010-008-9702-z.
175. Takahashi, M.; Tsujimoto, K.; Yamada, H.; Takagi, H.; Nakamori, S. The silk protein, sericin, protects against cell death caused by acute serum deprivation in insect cell culture. *Biotechnol. Lett.* **2003**, *25*, 1805–9.
176. Sahu, N.; Pal, S.; Sapru, S.; Kundu, J.; Talukdar, S.; Singh, N. I.; Yao, J.; Kundu, S. C. Non-Mulberry and Mulberry Silk Protein Sericins as Potential Media Supplement for Animal Cell Culture. *Biomed Res. Int.* **2016**, *2016*, 7461041, doi:10.1155/2016/7461041.
177. Aramwit, P.; Palapinyo, S.; Srichana, T.; Chottanapund, S.; Muangman, P. Silk sericin ameliorates wound healing and its clinical efficacy in burn wounds. *Arch. Dermatol. Res.* **2013**, *305*, 585–94, doi:10.1007/s00403-013-1371-4.
178. Aramwit, P.; Kanokpanont, S.; De-Eknamkul, W.; Srichana, T. Monitoring of inflammatory mediators induced by silk sericin. *J. Biosci. Bioeng.* **2009**, *107*, 556–61, doi:10.1016/j.jbiosc.2008.12.012.
179. Shi, L.; Yang, N.; Zhang, H.; Chen, L.; Tao, L.; Wei, Y.; Liu, H.; Luo, Y. A novel poly(γ-glutamic acid)/silk-sericin hydrogel for wound dressing: Synthesis, characterization and biological evaluation. *Mater. Sci. Eng. C. Mater. Biol. Appl.* **2015**, *48*, 533–40, doi:10.1016/j.msec.2014.12.047.
180. Salas Campos, L.; Fernándes Mansilla, M.; Martínez de la Chica, A. M. [Topical chemotherapy for the treatment of burns]. *Rev. Enferm.* **2005**, *28*, 67–70.
181. Saltz, A.; Kandalam, U. Mesenchymal stem cells and alginate microcarriers for craniofacial bone tissue engineering: A review. *J. Biomed. Mater. Res. Part A* **2016**, *104*, 1276–1284, doi:10.1002/jbm.a.35647.

182. Grant, G. T.; Mon, E. R.; David REES, S. A.; Jci Smiti-i, P.; Thom, id BIOLOGICAL INTERACTIONS BETWEEN POLYSACCHARtDES AND DIVALENT CATIONS: THE EGG-BOX MODEL.
183. Sweeney, I. R.; Miraftab, M.; Collyer, G. A critical review of modern and emerging absorbent dressings used to treat exuding wounds. *Int. Wound J.* **2012**, *9*, 601–12, doi:10.1111/j.1742-481X.2011.00923.x.
184. Gasperini, L.; Mano, J. F.; Reis, R. L. Natural polymers for the microencapsulation of cells. *J. R. Soc. Interface* **2014**, *11*, 20140817, doi:10.1098/rsif.2014.0817.
185. Abramov, Y.; Golden, B.; Sullivan, M.; Botros, S. M.; Miller, J.-J. R.; Alshahrour, A.; Goldberg, R. P.; Sand, P. K. Histologic characterization of vaginal vs. abdominal surgical wound healing in a rabbit model. *Wound Repair Regen.* **2007**, *15*, 80–86, doi:10.1111/j.1524-475X.2006.00188.x.
186. Doakhan, S.; Montazer, M.; Rashidi, A.; Moniri, R.; Moghadam, M. B. Influence of sericin/TiO_2 nanocomposite on cotton fabric: part 1. Enhanced antibacterial effect. *Carbohydr. Polym.* **2013**, *94*, 737–48, doi:10.1016/j.carbpol.2013.01.023.
187. Gulrajani, M. L.; Brahma, K. P.; Kumar, P. S.; Purwar, R. Application of silk sericin to polyester fabric. *J. Appl. Polym. Sci.* **2008**, *109*, 314–321, doi:10.1002/app.28061.
188. Khurana, G.; Arora, S.; Pawar, P. K. Ocular insert for sustained delivery of gatifloxacin sesquihydrate: Preparation and evaluations. *Int. J. Pharm. Investig.* **2012**, *2*, 70–7, doi:10.4103/2230-973X.100040.
189. Rao KM, Rao KSVK, Sudhakar P, Rao KC, S. M. Synthesis and characterization of biodegradable Poly(Vinylcaprolactam) grafted on to sodium alginate and its microgels for controlled release studies of and anticancer drug. *J. Appl. Pharamceutical Sci.* **2013**, *3*, 61–69.
190. Barth, A. Infrared spectroscopy of proteins. *Biochim. Biophys. Acta - Bioenerg.* **2007**, *1767*, 1073–1101, doi:10.1016/j.bbabio.2007.06.004.
191. Lee, K. Y.; Mooney, D. J. Alginate: properties and biomedical applications. *Prog. Polym. Sci.* **2012**, *37*, 106–126, doi:10.1016/j.progpolymsci.2011.06.003.
192. Rowley, J. A.; Madlambayan, G.; Mooney, D. J. Alginate hydrogels as synthetic extracellular matrix materials. *Biomaterials* **1999**, *20*, 45–53.
193. Steward, A. J.; Liu, Y.; Wagner, D. R. Engineering cell attachments to scaffolds in cartilage tissue engineering. *JOM* **2011**, *63*, 74–82, doi:10.1007/s11837-011-0062-x.
194. Driver, V. R.; Hanft, J.; Fylling, C. P.; Beriou, J. M.; Autologel Diabetic Foot Ulcer Study Group A prospective, randomized, controlled trial of autologous platelet-rich plasma gel for the treatment of diabetic foot ulcers. *Ostomy. Wound. Manage.* **2006**, *52*, 68–70, 72, 74 passim.
195. Martínez-Zapata, M. J.; Martí-Carvajal, A.; Solà, I.; Bolibar, I.; Ángel Expósito, J.; Rodriguez, L.; García, J. Efficacy and safety of the use of autologous plasma rich in platelets for tissue regeneration: a systematic review. *Transfusion* **2009**, *49*, 44–56, doi:10.1111/j.1537-2995.2008.01945.x.

196. Mosesson, M. W. Fibrinogen and fibrin structure and functions. *J. Thromb. Haemost.* **2005**, *3*, 1894–1904, doi:10.1111/j.1538-7836.2005.01365.x.
197. Nurden, A. T. Platelets, inflammation and tissue regeneration. *Thromb. Haemost.* **2011**, *105 Suppl 1*, S13-33, doi:10.1160/THS10-11-0720.
198. Etulain, J. Platelets in wound healing and regenerative medicine. *Platelets* **2018**, 1–13, doi:10.1080/09537104.2018.1430357.
199. Ulivi, V.; Tasso, R.; Cancedda, R.; Descalzi, F. Mesenchymal Stem Cell Paracrine Activity Is Modulated by Platelet Lysate: Induction of an Inflammatory Response and Secretion of Factors Maintaining Macrophages in a Proinflammatory Phenotype. *Stem Cells Dev.* **2014**, *23*, 1858–1869, doi:10.1089/scd.2013.0567.
200. Ren, B.; Hu, X.; Cheng, J.; Huang, Z.; Wei, P.; Shi, W.; Yang, P.; Zhang, J.; Duan, X.; Cai, Q.; Ao, Y. Synthesis and characterization of polyphosphazene microspheres incorporating demineralized bone matrix scaffolds controlled release of growth factor for chondrogenesis applications. *Oncotarget* **2017**, *8*, 114314–114327, doi:10.18632/oncotarget.23304.
201. Yin, J.; Qiu, S.; Shi, B.; Xu, X.; Zhao, Y.; Gao, J.; Zhao, S.; Min, S. Controlled release of FGF-2 and BMP-2 in tissue engineered periosteum promotes bone repair in rats. *Biomed. Mater.* **2018**, *13*, 25001, doi:10.1088/1748-605X/aa93c0.
202. Anitua, E.; Pino, A.; Troya, M.; Jaén, P.; Orive, G. A novel personalized 3D injectable protein scaffold for regenerative medicine. *J. Mater. Sci. Mater. Med.* **2018**, *29*, 7, doi:10.1007/s10856-017-6012-6.
203. Kunz, R. I.; Brancalhão, R. M. C.; Ribeiro, L. de F. C.; Natali, M. R. M. Silkworm Sericin: Properties and Biomedical Applications. *Biomed Res. Int.* **2016**, *2016*, 1–19, doi:10.1155/2016/8175701.
204. Zhang, Y.-Q.; Ma, Y.; Xia, Y.-Y.; Shen, W.-D.; Mao, J.-P.; Xue, R.-Y. Silk sericin–insulin bioconjugates: Synthesis, characterization and biological activity. *J. Control. Release* **2006**, *115*, 307–315, doi:10.1016/j.jconrel.2006.08.019.
205. Baba, T.; Hanada, K.; Hashimoto, I. The study of ultraviolet B-induced apoptosis in cultured mouse keratinocytes and in mouse skin. *J. Dermatol. Sci.* **1996**, *12*, 18–23.
206. Kato, N.; Sato, S.; Yamanaka, A.; Yamada, H.; Fuwa, N.; Nomura, M. Silk protein, sericin, inhibits lipid peroxidation and tyrosinase activity. *Biosci. Biotechnol. Biochem.* **1998**, *62*, 145–7.
207. Takeuchi, A.; Ohtsuki, C.; Miyazaki, T.; Kamitakahara, M.; Ogata, S.; Yamazaki, M.; Furutani, Y.; Kinoshita, H.; Tanihara, M. Heterogeneous nucleation of hydroxyapatite on protein: structural effect of silk sericin. *J. R. Soc. Interface* **2005**, *2*, 373–378, doi:10.1098/rsif.2005.0052.
208. Lim, K. S.; Kundu, J.; Reeves, A.; Poole-Warren, L. A.; Kundu, S. C.; Martens, P. J. The influence of silkworm species on cellular interactions with novel PVA/silk sericin hydrogels. *Macromol. Biosci.* **2012**, *12*, 322–32.
209. Cho, K. Y.; Moon, J. Y.; Lee, Y. W.; Lee, K. G.; Yeo, J. H.; Kweon, H. Y.; Kim, K. H.; Cho, C. S. Preparation of self-assembled silk sericin nanoparticles. *Int. J. Biol. Macromol.* **2003**,

32, 36–42.
210. Kundu, B.; Kundu, S. C. Silk sericin/polyacrylamide in situ forming hydrogels for dermal reconstruction. *Biomaterials* **2012**, *33*, 7456–7467, doi:10.1016/j.biomaterials.2012.06.091.
211. Aramwit, P.; Kanokpanont, S.; Nakpheng, T.; Srichana, T. The effect of sericin from various extraction methods on cell viability and collagen production. *Int. J. Mol. Sci.* **2010**, *11*, 2200–11, doi:10.3390/ijms11052200.
212. Terada, S.; Nishimura, T.; Sasaki, M.; Yamada, H.; Miki, M. Sericin, a protein derived from silkworms, accelerates the proliferation of several mammalian cell lines including a hybridoma. *Cytotechnology* **2002**, *40*, 3–12, doi:10.1023/A:1023993400608.
213. Aramwit, P.; Damrongsakkul, S.; Kanokpanont, S.; Srichana, T. Properties and antityrosinase activity of sericin from various extraction methods. *Biotechnol. Appl. Biochem.* **2010**, *55*, 91–98, doi:10.1042/BA20090186.
214. Mori, M.; Rossi, S.; Ferrari, F.; Bonferoni, M. C.; Sandri, G.; Riva, F.; Tenci, M.; Del Fante, C.; Nicoletti, G.; Caramella, C. Sponge-Like Dressings Based on the Association of Chitosan and Sericin for the Treatment of Chronic Skin Ulcers. II. Loading of the Hemoderivative Platelet Lysate. *J. Pharm. Sci.* **2016**, *105*, 1188–1195, doi:10.1016/j.xphs.2015.11.043.
215. Mori, M.; Rossi, S.; Ferrari, F.; Bonferoni, M. C.; Sandri, G.; Chlapanidas, T.; Torre, M. L.; Caramella, C. Sponge-Like Dressings Based on the Association of Chitosan and Sericin for the Treatment of Chronic Skin Ulcers. I. Design of Experiments–Assisted Development. *J. Pharm. Sci.* **2016**, *105*, 1180–1187, doi:10.1016/j.xphs.2015.11.047.

LIST OF PUBLICATION AND OTHER SCIENTIFIC ACTIVITIES

Publications

- **Platelet-rich plasma-based bioactive membrane as a new advanced wound care tool.**
  Spanò R., Muraglia A., Todeschi M.R., Nardini M., Strada P., Cancedda R., Mastrogiacomo M. *J. Tissue Eng Regen Med.* 2016 Nov 13. doi: 10.1002/term.2357.
- **Culture medium supplements derived from human platelet and plasma: cell commitment and proliferation support.**
  Muraglia M., Nguyen V.T., Nardini M., Mogni M, Coviello D., Strada P., Baldelli I., Formica M., Cancedda R., Mastrogiacomo M. *Front. Bioeng. Biotechnol.* doi: 10.3389/fbioe.2017.00066 *In publication*
- **Electrospun silk fibroin fibers for storage and controlled proteins release.**
  Pignatelli C., Perotto G., Nardini M., Mastrogiacomo M., Bayer S. I., Cancedda R. and Athanassiou A. *Acta Biomater. Submitted*
- **Sericin, alginate and platelet lysate combined in a biomembrane for the treatment of skin ulcers.**
  Nardini M., Perteghella S., Cancedda R., Torre M.L., Mastrogiacomo M. *In preparation*
- **Role of C-MYC in the proliferation stage of mesenchymal stem cells cultured and selected by platelet derivatives**
  Nardini M., Gentili C., Cancedda R., Castagnola P., Mastrogiacomo M. *In preparation*

National and International meeting

- Training Event "Il futuro terapeutico delle cellule stromali mesenchimali", GISM; Fondazione Poliambulanza; IZLER October 20, 2017 Brescia (IT)
- European Chapter Meeting of TERMIS 2017, TERMIS, June 26-30, 2017 Davos (CH) with the following poster: Platelet growth factor activated biomembrane as medical patch in skin regeneration
- Advance in stem cells and regenerative medicine, EMBO Conference, May 23-26, 2017 Heidelberg (DE) with the following poster: Platelet growth factor activated biomembrane as medical patch in skin regeneration
- Scientific Meeting "Life science for a better future", Associazione Italiana di Biologia e Genetica, May 11-13, 2017 Santa Margherita Ligure (IT) with the following oral presentation: Platelet growth factor activated biomembrane as a medical patch in skin regeneration
- GISM Annual Meeting 2016, GISM; Fondazione Poliambulanza; IZLER October 20-21, 2016 Brescia (IT) with the following poster: The c-Myc1 isoform is specifically induced by platelet lysate stimulation in mesenchymal stem cells.

- European Chapter Meeting of TERMIS 2016, TERMIS, June 28 July 1, 2016 Uppsala (SE) with the following poster: Smart platelet-rich-plasma based bioactive membrane as a new advanced wound care tool
- Training Event "Corso base sulla sperimentazione animale per la realizzazione di procedure su animali in ottemperanza al D. LGS 26/2014", Regione Liguria, November 11-12, 2015 Genova (IT)
- GISM Annual Meeting 2015, GISM; Fondazione Poliambulanza; IZLER October 8-9, 2015 Brescia (IT)
- Summer School on Biomaterials and Regenerative Medicine University of Trento July6-8 2015 Riva del Garda (IT)
- Stem Cells, Cancer, Immunology and Aging Fondazione Internazionale Menarini February 12-14 2015 Genova (IT)

Responsibilities

Support work for the practical laboratory experiences relative to the following academic courses:

- 2014/2015 Biologia Cellulare e dello sviluppo e Laboratorio di Colture Cellulari e di Biologia dello sviluppo, for the Bachelor's degree in Biotechnology (32 hours)
- 2015/2016 Biologia Cellulare e dello sviluppo e Laboratorio di Colture Cellulari e di Biologia dello sviluppo, for the Bachelor's degree in Biotechnology (32 hours)
- 2016/2017 Biologia Cellulare e dello sviluppo e Laboratorio di Colture Cellulari e di Biologia dello sviluppo, for the Bachelor's degree in Biotechnology (32 hours)
- 2017/2018 Biologia cellular II e Laboratorio, for Master degree in Farmaceutical and Medical Biotechnology (32 hours)

Training activities

- **From 31.07.17 to 01.08.17** Visiting PhD Student at Institute of Nanotechnology-Laboratory for Soft and Living Matter- National Research council (CNR), Università la Sapienza Rome, Italy under the supervision of Dr. Cedola Alessia to acquire specific know how on the elaboration of imagines acquired with Synchrotron Radiation
- **From 14.07.16 to 18.07.16** Training during PhD course at ESRF- European Synchrotron Radiation Facility- Grenoble (F) under the supervision of Dr. Alberto Gravin to execution of experiments.

Other activities

- **Co-author of a patent** regarding the validation of platelet derivatives associated to biomembranes useful as therapeutic agents (University of Genoa Partner) registered on February 21 2017 with n° 102017000117327.

- **Member of Participant Unit** in a Phase II randomized clinical trial (PATCH II) for the use of allogeneic platelet rich plasma for the treatment of skin chronic ulcers in diabetic patient as monocentric study approved from ethical committee of Ospedale Policlinico San Martino
  Study Chairman:
  Domenico Palombo, Chirurgia vascolare, IRCCS AOU San Martino-IST, Genova, Italia
  Ranieri Cancedda, Medicina Rigenerativa, DIMES Università di Genova, Italy
  Participant Units:
  Maddalena Mastrogiacomo, Marta Nardini, Medicina Rigenerativa DIMES Università di Genova
  Alessandro Poggi; Unità di Biologia Molecolare e angiogenesi, IRCCS Ospedale San Martino –IST
  Aurora Parodi, Cozzani Emanuele; Clinica Dermatologica Università di Genova- , IRCCS Ospedale San Martino –IST
  Pierluigi Santi, Baldelli Ilaria; Chirurgia plastica e ricostruttiva Università di Genova, IRCCS Ospedale San Martino –IST
  Paolo Bruzzi, Epidemiologia Clinica, IRCCS AOU San Martino-IST, Genoa, Italy
  Ferdinando Felli, Matteo Formica, Clinica Ortopedica, IRCCS AOU San Martino-IST, Genova, Italia
  The study started in June 2017 and is still going.